12-2015

IDENTIFYING PROTEIN KINASE TBK1 AS A NOVEL INHIBITOR OF INTESTINAL TUMORIGENESIS

Amber L. Mathews

IDENTIFYING PROTEIN KINASE TBK1 AS A NOVEL INHIBITOR OF INTESTINAL TUMORIGENESIS

by

Amber Lynn Mathews, M.S.

APPROVED:

_____
Dr. Shao Cong Sun, Ph.D.
Advisory Professor

_____
Dr. Qingyun Liu, Ph.D.

_____
Dr. Gary Gallick, Ph.D.

_____
Dr. Jagan Sastry, Ph.D.

_____
Dr. Kimberly Schluns, Ph.D.

APPROVED:

_____
Dean, The University of Texas
Graduate School of Biomedical Sciences at Houston

IDENTIFYING PROTEIN KINASE TBK1 AS A NOVEL INHIBITOR OF INTESTINAL TUMORIGENESIS

A

DISSERTATION

Presented to the Faculty of

The University of Texas

Health Science Center at Houston and

The University of Texas

M. D. Anderson Cancer Center

Graduate School of Biomedical Sciences

in Partial Fulfillment

of the Requirements

for the Degree of

DOCTOR OF PHILOSOPHY

By

Amber Lynn Mathews, M.S.

Houston, TX

December 2015

DEDICATION

I dedicate this dissertation to God who led me, supported me, comforted me, and has been my everything throughout this journey of life. I thank Him for His revelations which provides me with a better understanding of His creations. I also dedicate this to my mom and grandmother who encouraged me to pursue education, use my gifts and talents for the greater good, and believed in and supported me and my dreams.

ACKNOWLEDGEMENTS

It has truly been an amazing experience working on this project under the mentorship of Dr. Shao-Cong Sun. I have found myself many times pondering in amazement of the being given the opportunity to learn from someone with such an astute scientific mind as Dr. Sun. I am blessed to have been taught by someone who I admire and respect. In what seems like such a short time, I have learned a tremendous amount from Dr. Sun in scientific thinking, writing, and research management. Not only does he teach by instruction, but also he leads by example in his strong commitment to the advancement of science, his dedication to education and his integrity. I am grateful for all of his efforts in helping me achieve my academic and research goals.

I am also eternally grateful to the past and present members of Dr. Sun's lab who have become like big brothers and sisters to me. The members of the lab have offered me kindness, encouragement, and patience in teaching me. Additionally, we have formed true friendships and I sincerely thank you for sharing this experience with me. Each of you individually has provided me with valuable insight, perspective, and wisdom beyond science and the career, which I will always treasure. I am grateful for the opportunity to work in such a wonderful environment. Your continuous service and friendship turned the frustrations of a challenging project to joyful adventure. I especially would like to thank Xuhong Cheng for teaching me routine lab techniques and helping initiate the TBK1 project, Hongbo Hu

for help with other projects and Mikyoung Chang for help with TBK1 project and others.

I never would have thought to be so lucky to also have selected such an amazing advisory committee of Dr. Sun, Dr. Jagan Sastry, Dr. Kimberly Schluns, Dr. Gary Gallick, Dr. Qingyun Liu and Dr. Dingzhi Wang. While the anxiety typically builds prior to committee meetings from fear of unknown outcomes, my advisory committee members provided such a positive environment for sharing and learning that the meetings became fun and enjoyable. They presented helpful feedback for my project and challenged me in my research. I am also grateful to my committee for taking an interest in me, investing in me and my career through mentorship and sponsorship, and providing several letters of recommendations for my award applications. I would not have been granted some of the opportunities I've had in the GSBS were it not for this strong network of support.

I am also grateful for the support of my friends in the Immunology Program and the GSBS. As we struggled through challenging course work and project pitfalls, it was comforting to know that we had the support from one another. I thank you all, with a special thanks to Germaine Agollah, Rina Mbofung, Junchen Diao and Javier Ortiz. You have become like family to me and I thank you for your support, prayers and friendship.

My entry into the GSBS was equivalent to a miracle when submitting my application early Spring 2010. My first encounter with the GSBS faculty and administrators was incredible with an unusual individual interview day due to later

submission. After interviewing with Dr. Lane, Dr. Stancel, Dr. Sun, Dr. Watowich, Dr. Schluns and Dr. Gillet, I knew there was no better place for me than the GSBS. They made me feel welcomed while sharing the amazing research opportunities offered by the school. Additionally, by the end of the interview day, they provided me with two years of funding allowing me to matriculate into GSBS August 2010. The memory of that day will never fade as I truly believe divine intervention granted me favor to become a part such an incredible graduate program and learn from top experts in the field. I especially would like to thank Dr. Stephanie Watowich for her mentorship, support, and encouragement. I admire her for her professional achievements, service to GSBS and student learning, and her example as strong scientist.

While I have become part of a family here at GSBS, I would not have reached this point were it not for my biological family. My mother Jackie Stewart and grandparents Helen and Wilbert Mathews significantly contributed my achievements. My grandmother's example of hard work, dedication to family and community, and love during my adolescence served as an inspiration to me. My mother and grandparents instilled in me values of service to my community, pursuit of education, and strong work ethic, which I am eternally grateful. My aunts and uncles also significantly contributed to my development through the years, encouraging me and supporting me in my academic and personal endeavors. I am thankful for their understanding as I have been missing-in-action for the last several years in pursuit

of my endeavors. I am also grateful for my little sister Autumn Stewart who provides me with the medicine of laughter, which serves as a helpful reminder to enjoy life.

I am grateful to my husband David Rushworth, now GSBS alumni but whom I met as a fellow GSBS Immunology Program student. A person could not be so lucky to have such an amazing support system from family, lab family, GSBS faculty, staff and students as well as an incredibly talented, fun and supportive husband. I am grateful for the opportunity to share this wonderful experience together as husband and wife, as friends and as professional colleagues.

With all of the scientific and emotional support, I would not have accomplished much without the financial support I was afforded. I gratefully acknowledge the continuous funding made available by the GSBS in my first year and by the NIH-NCI T32 Fellowship under the Training Program in Cancer Immunobiology training grant for the last four years. I am also grateful to have received financial award from the generous donors of the American Legion Auxiliary for the last two years. A thank you also goes to FASEB for travel awards granted to me, which helped deepen my knowledge and skills to achieve my scientific career goals.

Lastly, but most certainly not least, I am grateful to my God, the Father, the Son and the Holy Spirit, who made this all possible though teaching me, guiding me, molding me and providing all that I needed through the people mentioned above.

IDENTIFYING PROTEIN KINASE TBK1 AS A NOVEL INHIBITOR OF INTESTINAL TUMORIGENESIS

Amber Lynn Mathews, M.S.

Advisory Professor: Shao-Cong Sun, Ph.D.

Colorectal cancer (CRC) is the third most common cancer diagnosed in women and men, causing almost 600,000 annual deaths worldwide. There is a clear need to understand how CRC forms and progresses in order to improve the strategies of CRC prevention and therapy. A major factor that drives the development of CRC is genetic mutations that lead to activation of oncogenes and inactivation of tumor suppressor genes in intestinal epithelial cells (IECs). In addition, the initiation and progression of CRC involve environmental and immunological factors. In particular, chronic inflammatory conditions are known as an important risk factor for CRC. Intestinal inflammation can be caused by deregulated signaling events in IECs or immune cells; and chronic inflammation is often associated with reduced production of immunosuppressive cytokines such as interleukin (IL)-10 and aberrant production of inflammatory cytokines. However, the signaling factors involved in the regulation of intestinal inflammation and tumorigenesis are still poorly defined. Given the complexity of the molecular and cellular components contributing to these pathogenic processes, animal models represent an important tool for CRC studies.

This dissertation focuses on the study of a serine/threonine kinase, TANK Binding Kinase 1 (TBK1). Although TBK1 is best known as a mediator of type I interferon induction in antiviral innate immunity, recent evidence suggests the involvement of TBK1 in several other biological processes including cancer development. Based on *in vitro* studies using cancer cell lines, TBK1 has been implicated as an oncogenic kinase that mediates survival of KRAS-dependent lung and other cancers. However, the oncogenic role of TBK1 is controversial, since this finding has been challenged by a more recent study. Moreover, the *in vivo* role of TBK1 in CRC development, particularly during the early phase of adenoma formation, has not been studied. This dissertation project took an *in vivo* approach that involves the generation and characterization of an innovative mouse model in which *Tbk1* is conditionally ablated in IECs. The data from my dissertation reveals an unexpected finding that TBK1 has a tumor-suppressive function in the intestine. IEC-specific *Tbk1* ablation promotes adenoma formation in mice carrying a mutation in the *Apc* gene, a tumor-suppressor gene commonly mutated in the early stages of colon cancer development. Interestingly, *Tbk1* expression is important for the crosstalk of IECs with intraepithelial lymphocytes that maintain the expression of immunosuppressive cytokine IL-10. These studies present the first *in vivo* model demonstrating the function of TBK1 during the process of intestinal adenoma development and suggest a mechanism of TBK1 action. These data also present a novel approach in determining the *in vivo* function of TBK1 early in the tumorigenic process as compared to previous findings based on the xenograft model of late-

staged cancers. In addition, because the use of TBK1 inhibitor has been suggested for possible treatment in cancers of other tissue types, my findings argue for the precaution in the selection of treatment modalities targeting TBK1 in these patients; it is possible that long-term use of TBK1 inhibitors may pose an increased risk for adenoma growth in the intestine.

TABLE OF CONTENTS

LIST OF FIGURES

LIST OF ABBREVIATIONS

+	positive
ABIN1	A20 binding inhibitor of NF-κB 1
Actb	β actin
ACF	aberrant crypt foci
AOM	azoxymethane
APC	adenomatous polyposis coli
Atg	autophagy related
BAFF	B cell activating factor
BCR	B cell receptor
BM	basement membrane
bp	base pairs
BrdU	bromodeoxyuridine
BubR1	bub1-related kinase
CCL	chemokine (C-C motif) ligand
CD	cluster of differentiation
cDNA	complementary DNA
Cdx2	caudal type homeobox 2
CNS	central nervous system
COX	cyclooxygenase
CRC	colorectal cancer
Cre	causes recombination

CRISPR	clustered regularly interspaced short palindromic repeats
CTD	C-terminus domain
CXCL	chemokine (C-X-C motif) ligand
CYLD	cylindromatosis
DMSO	dimethyl sulfoxide
DNA	deoxyribonucleic acid
DSS	dextran sodium sulfate
DTT	dithiothreitol
DTX	deltex E3 ubiquitin ligase
dUTP	deoxynucleotide triphosphates
EAE	experimental autoimmune encephalomyelitis
EDTA	ethylenediaminetetraacetic acid
Ephb	Eph receptor B
ER	estrogen receptor
FAP	familial adenomatous polyposis syndrome
FBS	fetal bovine serum
fl	floxed
Foxp3	forkhead box P
GALT	gut-associated lymphoid tissues
GFP	green fluorescent protein
GIN	gastrointestinal neoplasia
GTP	guanosine-5'-triphosphate

h	hours
H&E	hemotoxylin and eosin
HBSS	Hanks buffered salt solution
HEK	human embryonic kidney
HEPES	4-(2-hydroxyethyl)-1-piperazineethanesulfonic acid
HSP	heat shock protein
HUVEC	human umbilical vein endothelial cell
i.p.	intraperitoneally
IBD	inflammatory bowel disease
IEC	intestinal epithelial cells
IEL	intraepithelial lymphocytes
IFN	interferon
Ig	immunoglobulin
IKK	IκB kinase
IL	interleukin
Inh	inhibitor
IQGAP1	IQ motif containing GTPase activating protein 1
IRF	interferon regulatory factor
IkB	inhibitor of NF-κB
K	lysine
KD	kinase domain
KO	knockout

KRAS	Kirsten rat sarcoma viral oncogene homolog
LC3B	1B light chain 3
Lgr	leucine-rich Repeat containing G protein-coupled receptor
LOH	loss-of-heterozygosity
loxP	locus of crossing (x) over, P1
LP	lamina propria
Lys	lysine
M	microfold
MAVS	mitochondrial antiviral signaling proteins
MEF	mouse embryonic fibroblasts
mL	milliliter
Min	multiple intestinal neoplasia
mTORC	mammalian target of rapamycin complex
Muc	mucin
NaCl	sodium chloride
NAK	NF-κB-activating kinase
NEMO	NF-κB essential modifier
NF-kB	nuclear factor-κB
NIK	NF-κB-inducing kinase
NLRs	NOD like receptors
NOD	nucleotide-oligomerization domain
Nu/nu	nude

OPTN	optineurin
PAMP	pathogen-associated molecular patterns
PBS	phosphate buffered saline
PCR	polymerase chain reaction
PELI	pellino E3 ubiquitin protein ligase family member
PGE2	prostaglandin E2
PI3K	phosphatidylinositol 3-kinase
PLK	polo-like kinase
PPM1B	protein phosphatase $Mg^{2+/}Mn^{2+}$ dependent 1 B
PRR	pattern recognition receptors
PTEN	phosphatase and tensin homolog
qPCR	quantitative PCR
Rag	recombination activating gene
REGIII	regenerating islet-derived 3
RIG	retinoic acid-inducible gene
RLRs	RIG-I like receptors
RNA	ribonucleic acid
RNAi	RNA interference
RNF	RING finger protein
RPMI	Roswell Park Memorial Institute medium
S6	S6 ribosomal protein
SDD	scaffold dimerization domain

SDS-PAGE	sodium dodecyl sulfate-polyacrylamide gel electrophoresis
Sema	semaphoring
Ser	serine
SHIP	Src homology 2 domain-containing protein tyrosine phosphatase
shRNA	short hairpin RNA
SI	small intestine
Src	Rous sarcoma protooncogene
STING	stimulator of IFN genes
T2K	TRAF2-associated kinase
TANK	TRAF family member-associated NF-κB activator
TAX1BP1	Tax1 binding protein 1
TBK1	TANK binding kinase 1
TCR	T cell receptor
TGF	transforming growth factor
Thr	threonine
TLRs	toll-like receptors
TNF	tumor necrosis factor
TRAF	TNF-receptor-associated factor
Treg	regulatory T cells
TRIF	TLR/IL-1 receptor domain-containing adaptor protein inducing IFN-β
TUNEL	terminal deoxynucleotidyl transferase dUTP nick end labeling
ULD	ubiquitin-like domain

XIAP	X-linked inhibitor of apoptosis

CHAPTER 1: SPECIFIC AIMS OF THE DISSERTATION

Chapter 1: Specific Aims of the Dissertation

Colorectal cancer (CRC) is a major cause of cancer morbidity and mortality, and almost 150,000 people are diagnosed and approximately 50,000 die from this disease every year in the United States alone. The development of this disease results from dysregulated signal transduction in intestinal epithelial cells (IECs) that allows out-of-control growth and/or survival of dysfunctional cells. Several risk factors have been associated with CRC, including somatic and germline gene mutations, chronic intestinal inflammation, diet and lifestyle. While there has been progress in the field, the worldwide incidence of almost 1.2 million people and mortality rate of almost 600,000 suggest that there is indeed much to understand concerning the intestinal tumorigenic process in order to improve the strategies of CRC prevention and treatment. The molecular mechanisms that regulate the process of CRC initiation and progression are still poorly understood. The overall objective of my dissertation project has been to contribute to the understanding of the mechanisms that control intestinal adenoma development. This dissertation project contributes to this goal by specifically identifying TANK binding kinase 1 (TBK1) as a novel negative regulator of intestinal tumor growth using an innovative *in vivo* model.

TBK1 is a serine/threonine protein kinase that mediates type I interferon induction in antiviral innate immune responses. In addition, recent studies using *in vitro* cell culture and xenograft mouse models implicate TBK1 as an oncogenic

kinase that supports the survival and drug resistance of human cancer cell lines, including those derived from breast cancer, KRAS-driven lung cancers, melanoma, and prostate cancer. However, a more recent study showed that the viability of KRAS-mutant cancer cell lines did not correlate with the knockdown or pharmacological inhibition of TBK1 *in vitro*, thus creating controversy in the field. In addition, our understanding of the function of TBK1 in cancer is limited by the sole use of cell line studies, which models late stages of disease. Therefore, the role of TBK1 in regulating the early stage of tumor development, such as the initiation and growth of adenomas was not yet addressed. Secondly, the use of mouse xenograft models excludes the contribution of functional T lymphocytes to the understanding of disease progression. Third, the use of a limited number of human cancer cell lines may create variations in results due to the accumulation of different genetic alterations. To overcome these limitations, my dissertation project employed a new mouse model harboring TBK1 deficiency specifically in IECs. My hypothesis is that TBK1 modulates intestinal tumorigenesis *in vivo* by regulating IEC survival and immune homeostasis.

In testing this hypothesis, my project sought and accomplished the following specific aims. In **Specific Aim 1 (**discussed in Chapter 3), we examined the role of TBK1 in intestinal adenoma development by analyzing the effect of IEC-conditional *Tbk1* knockout on adenoma formation in $Apc^{min/+}$ mice and determined that TBK1 in IECs regulates intestinal tumorigenesis *in vivo*. These findings were consistent with a strong correlation between *TBK1* and *APC* mRNA expression in patient samples of

colorectal adenocarcinomas profiled in The Cancer Genome Atlas (TCGA). In **Specific Aim 2 (**also discussed in Chapter 3), we devised a series of immunological studies to examine whether TBK1 in IECs regulates intestinal immune homeostasis *in vivo* thus affecting the tumorigenic process. In this aim, we determined that TBK1 expression is important for the crosstalk of IECs with intraepithelial lymphocytes (IELs) that maintains an immunosuppressive environment during intestinal adenoma development. In addition to these *in vivo* studies, we carried out *in vitro* and xenograft studies in **Specific Aim 3** (discussed in Chapter 4) using *TBK1*-knockdown human CRC cell lines. We determined that TBK1 is dispensable for the growth of KRAS-competent xenograph tumor growth in immunocompromised hosts. The findings presented herein supporting the *in vivo* function of TBK1 in intestinal tumorigenesis provide a better understanding of the molecular mechanisms mediating the disease process. The significance of these findings is discussed within each chapter of the dissertation with a particular focus in Chapter 5 highlighting further implications.

CHAPTER 2: LITERATURE REVIEW

Chapter 2: Literature Review

Epidemiology

Colorectal cancer is one of the leading cancer diagnoses globally. The estimated new diagnoses of CRC is approximately 1.2 million being the second most common cancer diagnosis in women and third in men[1,2]. The rate of incidence is highest in Australia, New Zealand, North America and Europe. In fact, as compared to developing countries, the rates are as many as five times higher in developed countries, although differences in methods of medical diagnostics in these regions may have partially contributed to these epidemiological numbers. However, the recent trend is a steadily reduced incidence rate in economically developed countries as a result of screenings and adenomatous polyp removal. At the same time, a rise in incidence is observed in developing countries, which is attributed to environmental risk factors such as diet and lifestyle. The time of diagnosis also varies between developed and developing countries where late stage diagnosis is more common in developing counties and reflected in mortality rates. There are about 600,000 estimated worldwide deaths per year from CRC with highest mortality rate observed in Southern Africa, central and eastern Europe and Eastern Asia as of 2008.[1] Because of advancement in screenings, treatments and knowledge of disease course, there has been a decline in mortality in western countries.[1] However, the challenge remains as mortality rate for CRC is substantial.

It is estimated that nearly 140,000 Americans were diagnosed with CRC while 50,000 succumbed to the disease in 2014[3]. It is currently the third most common cancer diagnosis and cause of death among both women and men, despite a trend that has steadily declined since the early 1950s when CRC was the leading cause of cancer death[4,5]. The incidence and mortality rates for CRC is greater in men than in women. Reasons for gender differences are unknown but speculated to be related to differences in sex hormones, risk factors, and adherence to recommended screenings[6].

Those aged 65 years old and older hold the majority of new cases at 60 percent and CRC deaths at 70 percent[6]. While an overall decline has been observed in CRC incidence and mortality rates over the past few decades[5], a closer look at age related trends revealed that the decline in new cases is observed for those 50 years and older whereas a steady increase in CRC incidence amongst younger adults particularly those 49 years of age or younger[6,7]. It is predicted that this rate will continue upward in younger adults below the age of 50 years old, the traditional CRC screening age. Patients at higher risk, such as those with ulcerative colitis or family history of inherited CRC, are advised to undergo CRC screening prior to age 50 to allow for earlier diagnosis and treatment. It is believed that the disparity in age-related CRC incidence is associated with dietary risk factors such as the pervasiveness of obesity and an inactive lifestyle in the younger population[7], although further research is necessary to determine specifically the effects of these behavioral risk factors in CRC incidence in younger groups.

A study performed between 2006 and 2010 revealed a trend demonstrating differences amongst races and ethnicities, where African Americans have the highest rates of incidence and mortality while Asian and Pacific Islanders have the lowest[6]. There is an association between socioeconomic status and risk of incidence and mortality from CRC such that low socioeconomic status has higher risk for CRC. It is believed that the impact of disproportionately low social economic position of African Americans contributes to this imbalance of new cases and death between groups as the poverty rate was almost three times and two and half times higher amongst African Americans as compared to Caucasians and Asians, respectively.[6] However, other contributing factors, some of which are still unknown, are considered, as rates are still considerably higher in African Americans when compared with Caucasians who are within the same socioeconomic group. For example, one recent study suggests that behavioral risk factors may come into play such as obesity[6]. While there has been a decline over the more recent years in CRC rates[5,6], it is clear that there is a need to better understand the relationship between risk factors such as diet and lifestyle in addition to others including somatic and germline mutations and chronic intestinal inflammation in the development of CRC.

Intestinal epithelia and immune homeostasis – the norm

The intestine is an organ with diverse functions, including food digestion, nutrient and water absorption, gas exchange, microbial sensing and immunological regulation. Pivotal to the functions of intestine is the epithelium, the largest mucosal surface of the body that serves as both a physical barrier to commensal microbes

and an important component of the immune system. The intestinal epithelium is covered by a single layer of IECs, including enterocytes, goblet cells, paneth cells, endocrine cells and M cells, which work together to maintain homeostasis within the gut. These cells, originating from pluripotent intestinal epithelial stem cells, make up part of the mucosa, one of the four main vertical layers of the intestine[8]. Within the mucosa, IELs, predominately CD8+ T cells, are interspersed throughout and in direct contact with the epithelial cell layer as illustrated in Figure 1; this puts them along with the IECs at the forefront of the intestinal immune response. As part of the mucosa, the lamina propria, which lies beneath a basal membrane or thin layer of connective tissue under the IEC and IEL layer, is formed by a network of loose connective tissue that defines a compartment for heavily infused circulating immune cells, particularly T lymphocytes, macrophages, plasma cells, eosinophils, and mast cells[8]. These immune cells are less frequently within the submucosa, the second layer of the intestine, since a thin smooth muscle layer called the muscularis mucosa[8], a facilitator in movement and mucosal folding, acts as a divider between the mucosa and the submucosa[8,9]. Within the submucosa lie larger vessels of the blood and lymphatic systems, nerve fibers and ganglia supported by loose fibrous connective tissue. Surrounding the submucosa is the muscularis propria that consists of two layers of smooth muscle that function in contractility of the gut[9]. The outer most layer of the intestine is the serosa, a thin layer of loose connective tissue that connects to outer muscularis[8,9]. Throughout the intestine, there are widely dispersed gut-associated lymphoid tissues (GALT), such as Peyer's patches in the

small intestine and colonic patches and isolated lymphoid follicles in the large intestine, which are organized aggregates of immune cells mediating mucosal adaptive immune responses[9-11].

The epithelial tissues of the intestine undergo specific programs of self-renewal such that new cells are created every 10 to 14 hours from a dividing intestinal stem cell population, capable of differentiation while migrating from the crypt to the tip of the villus. As the cells continue to migrate toward the tip, they undergo apoptosis such that the layer of epithelium is regenerated every three to five days in a human and every two to three days in mice. The exceptions are Paneth cells in the small intestine and enteroendocrine cells, which are renewed less frequently, four weeks and 35-100 days, respectively[8,9]. A large portion of pluripotent intestinal stem cells differentiate into absorptive enterocytes while smaller specialized lineages include secretory enteroendocrine, goblet and Paneth cells. Enteroendocrine cells, neuroendocrine regulators in the intestine, secrete several hormones needed for proper digestion. Goblet cells are major producers of mucin proteins, especially mucin 2, which form a mucous layer over the mucosa. Goblet cells also produce proteins such as Trefoil factor 3, a protein that provides structural support for mucous layer integrity and signals the promotion of epithelial cell repair mechanism. Trefoil factor 3 together with muc2 adds additional level of protection against intestinal pathologic microbial stimuli. Paneth cells at the base of the crypt of the small intestine release antimicrobial molecules in larger quantities and variety than that of absorptive enterocytes. Whereas enterocytes secrete the C-type lectin

REGIII gamma, which targets destruction of peptidoglycan walls of gram-positive bacteria, Paneth cells secrete defensins, lysozymes, and cathelicidins which defend against broader groups of bacteria. By way of active transcytosis, IECs also facilitate the release of antibodies, particularly IgA produced by lamina propria plasma cells, into the lumen. This joint effort between plasma cells and IECs maintains homeostasis by regulating microbial populations in the luminal compartment[12].

IECs also have the ability to sample antigen from within the lumen. While it has traditionally been thought that epithelial microfold cells or M cells uniquely had the ability to engulf and transcytose microbial antigens into the Peyer's patches, a recent study has reported that goblet cells can function similarly, transporting antigen to lamina propria dendritic cells[12,13]. Intestinal dendritic cells that are in direct contact with IECs are also capable of sampling antigens directly within the lumen by using their dendrites that can cross the epithelial monolayer. It is not yet well understood how these different ways of antigen sampling functionally impact immune responses, but it is speculated that the different antigen-sampling cells may direct different types of immune responses[12].

In addition to mediate digestive process via digestive enzyme production, nutrient absorption, and antimicrobial peptide secretion, the IECs can actively sense commensal bacteria and pathogens and secrete cytokines and chemokines that are important for protective immunity and homeostasis of the intestine[14]. Recognition of microbe-associated molecular patterns by the IECs relies on the expression of a variety of pattern recognition receptors (PRRs), including toll-like receptors (TLRs),

RIG-I like receptors (RLRs) and nucleotide-oligomerization domain (NOD) like receptors (NLRs). Until recently, the focus of PRR studies has been on their role in eliciting a proinflammatory response in hematopoietic cells. However, it is increasingly clear that the PRRs of IECs play an important role in facilitating immune tolerance to commensal microbiota and maintaining intestinal immune homeostasis[12]. A major role of the IECs is to prevent invasion by the commensal bacteria, although it is also likely that IECs may interplay with immune cells to directly participate in immune tolerance. In this regard, several types of immune cells contribute to the establishment of immune tolerance to commensals and maintenance of immunosuppressive environment in the gut; these include IELs, regulatory T cells, and intestinal macrophages. These immunosuppressive cells are designed to promote a tolerogenic response and prevent active inflammation in response to nonthreatening commensals in the lumen or harmless antigen from the diet[11,14 15].

Colorectal cancer pathology

It is widely recognized that CRC develops in a stepwise fashion driven by accumulated genetic alterations and environmental factors. Genetic mutations in intestinal stem cells may result in deregulation of growth- or survival-related signaling events, thereby altering homeostatic conditions that lead to formation of aberrant crypt foci, in which crypts appear to be larger than normal[16,17]. These putative precancerous lesions are believed to eventually form gastrointestinal neoplasia (GIN) or microadenomas, microscopic areas of dysplasia. The continuous growth of these lesions results in the formation of macroscopic polyps termed macroadenoma or adenoma for short, characterized by grossly visible dysplastic epithelium that have not invaded through the muscularis mucosae[16,17]. Advancement of the adenoma growth through the muscular mucosae renders it an adenocarcinoma, the malignant and thus deadly stage of disease (Figure 1).

Apc mutant animal models for the study of CRC

Although the exact etiology for CRC is still elusive, several genetic mutations, both somatic and germline, as well as epigenetic changes have been linked to the development of this malignancy. In particular, patients with familial adenomatous polyposis syndrome (FAP) inherit a germline mutation in adenomatous polyposis coli (*APC*) gene in one allele. The loss of the second allele occurs within 30 years. As APC functions as a negative regulator of the Wnt signaling pathway, it controls the level of the active transcription factor β-catenin. The loss-of function mutation in the *APC* gene leads to accumulation of β-catenin within the nucleus, causing

uncontrolled induction of Wnt target genes and aberrant division of intestinal stem cells and IECs to form pre-cancerous cells and develop into microadenomas and adenomas[16]. Somatic mutation in *APC* is also commonly found in those with sporadic disease where the inactivation of *APC* gene occurs over time as a result of environmental exposures[18].

One of the first animal models of CRC was a randomly mutagenized mouse, carrying a mutation in the *Apc* gene that leads to expression of truncated form of APC protein[19]. The mutant mice spontaneously develop multiple intestinal neoplasia in the small intestine of the mice, from which the name Apc^{min} was given. While this first model involves *Apc* truncating mutation at codon 850, subsequent knock in mutations to introduce *Apc* truncations at codon 716 or 1638 resulted in a similar phenotype. The variation in truncating sites in the *Apc* gene was performed to test whether the shorter truncation in the $Apc^{min/+}$ model as compared to those seen in human patients altered the observed phenotype. Most of the various *Apc* truncating mutations resulted in overall similarity with polyp formation predominately in the small intestine of the mice except in a model where a frameshift at codon 1309, where polyps were distributed throughout the small intestine and colon, which more closely resemble the phenotype in patients who have colonic polyps as a result of *APC* LOH[20]. However, the $Apc^{min/+}$ model continues to be the primary model used in studies seeking to identify additional genes involved in intestinal tumorigenesis. Though the small intestine is the predominant location for adenoma formation in the $Apc^{min/+}$ mice, polyps form in the colon but less frequently[21]. However, high numbers

of microadenomas can be found in the colon of *Apc*$^{min/+}$ mice, which resemble those of the small intestine in that LOH of *Apc* and β-catenin nuclear accumulation are evident[22]. The *Apc*716 model demonstrated that the LOH of the *Apc* allele in proliferating cells located at the base of the crypt is the initiating step to aberrant crypt foci or early lesions in the mucosa[21]. Mice homozygous for the mutant *Apc*^{min} die during embryogenesis[22]. Additional evidence of APC interaction with microtubules and Rac-specific guanine nucleotide exchange factor Asef to regulate actin cytoskeletal rearrangement and cellular morphology supports the idea that APC is needed for proliferating cells to travel to the tip of the villus. Thus, the loss of APC in these cells would result in reduced Asef activity and decreased capacity to move and shed. Furthermore, APC interaction with proteins Asef2 and IQGAP1 also was reported to effect cell migration and polarity[21]. Additionally, mice heterozygous for *Apc*^{min} have displayed a gradual reduction in immature and mature T cells in the thymus and in immature and progenitor B cells in the bone marrow as well as a depletion of natural killer cells in the spleen. Further bone marrow transplant experiments revealed that this phenotype was due to an aberration in the nonhematopoietic compartment of the bone marrow of *Apc*$^{min/+}$ mice as a result of decreased mesechymal progenitor cell population where single mesenchymal precursors derived from *Apc*$^{min/+}$ mice displayed less colony forming units than that of wildtype mice[23].

The inability to maintain mucosal immunological homeostasis could influence the outcome of polyp formation in this model. In fact, not long after this study,

another group from MIT found that transferring wildtype CD4+CD25+ lymphocytes into the *Apc*$^{min/+}$ mice lessened tumor burden[24]. Based on these two studies, one could speculate that the depletion of thymocytes as *Apc*$^{min/+}$ mice age may result in reduced regulatory lymphocyte populations in the periphery tissues, specifically the small intestine where the maintenance of tolerance is compromised. By transferring CD4+CD25+ lymphocytes from interleukin (IL)-10 knockout mice, this study further showed that the IL-10 production by CD4+CD25+ cells was necessary for enhanced cellular apoptosis and diminished expression of cyclooxygenase- (COX-) 2 and proinflammatory cytokine genes within polyps of the *Apc*$^{min/+}$ mice[24]. A paper published in 2012 reported increased expression of several proinflammatory cytokines, including TNF-α, IL-6, and IL-1β, in the small intestine of older *Apc*$^{min/+}$ mice as compared to young *Apc*$^{min/+}$ mice, which is positively correlated with abundance of large polyps[25]. While the authors of this publication did not compare the levels of these proinflammatory mediators to wildtype animals, one could speculate that the loss of APC affects immunosuppressive mechanisms in the small intestine of the *Apc*$^{min/+}$ mice which may lead to a proinflammatory environment that favors the formation and growth of polyps.

The *Apc*$^{min/+}$ model has been used to identify several key players in the promotion and inhibition of intestinal adenoma development. Of particular importance is the proinflammatory enzyme COX-2, whose ablation reduces polyp formation in the *Apc*$^{min/+}$ model. Furthermore, *Cox-1* mutation in *Apc*$^{min/+}$ mice also causes reduction in polyp formation, similar to that of *Cox-2* deficiency. Further

studies demonstrate that both COX-1 and COX-2 stimulate angiogenesis in polyps by generating prostaglandin E2 (PGE2). COX-2 is expressed in both adenomatous polyps and malignant tumors and is now considered a common feature of tumors of the intestine. As a result of the findings from basic research, a COX-2 inhibitor, Celecoxib, has been developed and shown to significantly reduce the number of polys in FAP patients after six months of treatment[26]. However, some of the patients with sporadic disease treated with the COX-2 inhibitor in a later clinical trial suffered from cardiovascular side effects from the drug. As a result, physicians prescribing nonsteroidal anti-inflammatory drugs to patients must consider their level of risk for cardiovascular side effects and proceed with careful medical supervision[21]. In addition to *Cox-2*, the *BubR1* and *Cdx2* genes were identified as regulators of genomic stability in the *Apc*$^{min/+}$ and *Apc*716 models, respectively. Mutations in these genes resulted in higher numbers of intestinal polyps and rates of chromosomal instability in each respective model. The *Apc* models of CRC also gave insight into the effect of diet and exercise on the progression of disease. These models demonstrated that high fat diets accelerate with polyp formation while calorie-restricted diets significantly reduced polyp numbers. Exercise has also been shown to reduce polyp burden in the *Apc*$^{min/+}$ model, suggesting the need for dietary and exercise considerations in overall management of disease[21].

Apc mutant mice typically display only the formation of benign intestinal polyps that rarely advance to malignancy. This model was useful in identifying the gene *Smad4* as a player involved in progression of adenoma to adenocarcinoma.

Consistent with the involvement of Smad4 in TGF-β signaling, mice with Smad4 deficiency in the *Apc*$^{min/+}$ background display similarities to patients with colon cancer associated with TGF-β type II receptor mutations[21]. Phosphatidylinositol 3-kinase (PI3K)/Akt pathway has also been associated with colorectal cancer. *Apc*$^{min/+}$ mice with heterozygous mutation in the gene encoding PTEN, a negative regulator of PI3K pathway, development large invasive adenocarcinomas[21]. Similarly, invasion of polyps into the muscularis mucosae was observed in about half of a group of *Apc*$^{min/+}$ mice with *Ephb3* homozygous gene knockout[22].

Additional mouse models exist such as β-catenin mutant mouse model in recapitulating inherited disease syndromes which are less frequently used, likely due to greater percentage of sporadic colorectal patients, approximately 80 percent, who possess the *Apc* gene mutation as compared to 10 percent who carry mutation in β-catenin gene[21,27].

Inflammation and colon cancer

There was an early suggestion linking inflammation to cancer in the 19th century when pathologist Rudolf Virchow predicted that chronic inflammation and irritation may be a key player in cancer, an idea that was largely ignored as the main scientific focus was on intrinsic events within the premalignant cells that drive cancer development[28,29]. Most recently, many studies have provided evidence in support of the idea that cancer can evade immune destruction and is also stimulated by some inflammatory mediators or inflammatory disease conditions[16,28]. Now both cancer immune evasion and chronic inflammation have been included as hallmarks of

cancer[30]. Epidemiological studies over the last fifteen years have revealed an estimate of about 20 percent of cancer deaths occur in the context of inflammation and infection[28]. The idea of linking tumor formation and inflammation is particularly important in the intestine, where inflammatory disorders have been associated colorectal cancer. Increased risk for CRC has been observed in patients with chronic inflammatory diseases of the intestine, such as ulcerative colitis or chronic inflammatory bowel disease[31]. In fact, about 20 percent of patients with IBD develop colitis-associated cancer, a subtype of CRC that is fatal in more than 50 percent of these cases[16]. It has also been shown that an inflammatory component is involved in other types of CRC that lack grossly visible inflammation but have immune cell infiltrates and proinflammatory cytokine production within intestinal polyps[16]. In fact, the advancement of adenoma development in *Apc*$^{min/+}$ mice correlates with increased expression of proinflammatory mediators (Figure 2). As mentioned in a previous section, the use of the *Apc*$^{min/+}$ model identified that loss of *Cox-2*, an enzyme involved in promoting inflammation, reduced polyp numbers in the small intestine of mice. Similarly, *Cox-1* inhibition caused the same, suggesting that mediators of inflammation are involved in tumor development [16,21,31].

Regulation of inflammation and cancer by IL-10

One distinct feature of mucosal immunity as it compares to nonmucosal forms is that T cells of the gut have an activated or memory effector phenotype. They are poised for rapid induction of inflammation via cytokine production when necessary, a state that is tightly regulated by effector regulatory T cells in this environment that

are poised to suppress inflammation. These two mechanisms coexist, but the immunological environment at mucosal surfaces tends to be a default program of immunosuppression or tolerance. The T cells are designed to prevent active inflammation in response to commensals, which continuously interact with the surrounding epithelia[32,33].

One cytokine identified to have anti-inflammatory properties is IL-10. IL-10-deficient mice developed enterocolitis in the duodenum, jejunum, and colon, characterized by significant growth retardation and ultimately death. However, the inflammatory conditions of the *Il10* knockout mice were greatly attenuated when they were housed under specific pathogen free conditions, suggesting that IL-10 suppresses the immune response to intestinal antigens [34]. *Il10 receptor* knockout mice exhibited a similar phenotype, supporting the role of IL-10 in intestinal homeostasis[35].

Furthermore, *Il10* knockout weanlings, the age where gastrointestinal normal flora begin colonization, exhibited early signs of focal inflammatory lesions in the intestine which progresses to transmural inflammation, epithelial hyperplasia and then adenocarcinoma with age. Increased levels of proinflammatory cytokines, such as TNF-α, IL-6, IL-1β and IFN-γ, were present in the colons of IL-10 deficient mice as compared to wildtype mice. These sequelae were prevented in weanlings of *Il10* knockout mice who were treated with IL-10 intraperitoneally. While IL-10 had no statistically significant effect on the inflammation of adult mice, the IL-10 treatment did reduce the incidence of adenocarcinoma[36]. These early findings suggest that IL-

10 is required for maintaining intestinal homeostatic conditions and that its loss promotes intestinal inflammation and colorectal cancer. Further observations that colitis did not develop in IL-10-deficient mice treated with antibiotics or raised in a germ free environment corroborated these conclusions, demonstrating the role of IL-10 in suppressing immune cell reaction to intestinal microbiota[37].

A study using *Il10 green fluorescent protein* (*GFP*) reporter mice demonstrates that CD8+ intestinal epithelial lymphocytes (IELs) and CD4+ lymphocytes in the lamina propria cells are the major cells expressing IL-10[38]. In the same study, *in vivo* stimulation of IELs from the small intestine with anti-CD3 demonstrated that these cells were programmed to be IL-10 producing cells. Similarly, anti-CD3 stimulation of lamina propria lymphocytes induced a regulatory phenotype where GFP expression was observed. Both Foxp3+ Treg cells and IL-10-producing cells are responsible for homeostatic maintenance in the lamina propria while Foxp3- IELs assume this role in the epithelium demonstrated by IL-10-expressing GFP+ populations. Adoptive transfer of splenic CD4+ T cells to immunodeficient mice demonstrated that the gut microenvironment contributes to this phenotype where transferred cells found in the IEL compartment exhibited GFP expression after stimulation while those recovered from the spleen did not[38]. Furthermore, adoptive transfer of TCRαβ subpopulation of intestinal IEL into severe combined immunodeficiency mice prior to the induction of chronic colitis demonstrated that intestinal IELs suppress intestinal inflammation in an IL-10-dependent manner[39].

TBK1 structure and regulation

The serine/threonine protein kinase TBK1 is involved in several signaling pathways such as immune response to pathogen recognition, autophagy, cell survival and growth and oncogenesis[40]. Because of its molecular structure, its ubiquitous expression pattern, TBK1 is thought to serve as an important signal transducer, connecting various upstream signals to downstream biological processes[40]. It possesses a catalytic kinase domain (KD) at its N-terminus that interacts with its ubiquitin-like domain (ULD) and alpha helical scaffold dimerization domain (SDD) (Figure 3)[41,42]. Nearly full-length x-ray crystallography and TBK1 protein purification revealed that TBK1 exists in an homodimer conformation where KD are outward on opposite sides of the complex in the inactive form[41,42]. KD and SDD are conjugated with K63-linked ubiquitin chains at Lys 30 and Lys 401, respectively, which is a necessary modification for its activation[43]. An x-ray crystal structure from another group revealed that the KD of the active form of TBK1 is repositioned to perform its catalytic functions while remaining in dimer formation and keeping the C-terminus domain (CTD) facing away from the main body of the dimer. This configuration also allows for trans autophosphorylation between TBK1 dimers, resulting in phosphorylation of Ser172 in the activation loop of the KD domain[41]. In addition to mediating homodimerization of TBK1, the SDD also is required for substrate phosphorylation and has been speculated to facilitate adaptor protein recruitment needed for regulating substrate specificity[43,44]. Dimerization is not required, however, for adaptor protein interactions[41]. The CTD has been described

as an adaptor-binding motif involved in the recruitment of TBK1 to various other signaling mediators[45]. The adaptor-binding motif of TBK1 allows it to interact with a variety partners to transduce a signal within a cell[40]. Furthermore, adaptor proteins containing ubiquitin domains can bind to TBK1 via polyubiquitin chains, but the specificity of TBK1 binding to its substrates is likely dependent upon its cellular localization[40,46]. Cellular localization of TBK1 also regulates its activation by different stimuli. In response to upstream signals, TBK1 is recruited, by adaptor proteins, to specific signaling complexes, in which the concentrated TBK1 may be activated by autophosphorylation or phosphorylation by upstream kinases[40]. TBK1 also contains leucine zipper and helix-loop-helix motifs within the SDD region, although functions of these motifs are less well defined[45].

A major class of TBK1 stimuli is the pathogen-associated molecular patterns (PAMPs), which are components of various microorganisms such as DNA, single- and double-stranded RNA, and surface glycoproteins. PAMPs initiate innate immune responses through stimulation of pattern recognition receptors (PRRs). Several PRRs are able to target the activation of TBK1 and induce type I interferon production; these include the TRIF-dependent TLRs (TLR3 and TLR4), the NLR member NOD2, the intracellular RNA sensor RIG-I, and the intracellular DNA sensor STING. The activation and signaling function of TBK1 involve its recruitment to the PRR adaptors, such as TRIF (TLR/IL-1R domain-containing adaptor protein inducing IFN-β), MAVS (mitochondrial antiviral signaling proteins), and STING (stimulator of IFN genes). Upon activation by the PRRs, TBK1 phosphorylates IRF3, triggering the

dimerization and nuclear translocation of this anti-viral transcription factor and allowing IRF3 to induce expression of the type I interferon genes (Figure 3)[47]. While IRF3 is the most widely recognized substrate of TBK1, many others have been identified, including the interferon-responsive transcription factor IRF7, NF-κB members (p65 and c-Rel), signaling adaptors (TANK, MAVS, STING, and TRIF), kinases (NIK, AKT, IKKα, IKKβ, and NEMO), E3 ubiquitin ligases (PELI1 and XIAP), autophagy receptors (OPTN and p62), and the exocyst component Sec 5 in RalB signaling[40],[48,49].

As seen with other kinases, TBK1 activation is subject to control by negative regulators. One such TBK1 regulator is protein phosphatase Mg^{2+}/Mn^{2+}-dependent 1 B (PPM1B or PP2Cβ), which binds and dephosphorylates TBK1 at Ser172 and, thereby, inhibits virus-induced IRF3 phosphorylation and IFN-β expression[50]. Inositol 5' phosphatase SHIP1 (Src homology 2 domain-containing protein tyrosine phosphatase 1) has also been implicated as a negative regulator of TBK1; SHIP1 deficiency in macrophages resulted in hyperphosphorylation of TBK1 even under unstimulated conditions and TLR3-stimulated IFN-β production[51]. The authors though did not present evidence describing the mechanism and therefore it remains unknown whether SHIP1 directly or indirectly regulates TBK1 activity. Another phosphatase, SHIP2, inhibits TBK1 activation and IFN-β production by directly binding to the N terminal KD region of TBK1 and acting independently of the phosphatase activity of SHIP2[52].

As previously mentioned, ubiquitination of TBK1 plays an important role in its activation. Ubiquitin ligase Nrdp1 directly binds and polyubiquitinates TBK1 in macrophages after TLR stimulation, leading to IRF3 activation[47]. Conversely, the function of TBK1 is negatively regulated by deubiquitinases, proteases that cleave ubiquitin chains. The deubiquitinase CYLD has been shown to interact with TBK1 and removes K63-linked ubiquitin chains from it, resulting in reduced TBK1 kinase activity and IRF3 phosphorylation as well as downregulated type I IFN expression[53,54]. A20 is another deubiquitinase known to regulate TBK1 activation. A20 functions as a ubiquitin-editing complex, composed of A20, Tax1 binding protein 1 (TAX1BP1), and A20 binding inhibitor of NF-κB 1 (ABIN1), which negatively regulates TBK1 activation antiviral response by disrupting the association of TBK1 with its upstream activator TRAF3[47]. A similar function has also been demonstrated for the RING Finger Protein 11 (RNF11), which binds to TBK1 via TAX1BP1 and inhibits TBK1 activation and virus-induced IFNβ expression by blocking the association of TBK1 with TRAF3 and TBK1 K63 ubiquitination[55]. TBK1 is also negatively regulated through K48 type of ubiquitination, which targets TBK1 for proteasomal degradation, an event typically observed at longer time points likely involved in the resolution of a viral induced-inflammatory response. E3 ligases DTX4 and TRIP have been identified as mediators of this process[47].

TBK1 as a mediator of multiple signaling pathways

TBK1, also termed T2K[56] or NAK (NF-κB-activating kinase), was initially identified in a two-hybrid screen as a protein that interacts with TANK, a regulator of

NF-κB signaling pathway, and was proposed by Joel Pomerantz and David Baltimore at that time to mediate TANK-dependent NF-κB activation[18,57]. *Tbk1* deletion in mice results in embryonic death due to liver apoptosis and failure, a phenotype similar to mice deficient in other mediators of the NF-κB signaling pathway[56,58]. TBK1 was initially thought to serve as an upstream kinase of the classical IkB kinase (IKK) IKKβ; however, later studies demonstrated a dispensable role for TBK1 in the activation of IKK and NF-κB[57,58]. It is now clear that the canonical function of TBK1 is to phosphorylate and activate IRF3, mediating type I interferon induction during viral infection[58]. However, more recent studies have led to the identification of additional targets of TBK1 in various other signaling pathways. For example, TBK1 mediates CD40 and BAFF receptor-induced NIK degradation and negatively controls noncanonical NF-κB activation, a function that is crucial for maintaining normal production of the antibody IgA[48]. TBK1 also mediates proteolysis of AKT and negatively regulates the activation of the metabolic kinase mTORC1 by T-cell receptor, thereby modulating the activation and migration of T cells.[59] In cancer cells, TBK1 may play a role in mediating the expression of survival genes through activation of NF-κB family members, such as c-Rel and p65[45,60]. It is anticipated that additional signaling targets of TBK1 will be identified in normal and cancer cells.

TBK1 in the regulation of immune responses

Although TBK1 is expressed ubiquitously in numerous cell types, much of our knowledge about its functions comes from studies involving cells of the immune

system. It is well supported by both *in vitro* and *in vivo* studies that activated TBK1 targets IRF3 and IRF7 for phosphorylation and activation in response to TLR or nucleic acid sensor stimulation, resulting in the production of type I interferons necessary for an antiviral response (Figure 4). TBK1-mediated IRF3 regulation is also essential for preventing *de novo* viral replication *in vivo*[58].

Using B cell-conditional *Tbk1* knockout mice, our laboratory has revealed a new role for TBK1 in negatively regulating IgA antibody class switching by targeting the phosphorylation and degradation of NF-κB-inducing kinase (NIK), a key mediator of the noncanonical NF-κB signaling pathway[48]. The B cell-conditional *Tbk1* knockout mice had elevated levels of serum IgA and autoantibodies as well as antibody deposition to the kidney glomeruli, associated with nephropathy-like symptoms. Upon stimulation by some of the IgA inducers, such as stimuli of CD40 and BAFF receptor, the TBK1-deficient B cells have hyper-activation of noncanonical NF-κB as a result of increased NIK protein level. Thus, TBK1 controls the fate of NIK and the magnitude of noncanonical NF-κB activation in B cells to modulate antibody responses[48] (Figure 5).

TBK1 also plays a role in regulating T-cell activation and migration[59]. Mice with T cell-specific *Tbk1* ablation have increased frequency of T cells with activated effector- or memory-like surface markers, indicative of aberrant activation under homeostatic conditions. However, in a central nervous system (CNS) autoimmune inflammation model, the TBK1-deficient effector T cells display a defect in migration from the draining lymph nodes to CNS. Consequently, the T cell-conditional *Tbk1*

knockout mice are refractory to the induction of experimental autoimmune encephalomyelitis, an animal model for human multiple sclerosis. While previous studies suggest a role for TBK1 in activating AKT via direct phosphorylation and promoting human cancer cell survival[49,61,62], genetic ablation of *Tbk1* in T cells unexpectedly causes enhanced activation of AKT and its downstream target mTORC1[48,60,6159]. It appears that TBK1-mediated AKT phosphorylation serves as a trigger for AKT degradation (Figure 6). Ablation of one allele of *Akt*, to reduce its level of expression in TBK1-deficient mice, restores the ability of their T cells to migrate to CNS and renders them sensitive to EAE induction[59].

TBK1 in autophagy

The process of autophagy occurs as a means to recycle damaged proteins or cellular organelles in order to generate energy for the cell or to remove a molecular threat during starvation states. Autophagy can also occur in response to microbial infection as part of an innate immune response where an autophagosome forms around the bacteria to prevent their replication and possibly induce their destruction. This process involves ubiquitination of intracellular bacteria, a modification that recruits the Ubiquitin-binding autophagic adaptor protein optineurin (OPTN) and, thereby, triggers the assembly of the autophagic machinery. TBK1 has been implicated as an important regulator of autophagy responses to bacterial infections, in which TBK1 acts by phosphorylating OPTN and promoting its interaction with autophagic components, particularly Atg8[63]. Additional studies suggest that TBK1 also promotes the maturation of the autophagosome in macrophages during

bacterial infection by phosphorylating the autophagy adaptor sequestosome 1 (also called p62), which facilitates bacterial clearance[32]. These findings demonstrate another mechanism of action for TBK1 in the regulation of immune responses.

TBK1 in oncogenesis

One of the first clues of TBK1's potential involvement in cancer was presented in 2006 by the groups of Ulrich Brinkmann and Ira Paston who performed a high throughput screening using various cDNA expression libraries that revealed a potential role for TBK1 and IRF3 in regulating angiogenesis[64]. Overexpression of *TBK1* or its target transcription factor IRF3 induce secreted factors that promote the proliferation of human umbilical vein endothelial cells (HUVEC), a frequently used marker for the study of angiogenesis. In line with this finding, TBK1 expression is induced under hypoxic conditions[64], a physiological state within tumor microenvironment that promotes angiogenesis within solid tumors[65]. Some solid tumors, such as human breast and colon cancer, have been shown to have upregulated *TBK1* expression, although the significance of this finding warrants further studies since the data are quite variable among cancer patients[64].

Shortly thereafter, Michael White's group reported that *TBK1* downregulation by RNAi promotes apoptosis in HeLa, PANC-1 and MCF7 human cancer cell lines *in vitro* through its activity downstream of the Ras-like protein RalB[66]. RalB, a kinase implicated in tumorigenesis-associated processes[45,67,68], can activate TBK1 *in vitro*, signaling its interaction with downstream Sec proteins of the exocyst[44,66,6766]. This sequence of events is needed for the induction of oncogenic transformation by

Ras[45,66]. Specifically, TBK1-deficient mouse embryonic fibroblast (MEF) cells could not undergo transformation and eventually died after retroviral infection with mutant $KRAS^{G12V}$ as compared to wildtype MEFs that were transformed and grew in culture[66]. A few years later, William Hahn and Tyler Jack's group performed a screen in 19 cell lines that possessed either KRAS wildtype or mutant gene using RNA interference libraries targeting cell signaling mediators such as protein kinases, phosphatases and oncogenes. The screen revealed TBK1 as a synthetic lethal partner in *KRAS* mutant human lung cancer cell lines. Specifically, this paper showed that *in vitro* downregulation of *TBK1* using short hairpin (sh) RNAs resulted in decreased cell survival of lung cancer cells dependent upon KRAS. Additional experiments from this paper showed that knockdown of *TBK1* in *KRAS* mutant human lung cancer cell lines resulted in decreased tumor size over time in xenograft models using immunocompromised mice while human lung cancer lines exhibiting wildtype *KRAS* exhibited either increase or no difference in xerograph tumor growth after *TBK1* downregulation as compared to mice injected with *GFP* shRNA control[60].

The data from these high profile papers led to advanced studies in delineating mechanisms by which TBK1 promotes survival in human cancer cell lines. Using *in vitro* models, TBK1 was found to engage with and activate AKT after $KRAS^{G12V}$ transformation in a stimulant-dependent and -specific manner, thus promoting tumor cell survival [62]. It has also been suggested that TBK1 promotes human lung cancer cell survival through its regulation of autophagy, a cellular process that involves the lysosomal degradation of intracellular organelles and proteins to generate

macromolecules needed for cell survival and metabolism during starvation or to maintain intracellular integrity of proteins and organelles for proper functioning[69,70]. Similar to previous models, *TBK1* knockdown in A549 human lung cancer cells using RNA interference *in vitro* resulted in reduced punctate accumulation of microtubule-associated protein 1B light chain 3 (LC3B), an autophagosomal indicator of autophagy induction, which was associated with reduced nuclear translocation of RelB using immunofluorescent imaging. The authors proposed a model that TBK1 participated in the autophagic process in KRAS mutant human lung cancer cells thus leading to non-canonical NF-κB signal induction promoting cell survival or proliferation[69], although direct evidence is lacking for the latter. It is also remains unclear how autophagy is directly regulated by TBK1 in this model.

With the use of quantitative mass spectrometry as an approach to study protein phosphorylation, Eric Haura's research team identified over 2000 alterations in phosphorylation in nearly 400 proteins after *TBK1* knockdown in human A549 lung cancer cell line[71]. From this large number, the authors focused on diminished phosphorylation observed in the mitotic regulator polo-like kinase (PLK) 1 after *TBK1* RNAi. *In vitro* assays demonstrated that TBK1 binds to and phosphorylates PLK1 at Thr-210 during mitosis. In addition, the authors determined a correlation between cell viability after *TBK1* knockdown and cell viability after PLK1 pharmacological inhibition[71]. While the authors independently confirmed previous reports that *TBK1* knockdown in A549 cells reduces cell viability and separately demonstrated that treatment of lung cancer cells *in vitro* with PLK1 inhibitors decreased cell survival, it

remains to be determined whether TBK1-mediated PLK1 phosphorylation has a direct link with cancer cell survival[71].

While the study of the role of TBK1 in cancer has so far focused on KRAS-dependent lung cancer cells, a more recent work examined TBK1 using human breast cancer cell lines and suggested the involvement of TBK1 in mediating breast cancer resistance to tamoxifen treatment[72]. TBK1 binds and phosphorylates estrogen receptor alpha (ERα) at serine 305 in MCF7 breast cancer cell line, thereby affecting ERα's transcription activity. RNAi-mediated TBK1 silencing in MCF7 cells results in slower growth of the cell line, whereas TBK1 overexpression in MCF7 cells renders the cells more resistant to tamoxifen treatment. Immunohistochemical analyses revealed elevated expression of TBK1, as compared to normal tissue, and positive correlation of TBK1 expression with the expression and Ser-305 phosphorylation of ERα. The higher TBK1 expression is also associated with poorer disease-free survival in patients treated with tamoxifen, although this correlation is not seen in patients who are not treated with tamoxifen. These findings suggest that TBK1 may have a role in mediating breast cancer tamoxifen resistance[72].

Despite the many studies that demonstrate the association of TBK1 with cancer, a more recent work failed to demonstrate the requirement of TBK1 in cancer cell survival by using large panel of human cancer cell lines and similar experimental approaches employed by the others[73]. However, while the previous studies relied on a single or limited number of *TBK1* shRNAs, this later study used six different *TBK1* shRNAs targeting different coding and 3' untranslated regions. Although the *TBK1*

shRNA used previously (shT17) did reduce the viability of cancer cells, many other *TBK1* shRNAs did not produce this phenotype, despite their high efficiency in *TBK1* knockdown. Furthermore, overexpression of *TBK1* in the shT17-knockdown cells failed to rescue cell viability but restored the phosphorylation of IRF3, a primary substrate of TBK1[73]. These results suggest the possibility that some of the previous observations may have been due to off-target effect of the *TBK1* shRNAs. Consistently, treatment of cancer cell lines with three different TBK1 inhibitors efficiently inhibited IRF3 phosphorylation with only minimal effect on cell viability. Moreover, no correlation could be demonstrated between the degree of Ras activity in the cell lines and sensitivity to the inhibitors. Overall, the authors concluded that the growth or survival of KRAS-dependent cancer cell lines is not entirely TBK1-dependent[73]; thus creating controversy regarding this topic and raising the questions of whether and how TBK1 regulates cancer development and whether its function depends upon the type of tumor.

TBK1's role in colon cancer is unknown

A prior study revealed that colon tumor samples taken from patients display different patterns of TBK1 expression. Although some tumor samples have higher levels of TBK1 expression than normal tissue, some other tumor samples have greatly suppressed TBK1 expression[64]. These findings indicate the potential involvement of TBK1 in CRC pathogenesis. Of note, *TBK1* is localized to human chromosome 12q14.1[74,75], a region associated with chromosomal abnormalities such as deletions, inversions, duplications, insertions, and translocations in pancreatic,

ovarian, skin, breast, and prostate cancers and pulmonary chondroid hamartomas[73,7476-78]. Similarly, one report identified chromosome 12q14.1 copy-number losses in salivary duct carcinoma using a single-nucleotide polymorphism microarray platform[79]. Of particular interest, putative shallow deletions and gains of *TBK1* accounted for 20 percent and 30 percent of adenocarcinoma tissue samples sequenced from the large intestine of patients within validated and provisional datasets of The Cancer Genomics Atlas (TCGA) respectively[80,81] (Figure 7). The datasets are made publicly available through TCGA consortia using www.cbioportal.org that contain comprehensive large-scale genomic, transcriptomic and epigenomic profiling of various cancers including colorectal cancer [80,81]. In addition, point mutations were found in *TBK1* in nearly two percent of patient samples sequenced from adenocarcinoma tissues of the large intestine deposited in Catalogue of Somatic Mutations in Cancer (COSMIC) [82,83] (Figure 3; Table 2). These mutations were dispersed through all domains of *TBK1* (Figure 3; Table 2), all of which are necessary for its specific function[41-43,84]. Based on these findings, we hypothesized that TBK1 might play a role in intestinal tumorigenic processes *in vivo*, and we examined this hypothesis in this dissertation using a novel animal model.

Figure 1. Multiple factors play a role in colorectal cancer development.

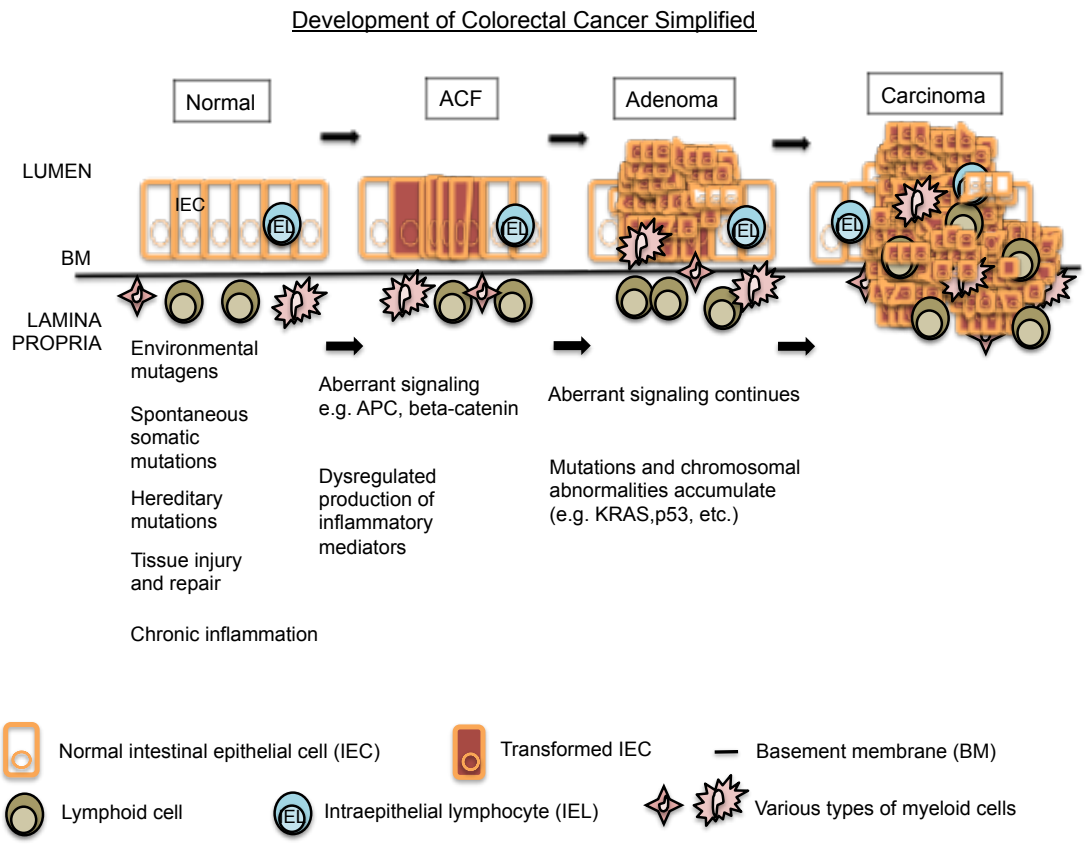

Figure 1. Multiple factors play a role in colorectal cancer development.

As a result of some genetic and/or environmental changes including hereditary and somatic mutations, injury and/or chronic inflammatory disease, aberrant crypt foci (ACF) form and accumulate within the intestinal epithelium. As abnormal cell signaling and diminished cellular protective functions such as DNA repair continues, adenomas form. The disease advances to carcinoma when the adenomas invade through the basement membrane (BM) into nearby tissues and lymph nodes. This stage of development is driven by the accumulation of mutations and chromosomal abnormalities and altered microenvironment. Advancement of the disease results in malignancy whereby cancer cells metastasize into distant tissues, organs and lymph nodes. Malignancy may result in death for patients with CRC.

Figure 2. Disruption of the immunological balance in the gut contributes to intestinal adenoma development.

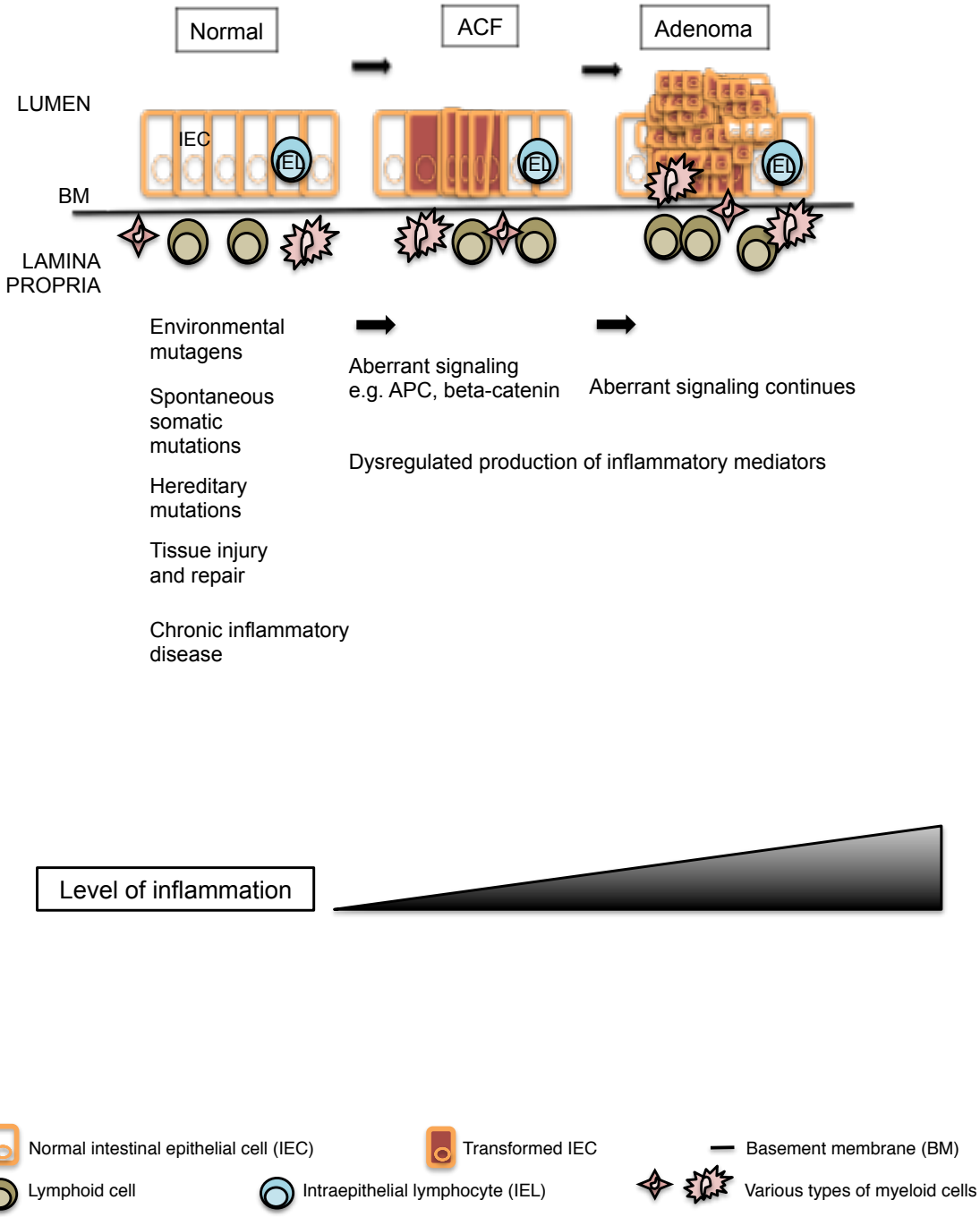

Figure 2. Disruption of the immunological balance in the gut contributes to intestinal adenoma development. Illustration of the relationship between intestinal tumorigenesis and inflammation. Disruption of intestinal epithelial cell homeostasis during the initiation and progression of intestinal adenoma development alters the behavior of intestinal immune cells, which influences disease progression.

Figure 3. Structure of TBK1 indicating point mutations identified in adenocarcinomas sampled from CRC patients.

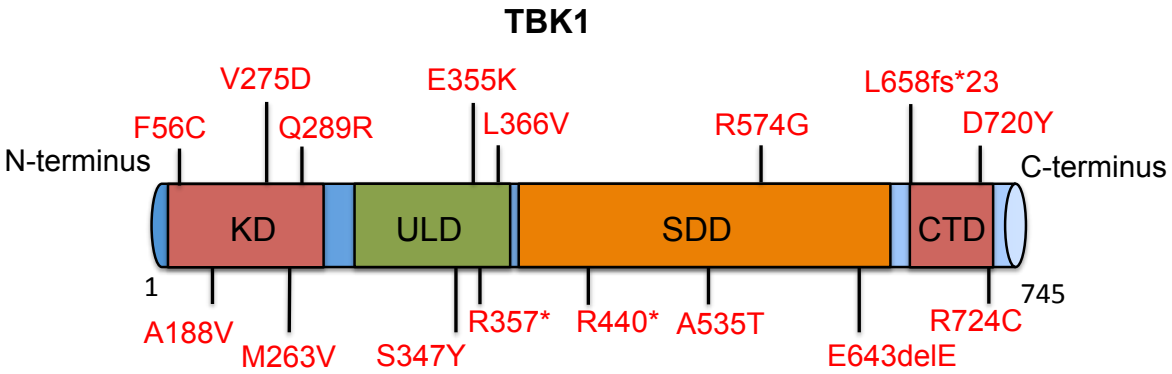

KD = kinase domain
ULD = ubiquitin-like domain
SDD = helical scaffold dimerization domain
CTD = C-terminal domain

Figure 3. Structure of TBK1 indicating point mutations identified in adenocarcinomas sampled from CRC patients.

Schematic of the structure of TBK1 indicating point mutations identified in almost two percent of 1,226 CRC patient tumor samples sequenced from adenocarcinoma tissues of the large intestine (deposited in Catalogue of Somatic Mutations in Cancer). These mutations, including truncating mutations (*) and frame-shift (fs) insertions and deletions (del), were located in the kinase domain (KD), ubiquitin-like domain (ULD), the helical scaffold dimerization domain (SDD) and the C-terminal domain (CTD), all of which are necessary for proper function of TBK1.

Figure 4. TBK1 regulates type I interferon innate immune response.

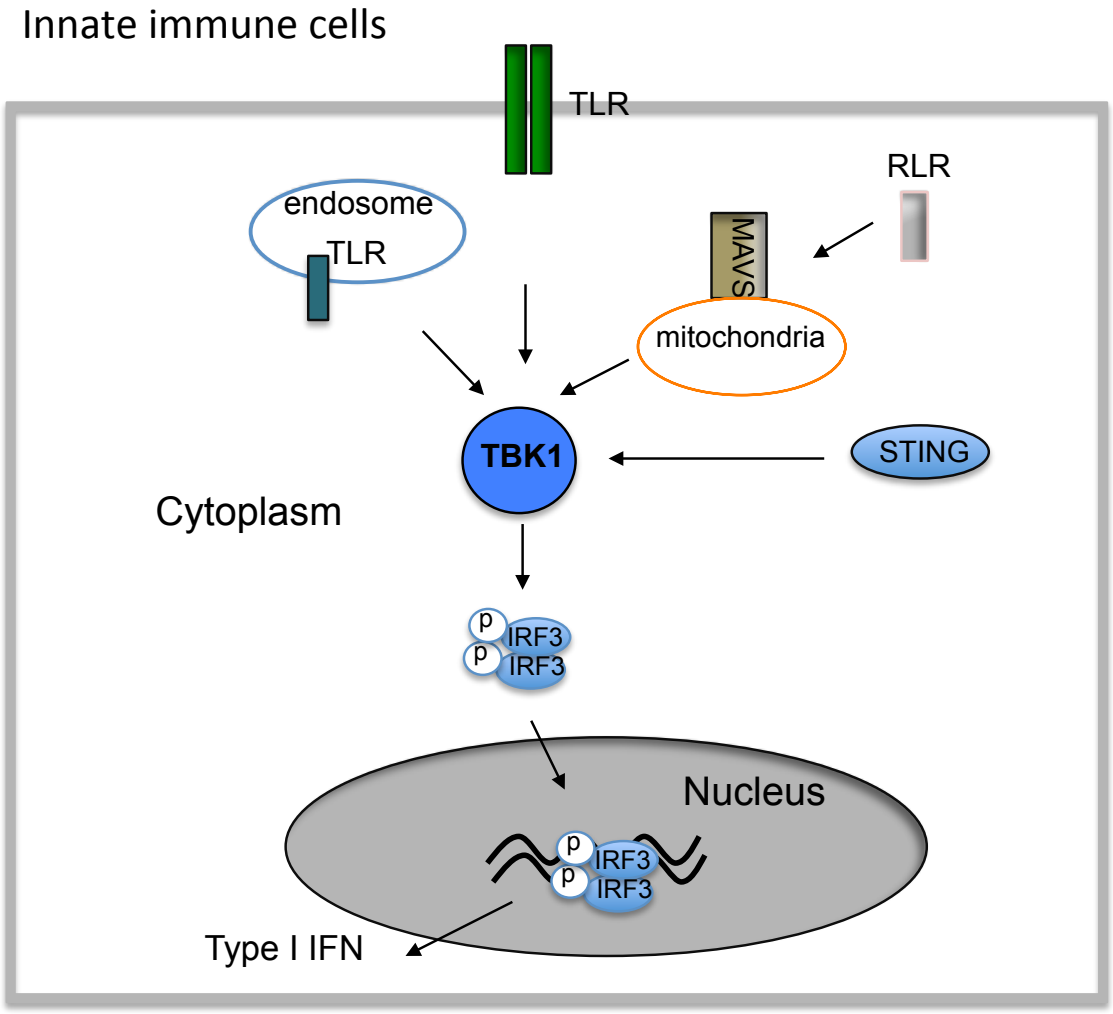

Figure 4. TBK1 regulates type I interferon innate immune response.

TBK1 mediates type I interferon expression upon PRR stimulation of innate immune cells by phosphorylating transcription factor IRF3. This leads to subsequent nuclear translocation dimerized IRF3 and activation of type I interferon gene expression.

Figure 5. TBK1 negatively regulates noncanonical NF-κB signaling and IgA production in B cells.

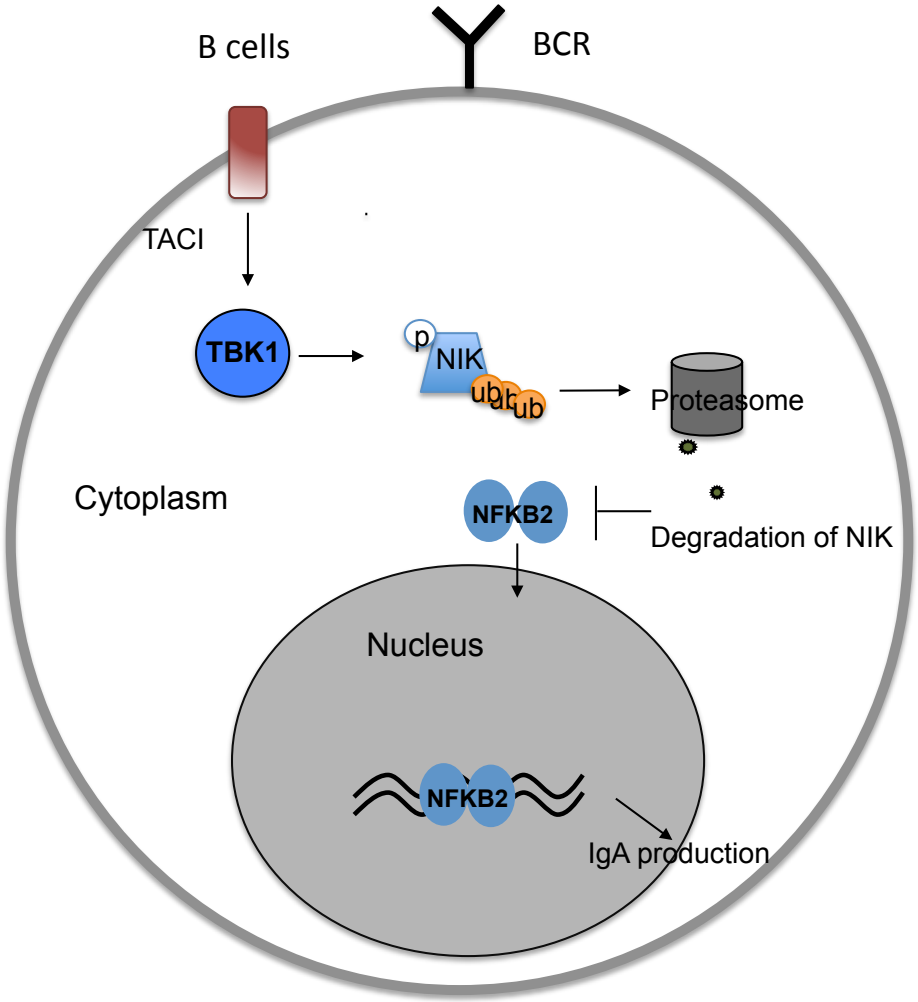

Figure 5. TBK1 negatively regulates noncanonical NF-κB signaling and IgA production in B cells.

In B cells, TBK1 negatively regulates IgA antibody class switching upon stimulation of TACI or BAFF receptor. TBK1 controls B Cell antibody responses by targeting the phosphorylation and degradation of NF-κB-inducing kinase (NIK), a key mediator of the noncanonical NF-κB signaling pathway.

Figure 6. TBK1 regulates T cell activation and egress from the lymph nodes by regulating AKT.

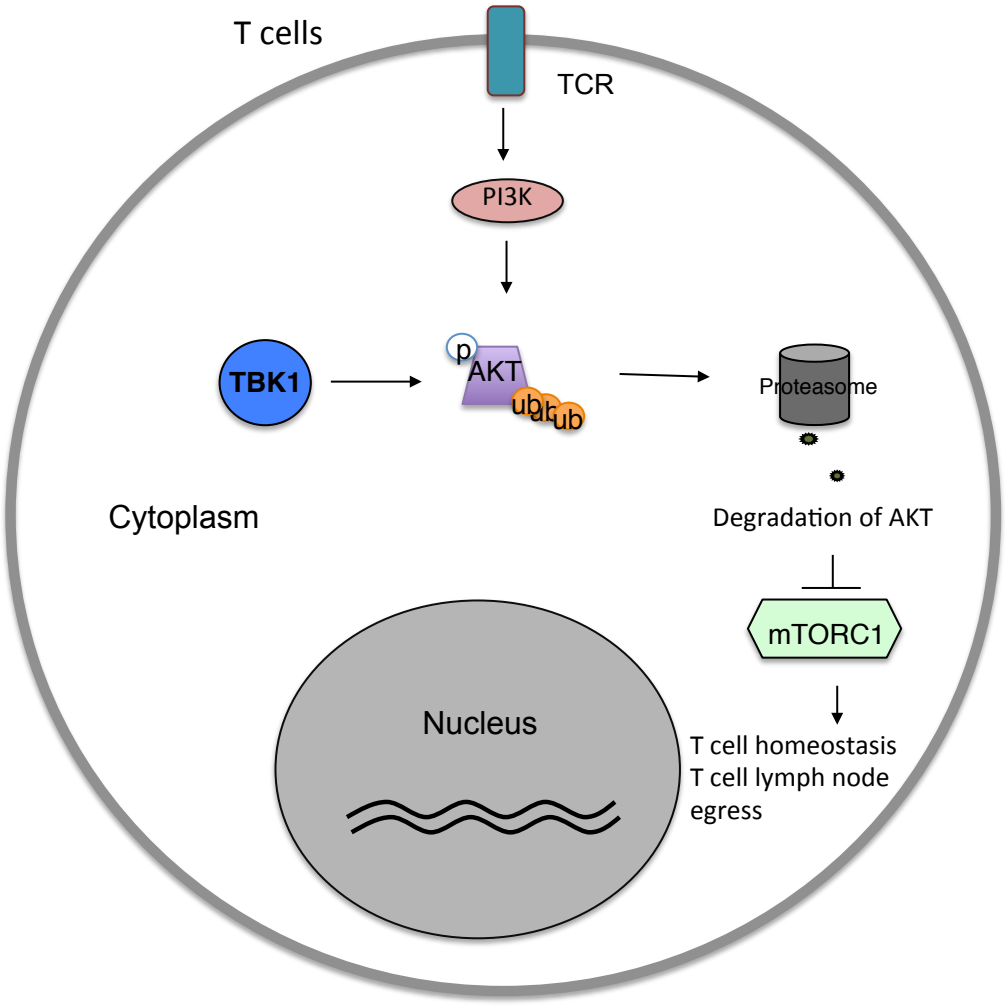

.

Figure 6. TBK1 regulates T cell activation and migration by regulating AKT.

In T cells, TBK1 regulates T cell activation and egress from lymph nodes to the central nervous system under inflammatory conditions. The TBK1 controls T cell migration from lymph nodes by targeting AKT for phosphorylation and degradation thus regulating downstream mediators such as mTORC1 involved in T cell egress.

Figure 7. Percentage of putative shallow deletion, diploid, gain and amplification of *TBK1* copy-number identified in adenocarcinomas sampled from CRC patients profiled in validated and provisional datasets of TCGA.

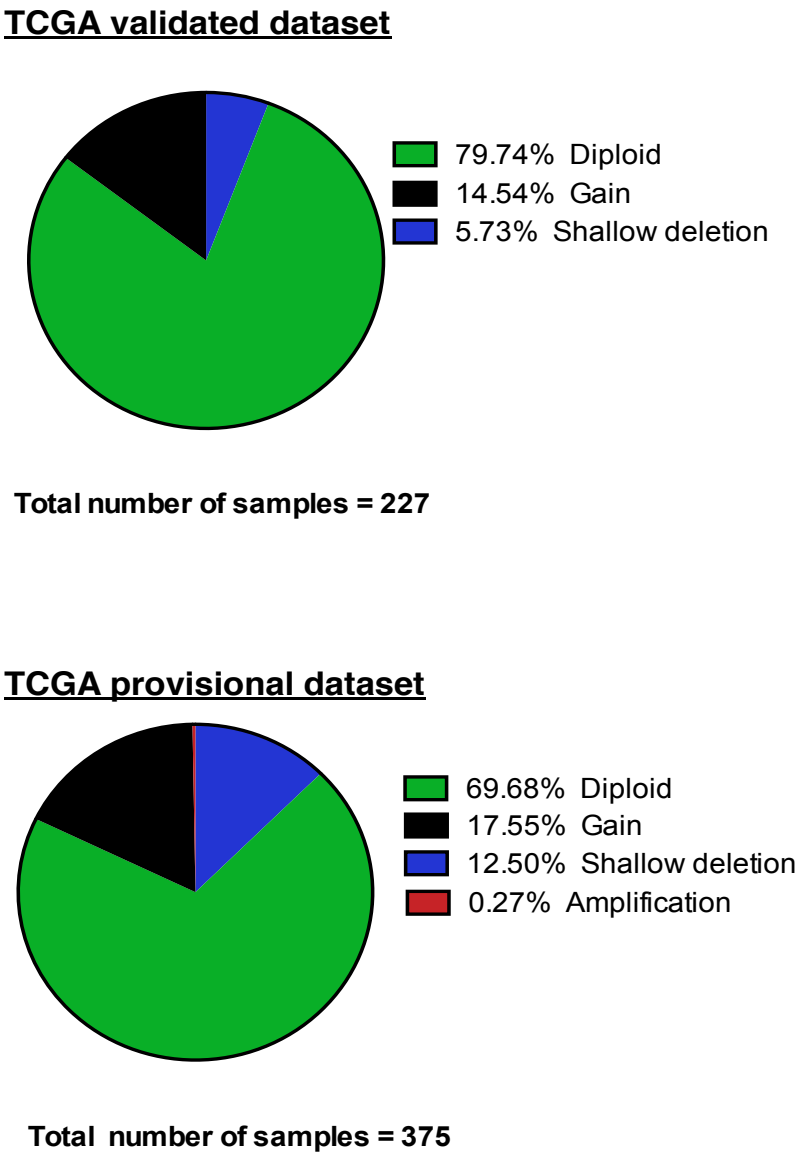

Figure 7. Percentage of putative shallow deletion, diploid, gain and amplification of *TBK1* copy-number identified in adenocarcinomas sampled from CRC patients profiled in validated and provisional datasets of TCGA.

Putative shallow deletions gains of *TBK1* accounted for 20 percent (top) and 30 percent (bottom) of adenocarcinoma tissue samples sequenced from the large intestine of patients within validated (top) and provisional (bottom) datasets of The Cancer Genomics Atlas (TCGA) respectively. The datasets are made publicly available through TCGA consortia using www.cbioportal.org.[80,81]

CHAPTER 3: INTESTINAL EPITHELIAL CELL-SPECIFIC TBK1 INHIBITS INTESTINAL ADENOMA GROWTH IN *APC*$^{MIN/+}$ MICE

Chapter 3: Intestinal epithelial cell-specific TBK1 inhibits intestinal adenoma growth in *Apc*$^{min/+}$ mice

Introduction

Colorectal cancer (CRC) is a major cause of cancer morbidity and mortality whereby almost 150,000 people are diagnosed per year and approximately one-third of individuals will die from disease per year in the United States alone. Worldwide, it affects almost 1.2 million people such that it is the third most common cancer diagnosed in women and men[2,85]. Globally, almost 600,000 persons die from colon cancer each year, which makes it one of the leading causes of cancer-related deaths for men and women combined[2]. Since the prognosis of CRC is still poor, it is critical to understand the process of intestinal tumor development and progression.

It is generally believed that CRC development results from dysregulated signaling events in IECs, causing out-of-control growth and/or survival and subsequent transformation of these cells. Several risk factors have been associated with CRC, including somatic and germline mutations, chronic intestinal inflammation, diet and lifestyle. For example, when the normal epithelium of the gut encounters inflammation, environmental mutagens including reactive oxygen and nitrogen species, tissue damage and repair, and/or inherited mutations within the intestine, cellular signaling pathways are induced in order to maintain or return the gut to homeostatic state. When these protective mechanisms are altered such that they do not properly function, adenoma formation eventually may occur and pose the risk for colorectal malignancies[16,86]. Understanding the biology and cellular mechanisms that

are involved in this early stage process is important for improving the approaches for CRC prevention and treatment.

The Wnt signaling pathway has been closely linked to the tumorigenic process in the gut. A central regulator of the Wnt pathway is the tumor suppressor adenomatous polyposis coli (APC), which functions by targeting the transcription factor β-catenin for proteolysis. Abnormal activation of the Wnt signaling pathway has been frequently observed in both hereditary and sporadic colorectal cancers and is often attributed to the loss-of-function mutations of *APC* or activating mutations in the transcription factor β-catenin[87]. A mouse model, $Apc^{min/+}$, has been frequently used in the study of CRC. The $Apc^{min/+}$ mice carry a heterozygous mutation in the *Apc* gene that leads to APC truncation[19]. This mouse model is particularly useful for the identification of novel factors involved in the regulation of intestinal tumorigenesis.

The serine/threonine protein kinase TBK1 is involved in several signaling pathways such as pathogen recognition and immune response, inflammatory response and Ras-dependent oncogenesis[40]. The current literature using human lung and breast cancer cell lines implicates TBK1 as having oncogenic activity[60,66,72]. Specifically, these *in vitro* studies and xenograft mouse models proposed that TBK1 supports cell survival of KRAS-driven lung cancers and tamoxifen-resistant breast cancers[60,66,72]. However, a more recent independent study challenged the conclusions of these studies, stating that TBK1 is dispensable for cancer cell survival[73]. The *in vivo* function of TBK1 in regulating intestinal tumorigenesis has not

yet been explored. By generating intestinal epithelial cell (IEC)-conditional *Tbk1* knockout mice, the present study addresses the role of TBK1 specifically in intestinal tumor development. Our work unexpectedly demonstrated a role for TBK1 to suppress intestinal tumorigenesis in the *Apc*$^{min/+}$ mice.

Results

IEC-specific *Tbk1* ablation promotes adenoma formation in *Apc*$^{min/+}$ mice.

To study the role of TBK1 in the gut, we generated IEC-conditional *Tbk1* knockout (hereafter called *Tbk1*$^{IEC\text{-}KO}$) mice by crossing mice with *Tbk1 lox*P-flanked (floxed) alleles with mice expressing Cre under the control of *villin* promoter (*villin*-Cre) (Figure 8A-C). Western blot demonstrates the loss of TBK1 protein from isolated primary IECs in the *Tbk1*$^{IEC\text{-}KO}$ (Figure 8C). The *Tbk1*$^{IEC\text{-}KO}$ mice appeared normal in growth and survival (data not shown). Based on gross examination, the IEC-specific *Tbk1* ablation did not appreciably alter the number (Figure 8A) or size of Peyer's patches in the small intestine. Histology analyses based on hemotoxylin and eosin (H&E) staining also did not reveal noticeable inflammation or tissue damage in the small intestines (Table 1) (Figure 9C and D).

We next crossed the *Tbk1*$^{IEC\text{-}KO}$ mice with the *Apc*$^{min/+}$ mice to examine the role of TBK1 in regulating intestinal adenoma development (Figure 8D). Western blot demonstrates the loss of TBK1 protein from isolated primary IECs in the *Apc*$^{min/+}$*Tbk1*$^{IEC\text{-}KO}$ mice (Figure 8E). Loss of TBK1 in IECs of *Apc*$^{min/+}$ mice resulted in increased polyp formation in the small intestines as compared to *Apc*$^{min/+}$ mice at four months of age (Figure 10A-B, D). Such a phenotype was detected in both the

distal and proximal regions of the small intestine of the *Apc*$^{min/+}$*Tbk1*$^{IEC\text{-}KO}$ mice, although the distal region had a more profound increase in the number of polyps (Figure 10B). These results suggest that the IEC-specific TBK1 plays a suppressive role in intestinal tumorigenesis. In addition to polyp number, polyp size was larger in *Apc*$^{min/+}$*Tbk1*$^{IEC\text{-}KO}$ mice compared to age-matched (four months) *Apc*$^{min/+}$ mice (Figure 10C). The effect of TBK1 deficiency on adenoma size was observed mainly in medium-sized adenomas. At an older age (six months), the *Apc*$^{min/+}$*Tbk1*$^{IEC\text{-}KO}$ mice also formed large multifocal adenomas in the distal region of the small intestine, which was not observed in the control *Apc*$^{min/+}$ mice (Figure 10E). These findings suggest a role for the IEC-specific TBK1 in negatively regulating the formation or growth of adenomas.

Since the distal region of small intestine, covering the ileum, has more abundant Peyer's patches and more diverse and abundant microbiota, we speculate that the promotion of tumor growth in this region might be due to the inflammatory nature of this environment, an idea which we are currently exploring.

Young *Apc*$^{min/+}$*Tbk1*$^{IEC\text{-}KO}$ mice exhibit earlier polyp formation as compared to *Apc*$^{min/+}$ mice.

To assess the mechanism by which TBK1 regulates intestinal adenoma formation, we examined whether the loss of TBK1 had an effect on the early stage of polyp formation. We analyzed the polyps in young *Apc*$^{min/+}$ and *Apc*$^{min/+}$*Tbk1*$^{IEC\text{-}KO}$ mice. Higher numbers of polyps were found in *Apc*$^{min/+}$*Tbk1*$^{IEC\text{-}KO}$ mice as early as six weeks of age (Figure 11A). However, the TBK1 deficiency did not significantly alter

the number of microadenomas (Figure 11B and C). Thus, it is likely that TBK1 regulates the growth, rather than initiation, of the intestinal adenomas in the *Apc*$^{min/+}$ mice.

TBK1 deficiency does not influence the proliferation of IECs or adenoma cells

To examine whether TBK1 regulates the proliferation of normal IECs or adenoma cells, we performed *in vivo* cell proliferation assays based on bromodeoxyuridine (BrdU) incorporation. Six-week old *Apc*$^{min/+}$ and *Apc*$^{min/+}$*Tbk1*$^{IEC\text{-}KO}$ mice were injected with BrdU intraperitoneally, and BrdU incorporation was assessed by immunohistochemical assays using an anti-BrdU antibody. We did not observe obvious differences in BrdU incorporation in normal mucosa between the *Apc*$^{min/+}$*Tbk1*$^{IEC\text{-}KO}$ and *Apc*$^{min/+}$ mice (Figure 11D-E). These animals also did not show significant differences in BrdU incorporation within their microadenomas (Figure 11F-G). In addition to BrdU incorporation, we examined the proliferative effects of the TBK1 deficiency by immunocytochemistry staining with Ki67, a commonly used indicator for cells in the state of proliferation. Immunohistochemical analyses did not reveal appreciable differences in the frequency of Ki67+ cells in either the normal tissue or larger adenomas between four month old *Apc*$^{min/+}$ and *Apc*$^{min/+}$*Tbk1*$^{IEC\text{-}KO}$ mice (Figure 12A-C).

TBK1 deficiency likely promotes cell survival of intestinal microadenomas

We examined the role of TBK1 in regulating apoptosis using a TUNEL assay that detects fragmented DNA in apoptotic cells**.** Analyses of the *Apc*$^{min/+}$ and *Apc*$^{min/+}$*Tbk1*$^{IEC\text{-}KO}$ intestinal tissues did not reveal major differences in the frequency

of TUNEL positive apoptotic cells in the normal mucosa (Figure 13A-B). Interestingly, analyses of TUNEL positive cells in microadenomas from *Apc*$^{min/+}$*Tbk1*$^{IEC\text{-}KO}$ intestinal tissues revealed a trend toward enhanced cell survival as compared to *Apc*$^{min/+}$ mice (Figure 13C-D). Because we did not achieve statistical significance with $p = 0.07$ (Figure 13D) using the arbitrary threshold of $p < 0.05$, we can not exclude the possibility that the observed difference may be due to chance. However, if we test with a less stringent threshold of 10 percent significance, then the difference of TUNEL positive cell frequency between the microadenomas in *Apc*$^{min/+}$ and *Apc*$^{min/+}$*Tbk1*$^{IEC\text{-}KO}$ may achieve statistical significance. Additionally, if we consider the 90 percent confidence intervals of 2.5 to 0.13 for these data, then it is likely that IEC-specific *Tbk1* deletion promotes cell survival in microdadenomas in *Apc*$^{min/+}$ mice. Further analyses are needed to make more solid conclusions. Additional sections of microadenomas will be analyzed to increase the number of observations per group. Furthermore, given that IEC-specific *Tbk1* ablation promotes enlargement in medium-sized tumors, we will assess the apoptotic indexes of medium sized tumors from *Apc*$^{min/+}$ and *Apc*$^{min/+}$*Tbk1*$^{IEC\text{-}KO}$.

IEC-specific *Tbk1* ablation does not cause visible intestinal inflammation

Recent findings have revealed a complex relationship between inflammation and cancer, suggesting that the immune response can both suppress and promote tumor development[16,88]. More recently, intestinal chronic inflammatory diseases have been identified as a risk factor for colon cancer[89,90]. Under normal conditions, the immune system does not mount strong responses to commensal microbes, which is

important for the maintenance of intestinal immune homeostasis and prevention of inflammation. Impaired barrier function or innate immune function in intestinal epithelia may cause bacterial invasion and chronic inflammation. Since TBK1 has been implicated in the regulation of innate immunity and inflammatory processes[40,72], we examined whether *Tbk1* ablation in IECs might impair immune homeostasis and cause intestinal inflammation.

To determine if TBK1 in IECs plays a role in immune homeostasis in the gut, we sacrificed wildtype and *Tbk1*$^{IEC-KO}$ mice and resected the colons and small intestines to count the number of Peyer's patches in the small intestine. Both the small intestine and colons were formalin-fixed, cut and H&E stained. We examined the colonic tissues and counted the number of colonic lymphoid follicles visible in two bi-level sections of swiss-rolled tissues. We observed no significant difference in the number of Peyer's patches nor colonic patches between *Tbk1* wildtype and *Tbk1*$^{IEC-KO}$ mice (Figure 9A-B). With the assistance of a pathologist, we blindly scored the tissues based on the presence of immune cells within the mucosa, submucosa, and/or transmural and on the extent of the mucosal damage (Table 1). We observed no overt histological difference in inflammation between *Tbk1* wildtype and *Tbk1*$^{IEC-KO}$ mice (Figure 9C-D). These data suggest that IEC-specific *Tbk1* deletion alone in the IECs does not impair immune homeostasis nor lead to spontaneous inflammation in the gut.

Intestinal tumorigenesis may be promoted by altered production of pro- versus anti-inflammatory cytokines without overt histological inflammation[91].

Therefore, we tested whether the TBK1 deficiency caused low-grade inflammation within the intestine by analyzing gene expression of inflammatory mediators using real-time quantitative PCR (qPCR). We detected the expression of pro- and anti-inflammatory cytokines, chemokines and cell markers such as *Tnfα*, *Il1β*, *Il17a*, *Il17f*, *Il10*, *Il12p35*, *Ccl2*, *Cox2*, *Foxp3*, *Tgfβ*, and interferons (IFNs) including *Ifnα*, *β* and *γ* by performing qPCR. These inflammatory mediators have previously been identified to play a role in tumor development. There was no detection of significant difference in any of these inflammatory proteins in *Tbk1*$^{IEC\text{-}KO}$ as compared to wildtype mice (Figure 14). Taken together, these data suggest that *Tbk1* deletion alone in IECs does not appreciably alter inflammatory environment in the gut nor does it spontaneously induce polyp formation even after aging the mice for one year (Figure 9D).

***Tbk1* ablation in IECs does not promote inflammation or adenoma formation in a chemically induced colitis-associated tumor model.**

Severe colitis can be induced by interrupting the epithelial barrier using chemicals, such as dextran sodium sulfate (DSS). The DSS-induced colitis has been frequently used for the study of inflammation and inflammation-associated cancer. DSS damages the colonic epithelial cell barrier thus inducing an immune response to the colonic microbes mediated by innate immune cells[70]. We treated *Tbk1*$^{IEC\text{-}KO}$ and wildtype mice with DDS for either five or seven days with two-day water recovery period (Figure 15A). The mice were weighed once per day during this treatment period and sacrificed at day two after DSS treatment. We observed no difference in

the weight or the histological score between wildtype and *Tbk1*$^{IEC-KO}$. Both groups of mice exhibited similar levels of decreased weight loss and colonic inflammation after treatment (Figure 15B-F).

To test the role of IEC-specific TBK1 in colitis-associated colon cancer, we treated wildtype and *Tbk1*$^{IEC-KO}$ mice with a single dose of azoxymethane (AOM), a genotoxic colon carcinogen, and several cycles of DSS and water[92] (Figure 16A). Consistent with the results obtained in mice treated with DSS alone, the IEC-specific TBK1 deficiency did not alter the level of inflammation in mice treated with DSS along with AOM, as shown by the similar level of bodyweight loss and colon shortening in the wildtype and *Tbk1*$^{IEC-KO}$ mice (Figure 16B and D). We also observed no difference in the number of polyps formed in the colons of wildtype and *Tbk1*$^{IEC-KO}$ mice (Figure 16C). Therefore, we hypothesize that TBK1 functions in IECs through another mechanism, possibly by modulating the adaptive immune cell component in the intestines. It is also possible that in our model, TBK1 in IECs may exert its functions in the context of *Apc* mutations.

The effect of TBK1 deficiency on adenoma formation is diminished in the absence of lymphocytes

To examine the role of adaptive immune system in regulating adenoma formation in *Apc*$^{min/+}$ and *Apc*$^{min/+}$*Tbk1*$^{IEC-KO}$ mice, we crossed these mice with *Rag1* knockout mice lacking mature T and B lymphocytes, key cellular mediators of the adaptive immune system[93]. We crossed *Apc*$^{min/+}$ *Tbk1* IEC mouse model with *Rag1* knockout mice. The small intestines of the mice were resected, fixed and counted for

number of polyps at age 2.5-3 months. As expected, *Apc*$^{min/+}$*Tbk1*$^{IEC\text{-}KO}$ mice had a substantially higher number of polyps than *Apc*$^{min/+}$ *Tbk1* mice under lymphocyte-competent conditions (Figure 17). When crossed to the *Rag1* knockout background, the number of polyps was greatly enhanced in both *Apc*$^{min/+}$*Tbk1*$^{IEC\text{-}KO}$ and *Apc*$^{min/+}$ mice (Figure 17), likely due to the loss of the immunosuppressive Treg cells and/or IELs[38, 39]. Moreover, under these lymphocyte-free conditions, the TBK1 deficiency only had a moderate, and statistically insignificant, effect on polyp formation.

The results described above suggest that TBK1 may regulate an aspect of adaptive immune homeostasis that is masked by the loss of Treg and other lymphocytes in the *Rag1* knockout conditions. We first examined the effect of TBK1 on immune homeostasis by analyzing the intestinal immune cell composition, specifically lymphocytes in addition to innate immune cells. We resected the small intestines of young mice and isolated both intestinal IELs and the lamina propria cells[94]. The *Apc*$^{min/+}$*Tbk1*$^{IEC\text{-}KO}$ and *Apc*$^{min/+}$ mice had a comparable frequency of TCRβ+ or γδTCR+ T cells (Figure 18 A-B; Figure 19 A-B) and myeloid CD11c+ and/or CD11b+ cells (Figure 18 C-D) in either the lamina propria or IEL compartments of the small intestine. The expression levels of *Foxp3*, a marker for Treg cells, were also similar between *Apc*$^{min/+}$*Tbk1*$^{IEC\text{-}KO}$ and *Apc*$^{min/+}$ mice (Figure 18E). These results suggest that loss of TBK1 in IECs does not alter the immune cell composition in the intestinal tissue, raising the question of whether the TBK1 deficiency may cause abnormal function of the intestinal lymphocytes.

TBK1 deficiency in the IECs of *Apc*$^{min/+}$ mice inhibits *Il10* production in the intestine

Although IEC-specific *Tbk1* deletion alone does not alter the expression of cytokines in the intestine (Figure 14), it remains possible that TBK1 plays a role in regulating cytokine protein in the context of *Apc* mutation. This possibility was suggested by the profound effect of TBK1 deficiency on adenoma formation in the *Apc*$^{min/+}$ mice. We therefore tested *Apc*$^{min/+}$ mice the effect of TBK1 deficiency in IECs on the expression of various cytokines and chemokines involved in the inflammatory process and cancer (Figure 20A). Because of the crucial role of TBK1 in regulating type I interferon induction, we also included interferon-responsive genes, such as *Il10*, *Cxcl11*, *Cxcl9*, *Cxcl10*, and *Irf7*, which have been shown to be effected by the loss of TBK1 in innate immune cells. In addition, we examined the β-catenin target genes *Axin2* and *Lgr5*, to assess the possible role of IEC-specific TBK1 in regulating Wnt signaling pathway, as well as genes involved in host defense (*Reg3β* and *muc2*). We quantitatively analyzed the expression of these genes from intestinal tissues of young 3.5-4 week old *Apc*$^{min/+}$ and *Apc*$^{min/+}$ *Tbk1*$^{\text{IEC-KO}}$ mice presumably before microscopic adenoma formation. Interestingly, the IEC-specific TBK1 deficiency in *Apc*$^{min/+}$ mice significantly inhibited the gene expression of the anti-inflammatory cytokine *Il10* in the intestine, although the expression of the rest of the genes was comparable between the *Apc*$^{min/+}$ and *Apc*$^{min/+}$ *Tbk1*$^{\text{IEC-KO}}$ mice (Figure 20A). *Il10* expression levels are sustained in mice after sole IEC-specific deletion of *Tbk1* or sole *Apc*$^{min/+}$ genotype (Figure 20B). Given the crucial role for IL-10 in

suppressing intestinal tumorigenesis, this finding provides important insights into the mechanism by which TBK1 regulates adenoma formation in the *Apc*$^{min/+}$ mice.

IEC-specific TBK1 regulates IL-10 production by IELs

As mentioned in Chapter 2, IECs can secrete cytokines and chemokines to initiate a mucosal immune response upon detection of commensal and pathogenic antigens, guiding homeostasis within the environment[14]. While there is little evidence of IECs expression of *Il10 in vivo*, it has been shown that human IECs can produce this anti-inflammatory cytokine *in vitro*[95,96]. In addition, IECs may stimulate IL-10 production by macrophages and lymphocytes, but the underlying mechanism has not been defined[97]. A large source of IL-10 in the intestine is produced by the IELs, although some cell types of the lamina propria (e.g. macrophages, dendritic cells, and regulatory T cells) can also produce IL-10[12,38]. In fact, intestinal IELs suppress chronic intestinal inflammation in an IL-10-dependent manner.[39] Therefore, analyzed *Il10* expression in highly purified IECs, intestinal epithelial lymphocytes, and lamina propria cells of the *Apc*$^{min/+}$ and *Apc*$^{min/+}$ *Tbk1*$^{IEC\text{-}KO}$ mice. To our surprise, the IEC-specific *Tbk1* knockout did not affect *Il10* expression in the IECs but impaired the *Il10* expression in IELs (Figure 21A-B). This effect was specific, since the TBK1 deficiency did not affect *Il10* expression in the lamina propria cells (Figure 21C). This finding supports the previous *in vitro* finding that IECs stimulate IL-10 production in lymphocytes and establishes TBK1 as an important factor mediating this crosstalk *in vivo*.

Discussion

The data presented in this study show that TBK1 functions in IECs to inhibit intestinal adenoma growth in *Apc*$^{min/+}$ mice. Loss of TBK1 in IECs of *Apc*$^{min/+}$ mice resulted in increased polyp formation in the small intestines, a phenotype observed as early as six weeks of age. The increase in polyp number in the *Apc*$^{min/+}$*Tbk1*$^{\text{IEC-KO}}$ mice was seen in both the proximal and distal regions of small intestine, but this phenotype was more pronounced in the distal region. Polyp size was greater in the *Apc*$^{min/+}$*Tbk1*$^{\text{IEC-KO}}$ mice as compared to *Apc*$^{min/+}$ mice, specifically in the medium sized adenomas.

TBK1 has previously been shown to be important in regulating the immune response by mediating type I interferon production, IgA production, and T cell activation and migration[48,59,98]. In addition, previous *in vitro* studies using human lung and breast cancer cell lines implicate TBK1 to have tumor-promoting activity[45,60,62,66,72]. TBK1 knockdown promotes apoptosis and reduces xenograft tumor growth of KRAS-dependent lung cancer cells but not of KRAS-independent tumor cell lines[60]. TBK1 appears to also contribute to the resistance of breast cancer cells to tamoxifen resistance[72]. However, a more recent publication challenged some of these findings and suggest that some of the phenotypes of TBK1 knockdown cancer cell lines may be due to off-target effect of the TBK1 shRNAs[73]. In addition to the controversy, the previous work also had several limitations in addressing the cancer-regulatory function of TBK1. First, the use of mouse xenograft models, which rely on immunodeficient recipient mice, excludes the contribution of immune system,

a major component of the tumor microenvironment that regulates tumor growth and progression. Second, since human cell lines often have accumulated genetic alterations, the cell line studies cannot assess the role of TBK1 in regulating the early-stages of tumorigenesis. Furthermore, the use of shRNA-mediated knockdown approach or pharmacological inhibitors of TBK1 have the issue of specificity due to off-target effect shRNAs and pharmacological inhibitors. Our conditional *Tbk1* KO mouse model allowed us to study the *in vivo* role of TBK1 during the early stages of intestinal tumorigenesis in immunocompetent mice. With our new approach, we discovered an unexpected function of TBK1 in suppressing the formation of intestinal adenoma, an early stage of CRC development.

Within the mucosa, IELs, predominately CD8+ T cells, are interspersed throughout and in direct contact with the epithelial cell layer; this puts them along with the IECs at the forefront of the intestinal immune response. As part of the mucosa, the lamina propria, which lies beneath a basal membrane under the IEC and IEL layers, defines a compartment for heavily infused circulating immune cells particularly T lymphocytes including effector T cells and Treg cells, macrophages, plasma cells, eosinophils, and mast cells. The IECs can express immunological mediators to help guide the appropriate response to commensal microbes or pathogens, a delicate balance required to achieve homeostasis within the environment[14]. We found that TBK1 in IECs function to regulate *Il10* expression in IELs to produce IL-10 during the early stages of the tumorigenic process, which is illustrated in a schematic in Figure 22. Previous studies showed that IL-10-deficient

mice developed enterocolitis in the duodenum, jejunum, and colon and that *Il10* knockout weanlings, the age where gastrointestinal normal flora begin colonization, exhibited early signs of focal inflammatory lesions in the intestine which progresses to transmural inflammation, epithelial hyperplasia and then adenocarcinoma with age[34,36]. Higher levels of proinflammatory cytokines such as TNF-α, IL-6, IL-1β and IFN-γ were present in the colons of IL-10-deficient mice as compared to wildtype control mice. These sequelae were prevented in weanlings of *Il10* knockout mice when treated with IL-10 intraperitoneally such that the incidence of adenocarcinoma in these mice was reduced[36]. These early findings suggest that IL-10 is required for maintaining intestinal homeostatic conditions and its loss can lead to intestinal inflammatory disease and colorectal cancer. Impaired IL-10 production in the intestine is also linked to enhanced intestinal tumorigenesis in other knockout mouse models crossed with the *Apc*$^{min/+}$ mice[91]. Thus, our finding that TBK1 deficiency in IECs inhibits IL-10 production provides mechanistic insight into the role of TBK1 in regulating intestinal adenoma formation.

We demonstrated that the tumor-regulating function of TBK1 is diminished when the *Apc*$^{min/+}$*Tbk1*$^{\text{IEC-KO}}$ mice were crossed to the lymphocyte-deficient *Rag1* knockout background. Under these conditions, the number of polyps was greatly increased in both the *Apc*$^{min/+}$ and *Apc*$^{min/+}$*Tbk1*$^{\text{IEC-KO}}$ mice. Since *Rag1* knockout mice lack both conventional T cells and Treg cells, it is likely that the lack of immunosuppressive Treg cells may contribute to an inflammatory environment that promotes tumor formation[33-86]. Indeed, transfer of wildtype Treg cells into the *Apc*$^{min/+}$

mice reduces tumor burden[24]. More importantly, the tumor-suppressing function of Treg cells requires their production of the immunosuppressive cytokine IL-10[24]. Of note, intestinal IELs suppress intestinal inflammation in an IL-10-dependent manner[39]. Our finding that TBK1 regulates *Il10* expression in the intestine thus has important implications. Although TBK1 does not seem to regulate *Il10* expression in Treg cells, the IEC-specific TBK1 is required for IL-10 production by another major source of IL-10 producing cells, the IELs. Additional studies are required to elucidate the mechanism underlying this novel and intriguing function of TBK1. One hypothesis is that TBK1 may regulate the production of a secreted factor(s) in IECs, which in turn stimulate the IELs for IL-10 expression.

Clinical Importance

As previously mentioned in Chapter 2, the localization of human chromosome 12q14.1, the region where *TBK1* lies, is associated with chromosomal abnormalities in cancers including in pancreatic, ovarian, skin, breast, prostate, and salivary duct cancers and pulmonary chondroid hamartomas[74-79]. Of particular interest, shallow deletions and gains of *TBK1* accounted for 20 percent and 30 percent of adenocarcinoma tissue samples sequenced from the large intestine of patients within validated and provisional (Figure 7) datasets of The Cancer Genomics Atlas (TCGA) respectively. Publicly available through TCGA consortia using www.cbioportal.org, these datasets contain comprehensive large-scale genomic, transcriptomic and epigenomic profiling of various cancers including colorectal cancer [80,81]. The copy numbers of *TBK1* significantly correlated with *TBK1* mRNA

expression in these samples (Figure 23A), where *TBK1* mRNA expression significantly decreased or increased in samples with putative shallow deletions or gains as compared to diploid *TBK1* copy-number respectively (Figure 23B). However, neither *TBK1* copy number nor mRNA expression levels significantly correlated with the overall survival of these patients (Figure 24). However, analysis of *TBK1* mRNA expression levels within different stages of colorectal cancer, from stage I through stage IV, revealed a significant correlation between *TBK1* mRNA expression in tumors sampled during stage IIIC and the overall survival of those patients (Figure 25 A-B). During stage IIIC of disease, the cancer has grown through the outer layers of the intestine into the visceral peritoneum and has spread to nearby lymph nodes but has not yet reached nearby tissues or distant organs[99]. In addition, a moderately high correlation existed between *TBK1* mRNA expression in tumors during early stage of disease to *TBK1* mRNA expression in tumors during later stages (Figure 25 C), suggesting a strong relationship between the degree to which *TBK1* is expressed in early staged tumors and in later stages as the cancer progresses.

Further analyses using these profiles were performed to determine the clinical relevance for the role of TBK1 in colon cancer. Similar to the trends found with *TBK1* mRNA expression using TCGA data were trends found with expression of *APC*, *TP53*, *KRAS*, and *PIK3CA* genes (Figure 26), well-known regulators of the tumorigenic process[17,30,87,100,101]. In fact, *APC*, *TP53*, *KRAS*, and *PIK3CA* are among the top five most frequently mutated genes, with a frequency of mutation at

61 percent, 43 percent, 34 percent, and 16 percent respectively in the validated dataset of TCGA (Figure 26A). Although copy numbers of these genes - *APC*, *TP53*, *KRAS*, and *PIK3CA* - significantly correlated with its respective mRNA expression (Figure 26B) as did *TBK1* copy number and its mRNA expression (Figure 23A), no correlations were found between the copy number (Figure 27A) or mRNA expression levels (Figure 27B) of either gene and the overall survival of the patients as observed with TBK1 and overall survival irrespective of disease stage (Figure 24). This suggest that the correlation between patient overall survival and gene expression of recurrently mutated genes may not be sufficient to predict its role in cancer development.

As an important signal transducer in various downstream biological processes, TBK1 function is dependent upon its molecular structure as well as its expression pattern[40]. Interestingly, point mutations in *TBK1* were found in approximately two percent of the large intestinal genomic profiles from 1,226 patient tumor samples deposited in Catalogue of Somatic Mutations in Cancer (COSMIC)[82,83]. Twenty-two different *TBK1* mutations (Table 2) in these patient samples included missense, nonsense and synonymous substitutions as well as frame-shift deletion and insertion, and in-frame deletion and were relatively dispersed throughout the KD, ULD, SDD and CTD of *TBK1* with missense mutations accounting for the majority (Table 2; Figure 3; Figure 28). Mutationassessor.org software offered by cBio@MSKCC uses evolutionary conservation patterns of intra- and interspecies homologues in families and sub-families empirically to predict the impact of amino acid substitutions on protein function. With this software, functional

impact scores are calculated using multiple sequence alignments, with the assumption that protein function is likely affected by specific substitutions of conserved residues[102]. To predict the functional impact of the missense *TBK1* mutations listed in Table 2, each mutation was assessed using the algorithm provided. Only two of the 14 missense mutations were classified as a "medium" level of functional impact, predicting that these mutations may alter the function of TBK1 (Table 2). Both of these mutations, F56C and A188V, were localized within the catalytic and activation loops of the KD of *TBK1* respectively. A change in conserved residues within these loops could potentially alter the function of TBK1 since the structural configuration of these loops within the KD influence the activation state of TBK1[41]. Experimental validation is needed to test this prediction.

Almost half of missense mutations found in *TBK1* were given a "low" score for functional impact, predicting that these specific mutations would have no influence on TBK1 function (Table 2). These mutations were primarily localized within the ULD and SDD of TBK1. Each domain of TBK1 influences its context-specific function[41-43,84]. Particularly, the ULD of TBK1 interacts with its own KD and SDD and is required for the full activity of TBK1 KD; this is critical for the regulation of IFN-inducible gene transcription during an immune response[42,84]. Furthermore, the ULD and KD of TBK1 interact with the SDD of the other TBK1 subunit in the dimer, while the CTD serves as a binding site for several adaptor proteins involved in TBK1-mediated signal transduction[41-43,103]. These intricacies in the structure of TBK1 become particularly important as we determine the functional implications for *TBK1*

sequence alterations revealed in the TCGA and COSMIC databases. For example, mutationassessor.org predicted that E355K substitution would not influence the function of TBK1 (Table 2). However, E355 is a key residue at the ULD interface that participates in TBK1 homodimerization. TBK1 E355A, R357D, and E355A/R357D double mutations disrupted the activation of TBK1 and downstream signaling events, which diminished TLR-induced type I interferon gene expression *in vitro* [43]. These findings support the need for experimental validation of all predicted outcomes of amino acid substitutions determined by mutationassessor.org, including TBK1 E355K. While mutationassessor.org is limited to predicting the effect of missense mutations, one could predict that nonsense mutations such as *TBK1* R357* found in the COSMIC database (Table 2) may alter the activity of TBK1 given that R357D mutation impaired its function and truncation within the ULD would likely alter TBK1 homodimerization, activation and substrate specificity [41-43,84].

The molecular structure, the subcellular localization, the specificity of binding partners and substrates, and the expression pattern directs the activity of TBK1 in various cellular processes[40]. Further analyses of colorectal cancer patient profiles from TCGA using www.cbioportal.org indicated a strong relationship between the expression of TBK1 and other well-known factors involved in colorectal cancer initiation and progression, including APC, KRAS, and PIK3CA (Figure 29). *TBK1* mRNA expression highly and significantly correlated with the *APC*, *KRAS* and *PIK3CA* mRNA expression - three of the top five genes most frequently mutated in colorectal cancer patient samples (Figure 26A). Our *in vivo* model presented earlier

in this chapter revealed that TBK1 functions in IECs to inhibit intestinal adenoma growth in *Apc*$^{min/+}$ mice (Figure 10), a model of early staged disease[19]. Our *Tbk1* IEC conditional knockout model provides a mechanism that explains the strong positive association between *TBK1* and *APC* gene expression gleaned from the transcriptomic profiles from TCGA (Figure 29). A significantly strong positive association also existed between *TBK1* and *KRAS* and *TBK1* and *PIK3CA* gene expression. The question still remains whether TBK1 negatively regulates intestinal adenoma growth in KRAS or PIK3CA mutant backgrounds. Furthermore, TCGA patient sample data revealed a positive correlation between the mRNA expression of *TBK1* and *IL10* (Figure 30), which is consistent with the results of our *in vivo* model where IEC-specific deletion of *Tbk1* diminished *Il10* expression in the intestine. Taken together, these data support the clinical relevance of our model, providing a mechanism for the link between APC, TBK1 and IL-10 during intestinal adenoma development.

The findings presented in this chapter illustrate the role of TBK1 during early stage develop of intestinal adenomas. Because TBK1 currently serves as an attractive target in the discovery of anti-inflammatory and anti-cancer therapeutics where its pharmacological inhibitors are now readily available, the findings of the present study could have significant impact in the field. It suggests the need for careful consideration regarding the context in which TBK1 functions, which would ultimately aide in the selection of treatment modalities and preventative strategies for patients and influence the outcomes of treatments used to target this protein kinase.

My project studies suggest a need for careful consideration in the selection of treatment modalities targeting TBK1 in cancer patients of other tissue types as it is possible that long term use of TBK1 inhibitor could possible increase the risk for adenoma growth in the intestine.

Figure 8. Generation of intestinal epithelial cell conditional *Tbk1* mouse model.

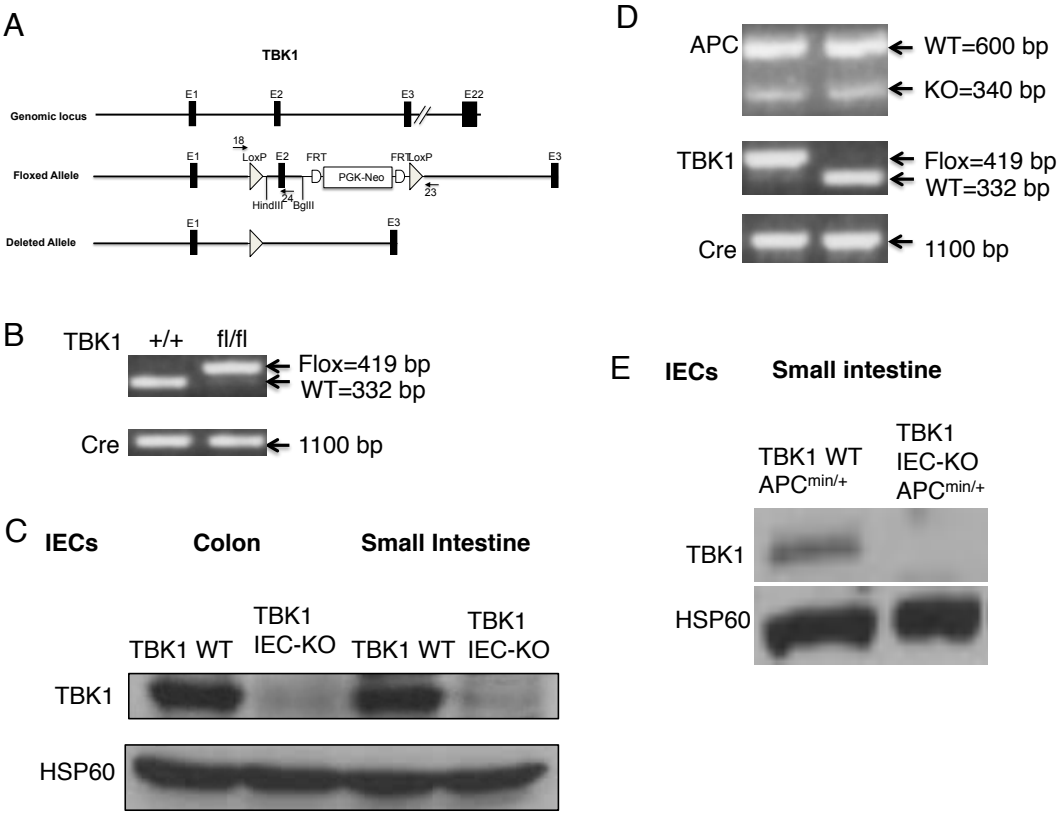

Figure 8. Generation of intestinal epithelial cell conditional *Tbk1* and *Apc*$^{min/+}$ *Tbk1* mice. Conventional *Tbk1* KO mice are embryonic lethal[56]; therefore, to address our hypothesis, we generated *Tbk1* intestinal epithelial cell-conditional KO (*Tbk1*$^{IEC\text{-}KO}$) mice by crossing *Tbk1* floxed mice with *villin*-Cre mice. A) Schematic image of *Tbk1* gene targeting in IECs. Two *lox*P sites were inserted adjacent to coding exon. Deleted allele depicts the removal of exon 2 after *villin*-Cre-mediated *lox*P recombination. B) PCR was used to detect the *Tbk1* floxed and wildtype alleles and cre transgene in tail DNA. The +/+ Cre+ are indicated as *Tbk1* wildtype while fl/fl Cre+ are indicated as *Tbk1*$^{IEC\text{-}KO}$. C) Western blot was used to detect TBK1 protein levels from isolated primary IECs of the mice. D) IEC-conditional *Tbk1* mice were crossed with *Apc*$^{min/+}$ mice to generate well-known *Apc*$^{min/+}$ colon cancer model.

Figure 9. *Tbk1*$^{IEC\text{-}KO}$ mice have normal development and intestinal homeostasis. IEC-specific ablation of *Tbk1* does not induce spontaneous tumor formation as mice age.

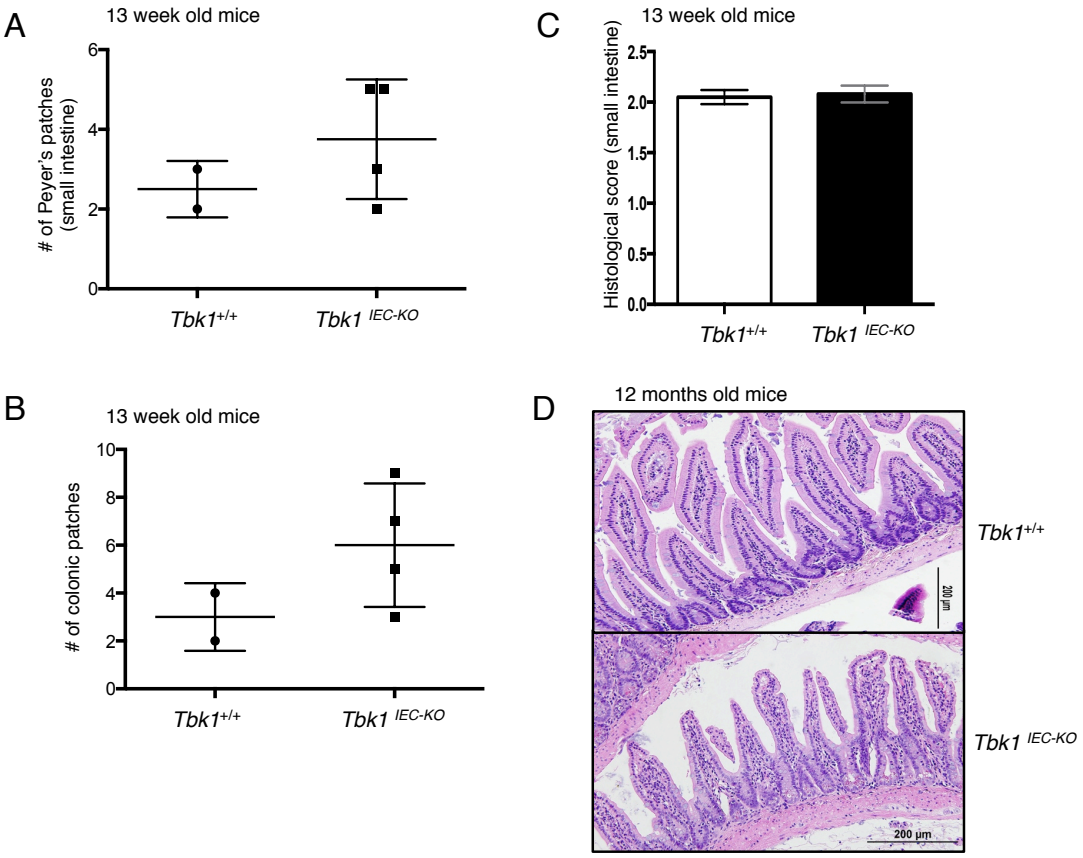

Figure 9. *Tbk1*$^{IEC\text{-}KO}$ mice have normal development and intestinal homeostasis. IEC-specific ablation of *Tbk1* does not induce spontaneous tumor formation as mice age. After sacrificing 13 week old mice, small intestines and colons were resected. A) Peyer's patches in the small intestine were identified grossly and counted. Data presented as the mean ± SD. (n=2 wildtype; n=4 *Tbk1*$^{IEC\text{-}KO}$) B) Colonic patches were identified histologically and counted. Data presented as the mean ± SD. (n=2 wildtype; n=4 *Tbk1*$^{IEC\text{-}KO}$) C) Small intestines were formalin-fixed and histologically scored (based on inflammation extent and mucosal damage in Table 1) to determine alterations in tissue morphology. Data presented as the mean ± SD. (n=2 wildtype; n=4 *Tbk1*$^{IEC\text{-}KO}$) D) Representative image of H&E stained tissue section of wildtype and *Tbk1*$^{IEC\text{-}KO}$ small intestines at one year of age. (n=3 wildtype; n=4 *Tbk1*$^{IEC\text{-}KO}$)

Figure 10. IEC-specific TBK1 ablation greatly promotes adenoma development in *Apc*$^{min/+}$ mice.

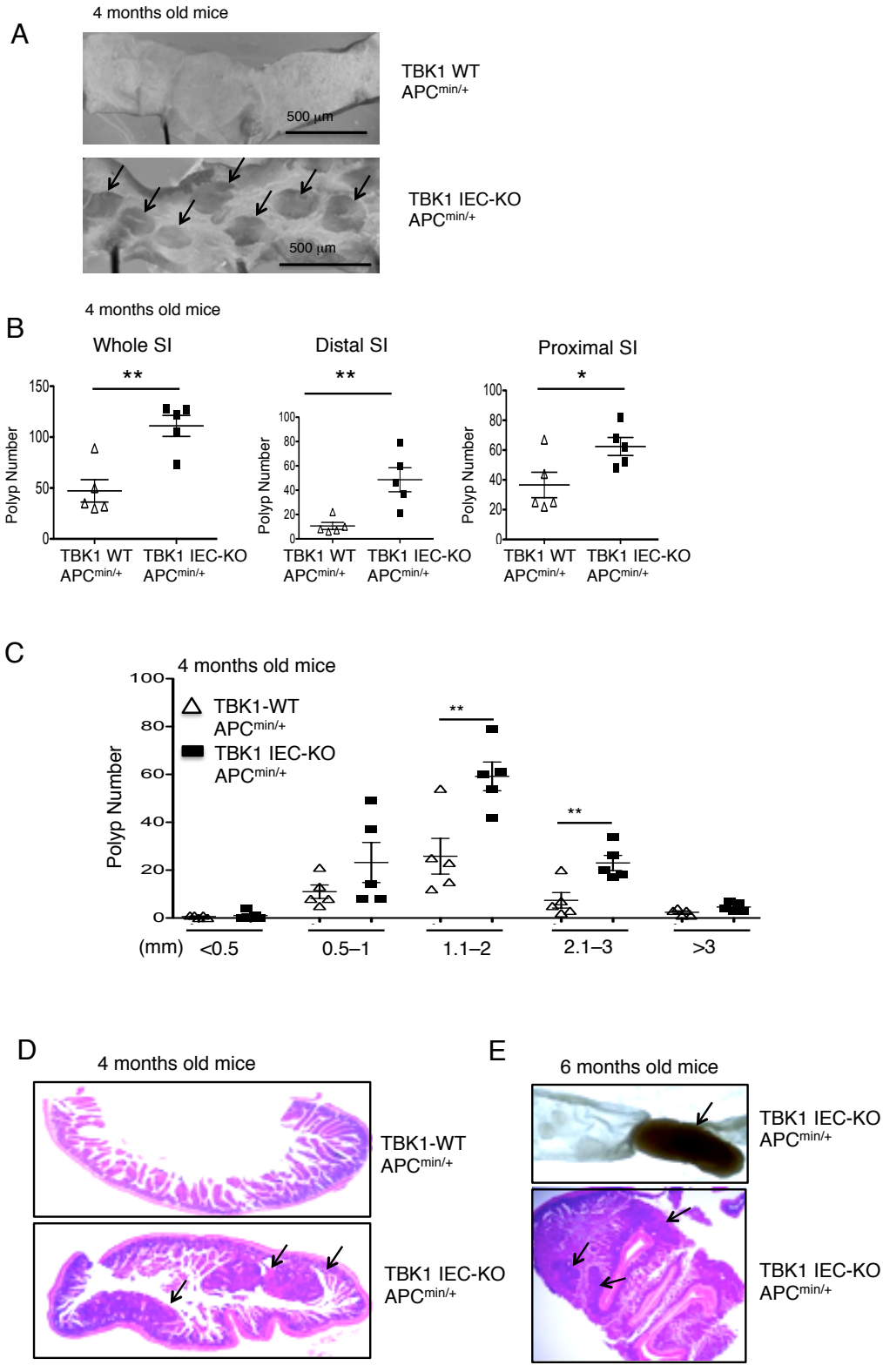

Figure 10. IEC-specific TBK1 ablation greatly promotes adenoma formation in *Apc*$^{min/+}$ mice. A) Representative images of tumor development in the small intestines of *Apc*$^{min/+}$ and *Apc*$^{min/+}$*Tbk1*$^{IEC\text{-}KO}$ mice at four months of age. B) Polyp numbers in the entire small intestine, distal region (13cm from the caecum) and proximal regions. C) Summary of tumor sizes in the entire small intestine. D) H&E staining of the distal region of the small intestine showing increased adenomas in *Tbk1*$^{IEC\text{-}KO}$ mice at four months of age. E) Representative picture of large multifocal adenomas in the distal region of the small intestine from the *Apc*$^{min/+}$*Tbk1*$^{IEC\text{-}KO}$ mice at six months of age. Each symbol in the graphs represents an individual mouse. The data are presented as mean ± SEM. The symbol * represents $p < 0.05$ and ** represents $p < 0.01$.

Figure 11. TBK1 deficiency in IECs promotes polyp formation in young mice *Apc*$^{min/+}$ mice.

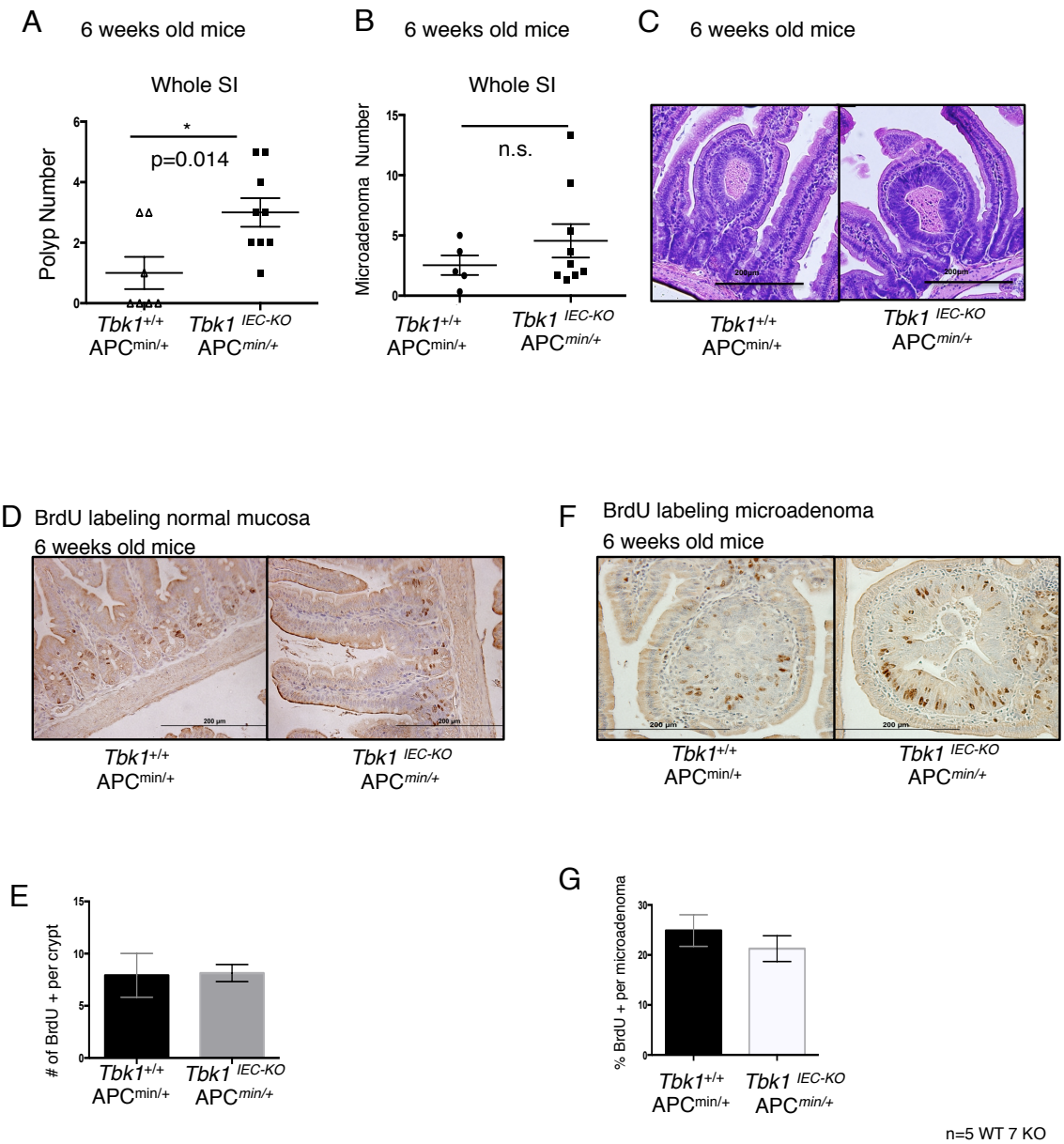

Figure 11. Young *Apc*$^{min/+}$*Tbk1*$^{IEC\text{-}KO}$ mice exhibit earlier polyp formation as compared to *Apc*$^{min/+}$ mice. A) Polyp (gross macroadenoma) numbers in the entire small intestine at six weeks of age. B) Microadenoma numbers in the entire small intestine histologically-identified (tri-level) at six weeks of age. C) Representative images of histologically-identified microadenomas of the small intestines of *Apc*$^{min/+}$ and *Apc*$^{min/+}$*Tbk1*$^{IEC\text{-}KO}$ mice at six weeks of age. D) Representative images of BrdU immunohistochemical staining of the normal mucosa in the small intestines of *Apc*$^{min/+}$ and *Apc*$^{min/+}$*Tbk1*$^{IEC\text{-}KO}$ mice at six weeks of age. E) Enumeration of the of BrdU+ cells per crypt within the normal mucosa of the small intestines of *Apc*$^{min/+}$ and *Apc*$^{min/+}$*Tbk1*$^{IEC\text{-}KO}$ mice at six weeks of age. F) Percentage of BrdU positive (+) cells per microadenoma determined as the percentage of BrdU+ nuclei per DAPI stained nuclei per microadenoma. All microadenomas identified per swiss-rolled intestinal tissue section were analyzed. The data are presented as mean ± SEM values (n= 5 *Apc*$^{min/+}$ mice; n=7 *Apc*$^{min/+}$*Tbk1*$^{IEC\text{-}KO}$ mice. Each symbol in the graphs represents an individual mouse. The symbol * represents $p < 0.05$.

Figure 12. IEC-specific TBK1 ablation does not influence the proliferation of IECs or adenoma cells in older *Apc*$^{min/+}$ mice.

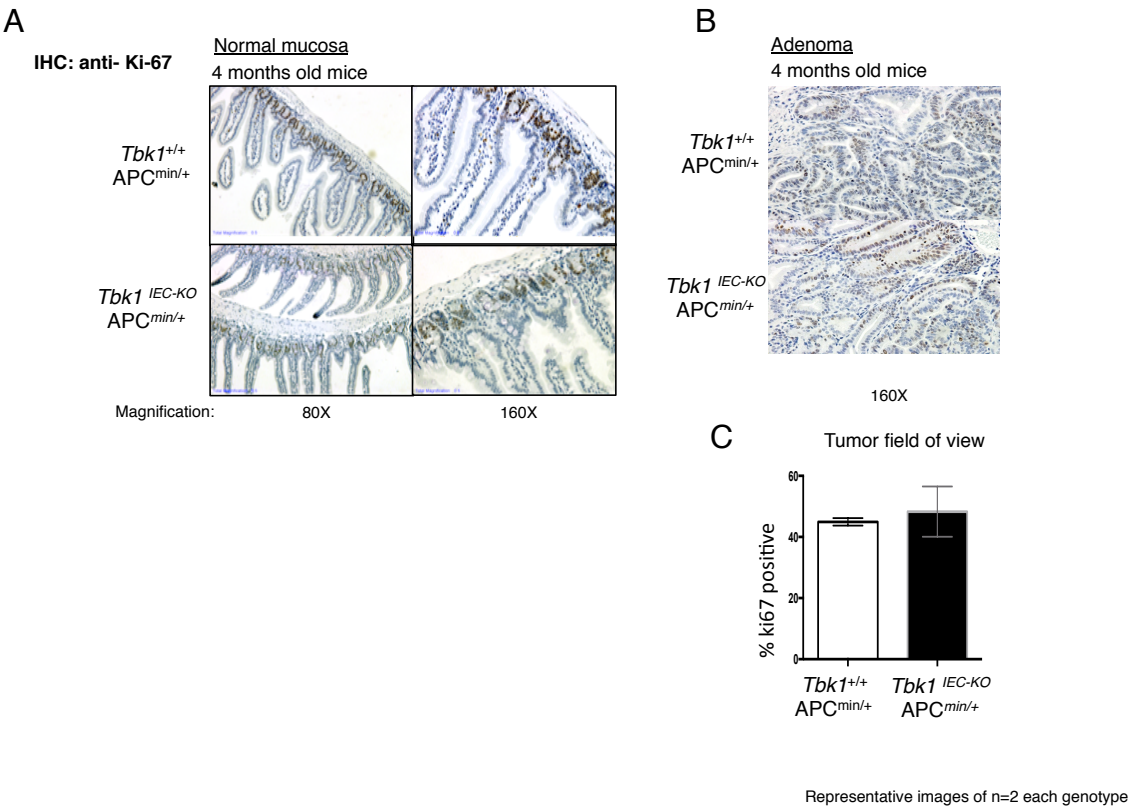

Representative images of n=2 each genotype

Figure 12. IEC-specific TBK1 ablation does not influence the proliferation of IECs or adenoma cells in older *Apc*$^{min/+}$ mice. A) Representative images of Ki67 immunohistochemical staining of the normal mucosa of the small intestines of *Apc*$^{min/+}$ and *Apc*$^{min/+}$*Tbk1*$^{IEC\text{-}KO}$ mice at four months of age. B) Representative images of Ki67 immunohistochemical staining of the adenomas in the small intestines of *Apc*$^{min/+}$ and *Apc*$^{min/+}$*Tbk1*$^{IEC\text{-}KO}$ mice at four months of age. C) Enumeration of the percentage of Ki67 + cells per field of view for the large adenomas in the small intestines of *Apc*$^{min/+}$ and *Apc*$^{min/+}$*Tbk1*$^{IEC\text{-}KO}$ mice at four months of age.

Figure 13. IEC-specfic-TBK1 deficiency promotes cell survival in the intestinal microadenomas of *Apc*$^{min/+}$ mice.

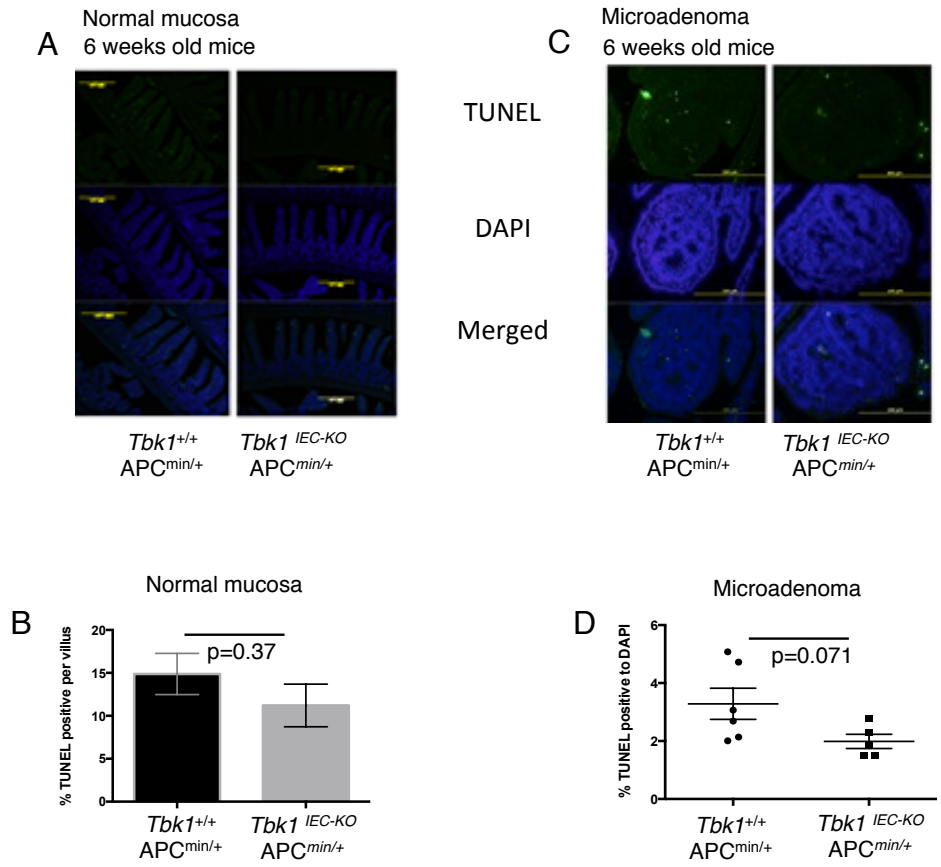

Figure 13. IEC-specfic-TBK1 deficiency likely promotes cell survival in the intestinal microadenomas of *Apc*$^{min/+}$ mice. A) Representative images of TUNEL fluorescent and DAPI staining of the normal mucosa of the small intestines of *Apc*$^{min/+}$ and *Apc*$^{min/+}$*Tbk1*$^{IEC\text{-}KO}$ mice at six weeks of age. B) Percentage of TUNEL positive (+) cells per villus determined as the percentage of GFP positive nuclei per DAPI positive nuclei per villus. Graph presents mean ± SEM values (n=3 mice per genotype; at least 6-9 images of different intestinal tissue focal areas were analyzed per mouse counting cells of at least 6-7 villi per area). C) Representative images of TUNEL fluorescent and DAPI staining of microadenomas of the small intestines of *Apc*$^{min/+}$ and *Apc*$^{min/+}$*Tbk1*$^{IEC\text{-}KO}$ mice at six weeks of age. D) Percentage of TUNEL positive cells per microadenoma determined as the percentage of GFP positive nuclei per DAPI positive nuclei per microadenoma. Graph presents mean ± SEM values (n= 6 *Apc*$^{min/+}$ mice; n=5 *Apc*$^{min/+}$*Tbk1*$^{IEC\text{-}KO}$ mice; p=0.071; 90% CI = 2.45, 0.135). Each symbol in the graph represents mean percentage of an individual mouse. All microadenomas identified per swiss-rolled intestinal tissue section were analyzed.

Table 1. Histological colitis and small intestinal inflammation scoring method.

Table 1

A. Histological Colitis Scoring Method (modified from K. Williams et. Al, *Gastroenterology* (2001))

Feature scored	Score	Description
Inflammation extent	0	none
	1	mucosa
	2	mucosa and submucosa
	3	transmural
Mucosal damage	0	none
	0	intraepithelial neutrophils and crypt abscess
	1	crypts lost; surface epithelium present
	2	focal ulcers present (cypts and surface epithelium lost)
	3	diffuse/extensive ulcer

B. Small intestine histological scoring method (Modified from Gomes-Santos et. al*; Clinical and Developmental Immunology* (2012)

Feature scored	Score	Description
extent of damage to mucosal architecture	0	normal
	1	mild
	2	moderate
	3	extensive
degree of cellular infiltration	0	normal
	1	mild
	2	moderate
	3	transmural
extent of muscle thickening	0	normal
	1	mild
	2	moderate
	3	extensive
crypt abscesses	0	absent
	1	present
loss of goblet cells	0	absent
	1	present

Table 1. Histological colitis and small intestinal inflammation scoring method. Tissue sections from either the colon or the small intestine of *Tbk1*$^{IEC\text{-}KO}$ and wildtype mice were H&E stained and blindly scored based on the presence of immune cells within the mucosa, submucosa, and/or transmural and on the extent of the mucosal damage.

Figure 14. *Tbk1* deletion in IECs does not alter the expression of inflammatory mediators in the gut.

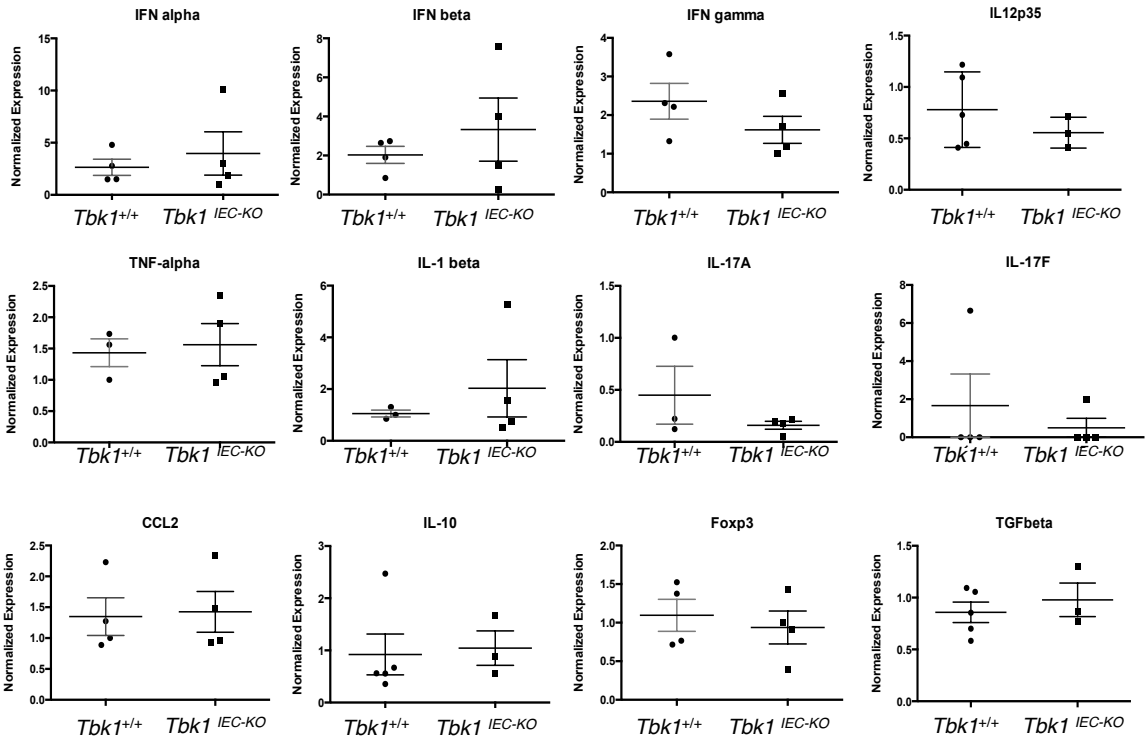

Figure 14. *Tbk1* deletion in IECs does not alter the expression of inflammatory mediators in the gut. qPCR analysis of indicated genes using the distal small intestines (13cm from caecum) wildtype or *Tbk1*$^{IEC\text{-}KO}$ mice. Normalized expression levels were calculated relative to the expression of internal control *Actb*. Data are presented as mean ± SEM based on multiple samples and representative of one experiment. Each symbol represents a mouse.

Figure 15. *Tbk1* ablation in IECs does not promote inflammation in a chemically induced colitis model.

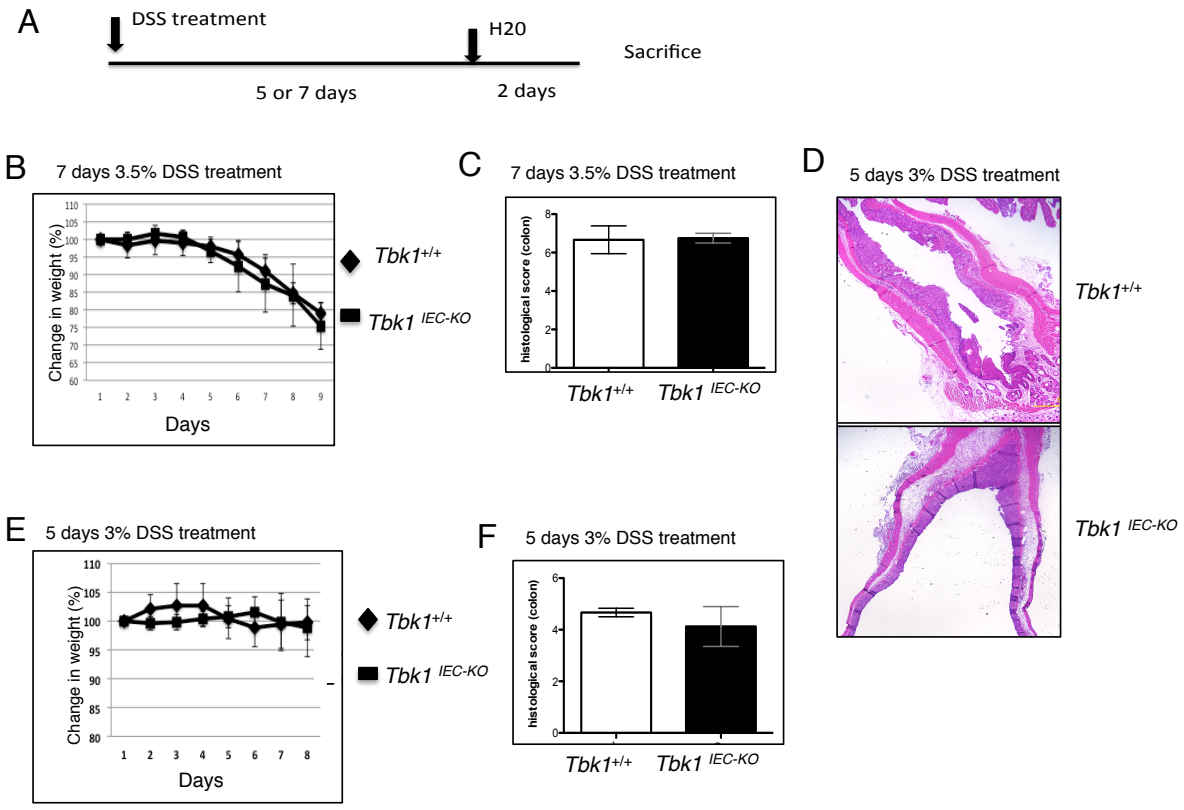

Figure 15. *Tbk1* ablation in IECs does not promote inflammation in a chemically induced colitis model. A) Schematic of treatment with DSS for five or seven days followed by two-day recovery with water before sacrificing *Tbk1*$^{IEC-KO}$ and wildtype mice. B) *Tbk1*$^{IEC-KO}$ and wildtype mice were weighed each day during 3.5% DSS treatment for seven days followed by two day recovery with water. Data presented as mean change in weight ± SD as percentage (n=5 per genotype). C) After treatment and recovery, colons were resected, formalin-fixed, H&E stained and histologically scored for evidence of inflammation (based on inflammation extent and mucosal damage in Table 1). Data presented as the mean ± SD (n=5 each group). D) Representative H&E stained colonic tissue section from mice treated with 3.5% DSS for seven days. The extent of tissue damage in both groups was similar in tissue sections from mice treated with 3% DSS (data not shown). E) *Tbk1*$^{IEC-KO}$ and wildtype mice were weighed each day during 3.0% DSS treatment for five days followed by two day recovery with water. Data presented as mean change in weight ± SD as percentage (n=5 per genotype).

Figure 16. *Tbk1* ablation in IECs does not promote inflammation or adenoma formation a chemically induced colitis-associated tumor model.

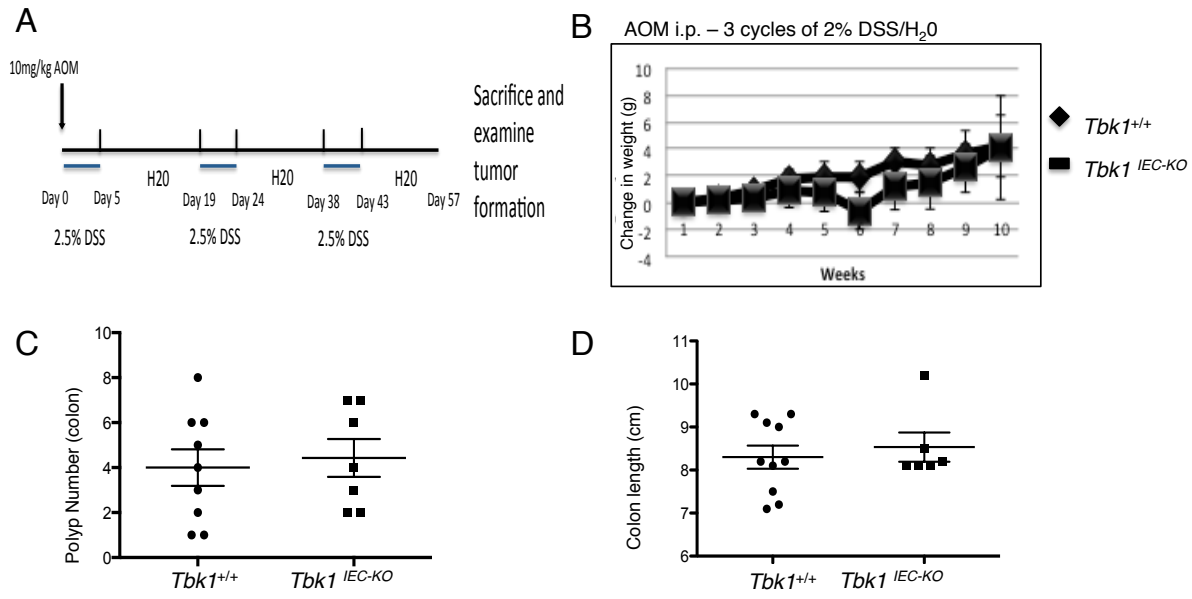

Figure 16. *Tbk1* ablation in IECs does not promote inflammation or adenoma formation a chemically induced colitis-associated tumor model. A) Schematic of treatment with a single dose of azoxymethane (AOM) followed by three cycles of DSS and water before sacrificing *Tbk1*$^{IEC\text{-}KO}$ and wildtype mice. B) *Tbk1*$^{IEC\text{-}KO}$ and wildtype mice were weighed as indicated during treatment. Data presented as mean ± SD (n=9 wildtype; n=7 *Tbk1*$^{IEC\text{-}KO}$). C) After three cycles of DSS/water treatments, colons were resected and measured for length. Data presented as mean ± SEM. D) Colons were formalin-fixed and number size of gross polyps was determined. Data presented as mean ± SEM. Each symbol in the graphs (C and D) represents an individual mouse.

Figure 17. The effect of TBK1 deficiency on adenoma formation is diminished in the absence of lymphocytes.

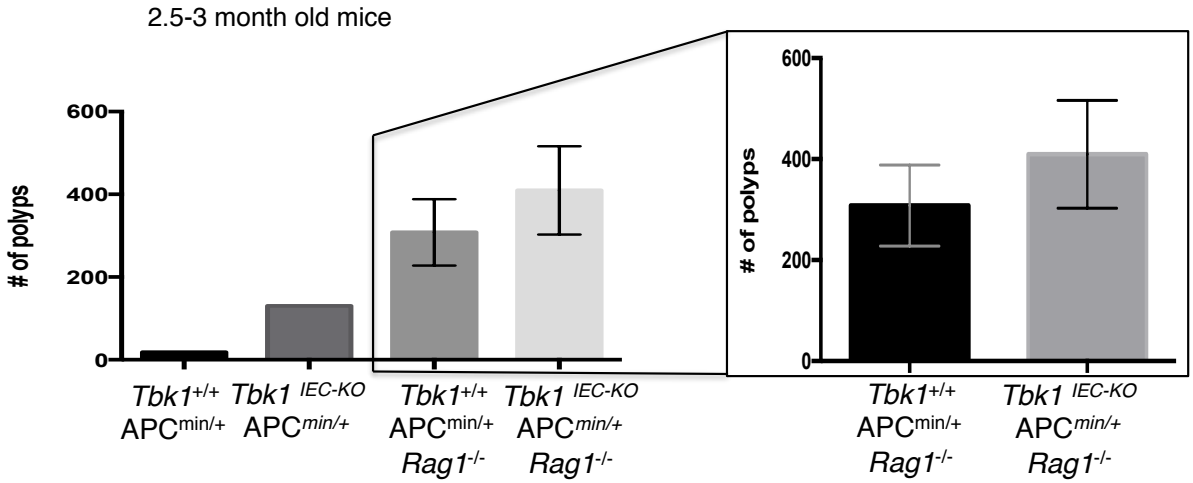

Figure 17. The effect of TBK1 deficiency on adenoma formation is diminished in the absence of lymphocytes. Gross adenomas in the entire small intestine 2.5 to 3 months old *Apc*$^{min/+}$ *Rag1* knockout and *Apc*$^{min/+}$*Tbk1*$^{IEC\text{-}KO}$ *Rag1* knockout mice were counted. The data are presented as mean ± SD (n=3 for *Apc*$^{min/+}$ *Rag1* knockout mice and n=2 for *Apc*$^{min/+}$*Tbk1*$^{IEC\text{-}KO}$ *Rag1* knockout mice).

Figure 18. IEC-specific *Tbk1* ablation in *Apc*$^{min/+}$ mice does not alter the frequency of immune cell composition in intestinal lamina propria.

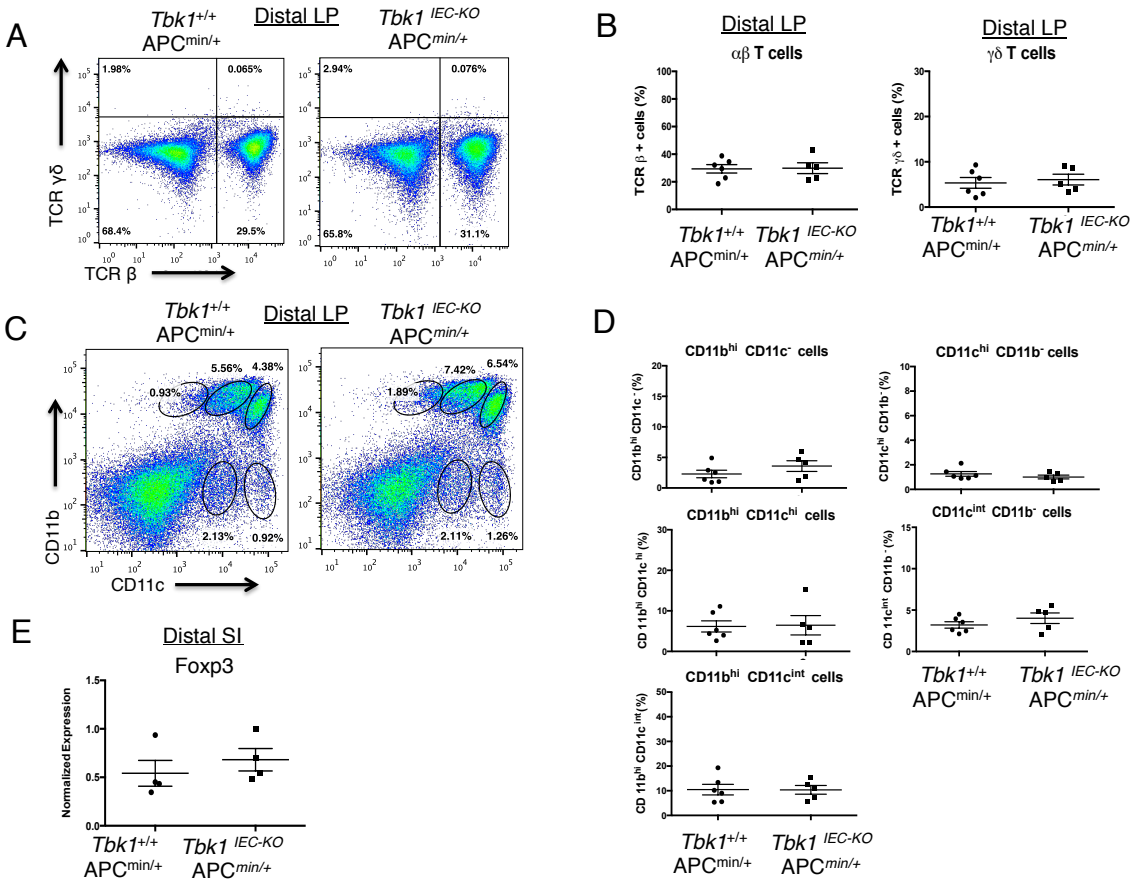

Figure 18. IEC-specific *Tbk1* ablation in *Apc*$^{min/+}$ mice does not alter the frequency of immune cell composition in intestinal lamina propria. A) Flow cytometric analysis of CD45^{+} subpopulations of αβ T cells (TCRβ^{+}) or γδ T cells (TCRγδ^{+}) from the lamina propria of *Apc*$^{min/+}$ and *Apc*$^{min/+}$*Tbk1*$^{IEC\text{-}KO}$ mice distal small intestines at three and one-half to four weeks old. Data are presented as a representative dot plot with each quadrant indicating the percentage of cells among total CD45^{+} cells. B) Summary graphs of mean ± SEM of lamina propria subpopulations of ab T cells and gd T cells based on two independent experiments. Each symbol represents a mouse. Data represent two independent experiments. C) Flow cytometric analysis of CD45^{+} myeloid populations of CD11c$^{hi/int/-}$ and/or CD11b$^{hi/int/-}$ cells from the lamina propria of *Apc*$^{min/+}$ and *Apc*$^{min/+}$*Tbk1*$^{IEC\text{-}KO}$ mice distal small intestines at three and one-half to four weeks old. Data are presented as a representative dot plot with each quadrant indicating the percentage of cells among total CD45^{+} cells. D) Summary graphs of mean ± SEM of lamina propria subpopulations of CD11c$^{hi/int/-}$ and/or CD11b$^{hi/int/-}$ myeloid cells based on two independent experiments. Each symbol represents a mouse. Data represent two independent experiments. E) Distal small intestinal (SI) tissues were analyzed for *Foxp3* mRNA expression using qPCR. Normalized expression levels were calculated relative to the expression of internal control *Actb*. Data are presented as mean ± SEM based on multiple samples and representative of one experiment. Each symbol represents a mouse.

Figure 19. *Tbk1* ablation in IECs of *Apc*$^{min/+}$ mice does not alter the frequency of IEL subpopulations of αβ or γδ T cells in the small intestine.

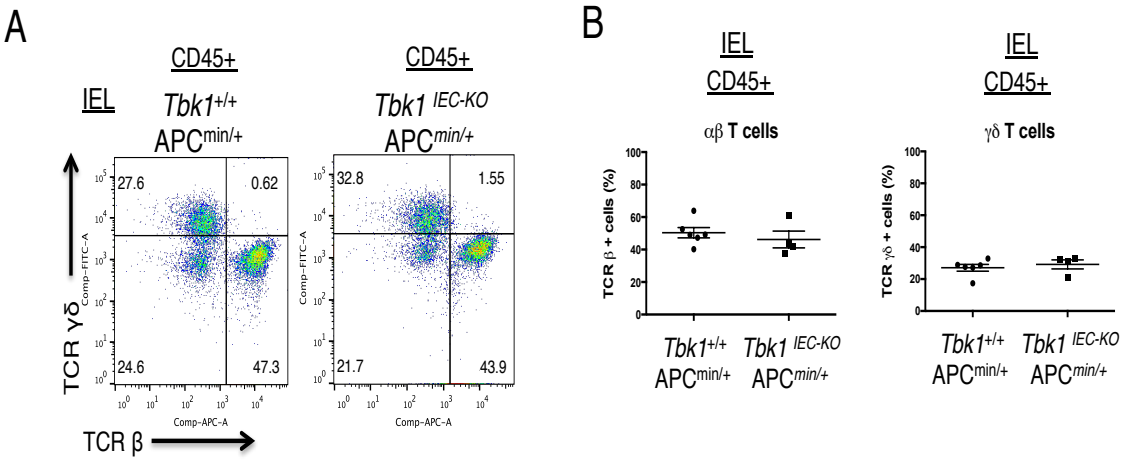

Figure 19. *Tbk1* ablation in IECs of *Apc*$^{min/+}$ mice does not alter the frequency of IEL subpopulations of $\alpha\beta$ or $\gamma\delta$ T cells in the small intestine. Flow cytometric analysis of CD45^{+} IEL subpopulations of $\alpha\beta$ T cells (TCRβ^{+}) or $\gamma\delta$ T cells (TCR$\gamma\delta^{+}$) from the small intestines of *Apc*$^{min/+}$ and *Apc*$^{min/+}$*Tbk1*$^{\text{IEC-KO}}$ mice at three and one-half to four weeks old. A) Data are presented as a representative dot plot with each quadrant indicating the percentage of cells among total CD45^{+} cells. B) Summary graphs of mean ± SEM of IEL subpopulations of ab T cells and gd T cells based on two independent experiments. Each symbol represents a mouse. Data represent two independent experiments.

Figure 20. TBK1 deficiency in IECs leads to defective *IL10* expression in *Apc*$^{min/+}$ mice small intestines.

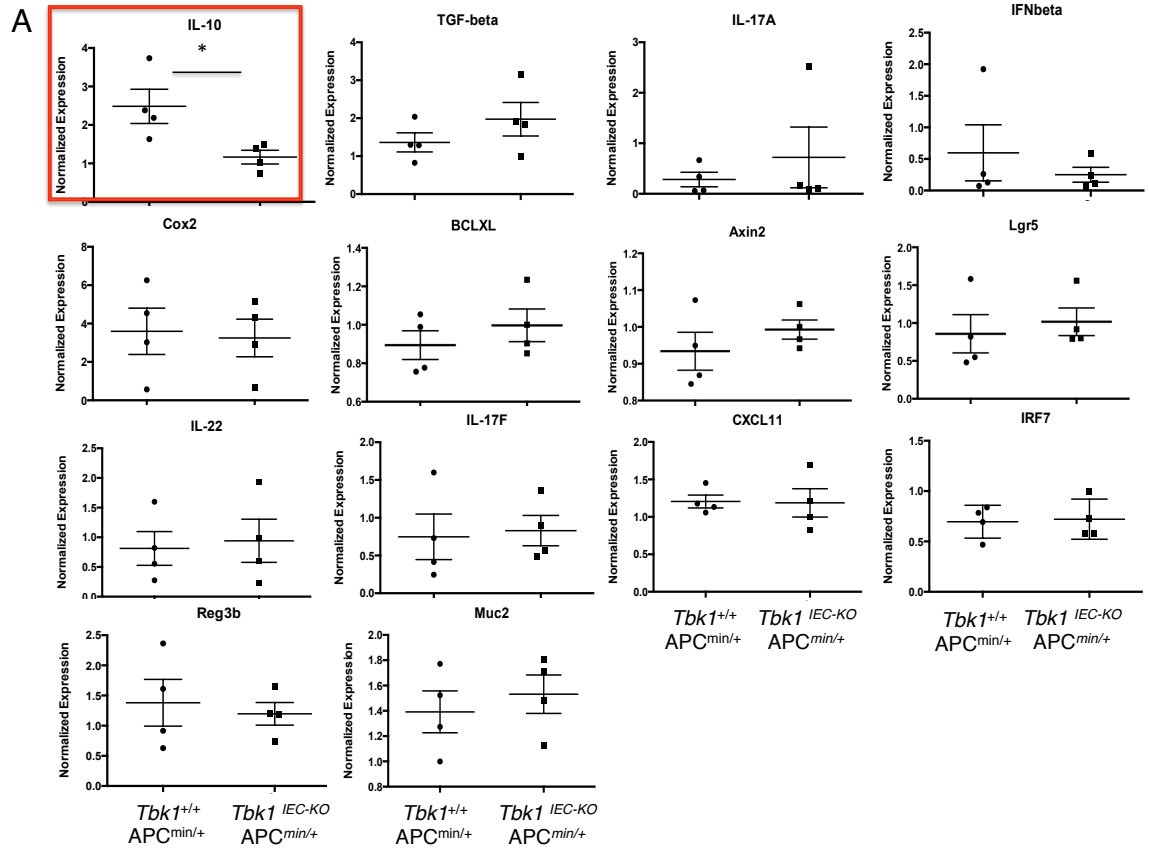

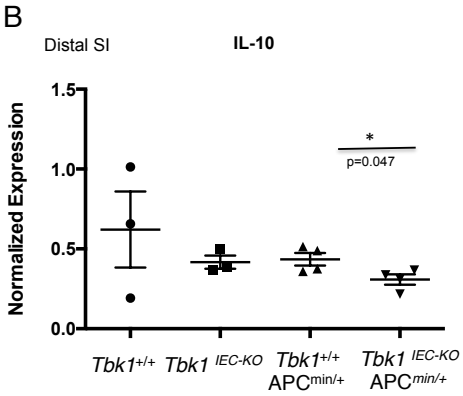

Figure 20. TBK1 deficiency in IECs leads to defective *IL10* expression in the intestines of *Apc*$^{min/+}$ mice. qPCR analysis of indicated genes using the distal small intestines (13cm from caecum) from A) *Apc*$^{min/+}$ and *Apc*$^{min/+}$*Tbk1*$^{IEC\text{-}KO}$ mice or B) wildtype, *Tbk1*$^{IEC\text{-}KO}$, *Apc*$^{min/+}$ and *Apc*$^{min/+}$*Tbk1*$^{IEC\text{-}KO}$ mice. Normalized expression levels were calculated relative to the expression of internal control *Actb*. Data are presented as mean ± SEM based on multiple samples and are representative graphs of two independent experiments. Each symbol represents a mouse. The symbol * represents $p < 0.05$.

Figure 21. Loss of TBK1 in IECs results in diminished levels of *IL10* expression by intestinal IELs *Apc*$^{min/+}$ mice.

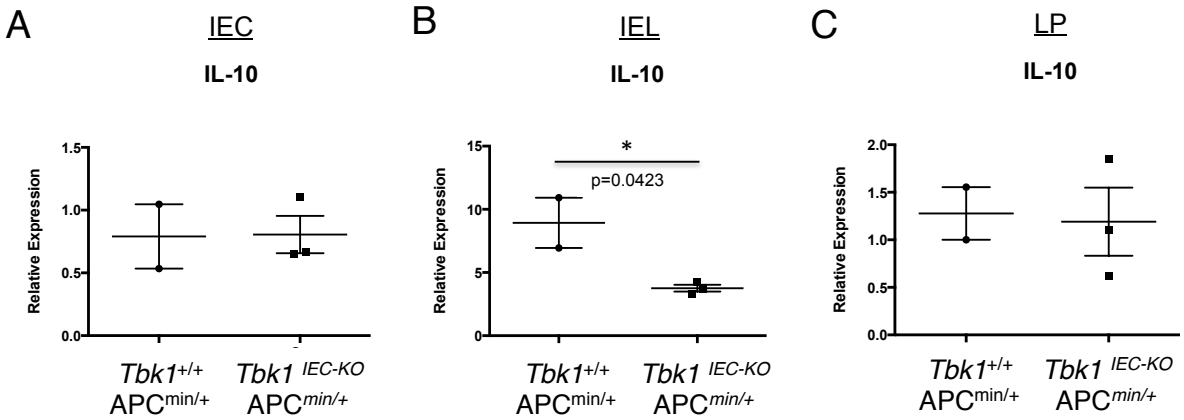

Figure 21. Loss of TBK1 in IECs results in diminished levels of *IL10* expression by intestinal IELs *Apc*$^{min/+}$ mice. qPCR analysis of *IL10* mRNA expression using A) primary IECs, B) primary IELs, or C) primary immune cells from the lamina propria (LP) of distal the small intestines from *Apc*$^{min/+}$ and *Apc*$^{min/+}$*Tbk1*$^{IEC\text{-}KO}$ mice. Normalized expression levels were calculated relative to the expression of internal control *Actb*. Data are presented as mean ± SEM based on multiple samples and are representative graphs of two independent experiments. Each symbol represents a mouse. The symbol * represents $p < 0.05$.

Figure 22. A schematic representing our proposed model of IEC-specific TBK1 regulation of intestinal adenoma growth *in vivo*.

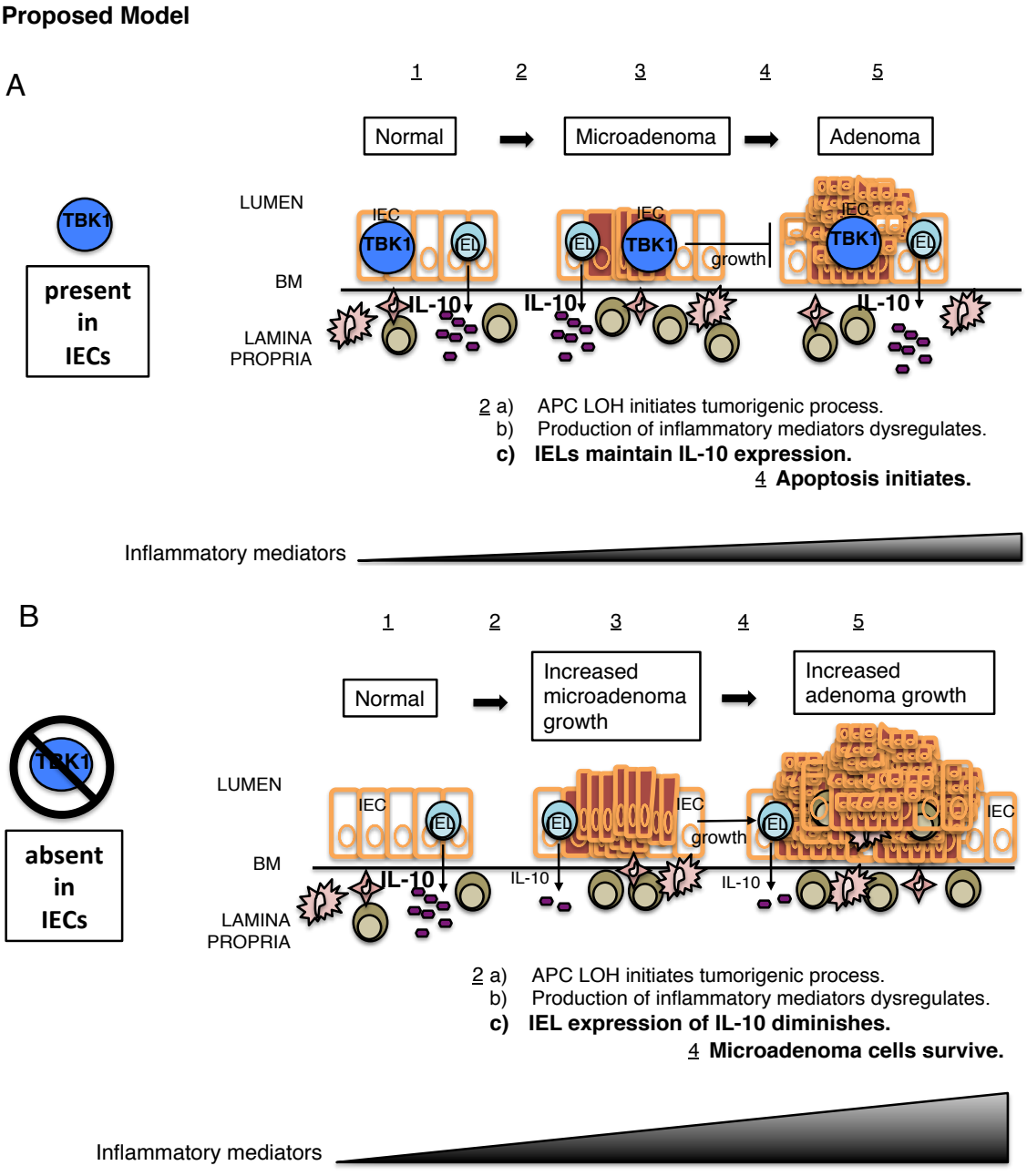

Figure 22. A schematic representing our proposed model of IEC-specific TBK1 regulation of intestinal adenoma growth *in vivo*. A) Under normal conditions, intestinal homeostasis is maintained with IECs forming a single-layer barrier between the lumen and lamina propria. Abnormal loss-of-heterozygosity (LOH) of tumor suppressor APC triggers deregulated cellular signaling and inflammation leading to microadenoma formation. TBK1 in IECs negatively regulates microadenoma to macroadenoma growth by maintaining the levels of immunosuppressive cytokine IL-10 produced by intestinal IELs during the tumorigenic process, resulting in apoptosis of adenoma cells. B) However, upon initiation of the adenoma formation in the absence of TBK1 in IECs, intestinal IELs express diminished levels of *Il10*. With continued aberrant cell signaling and inflammation after LOH of *Apc*, the absence of TBK1 in IECs promotes intestinal adenoma growth through increased adenoma cell survival.

Figure 23. Copy numbers of *TBK1* significantly correlated with *TBK1* mRNA expression in colorectal adenocarcinoma samples deposited in TCGA.

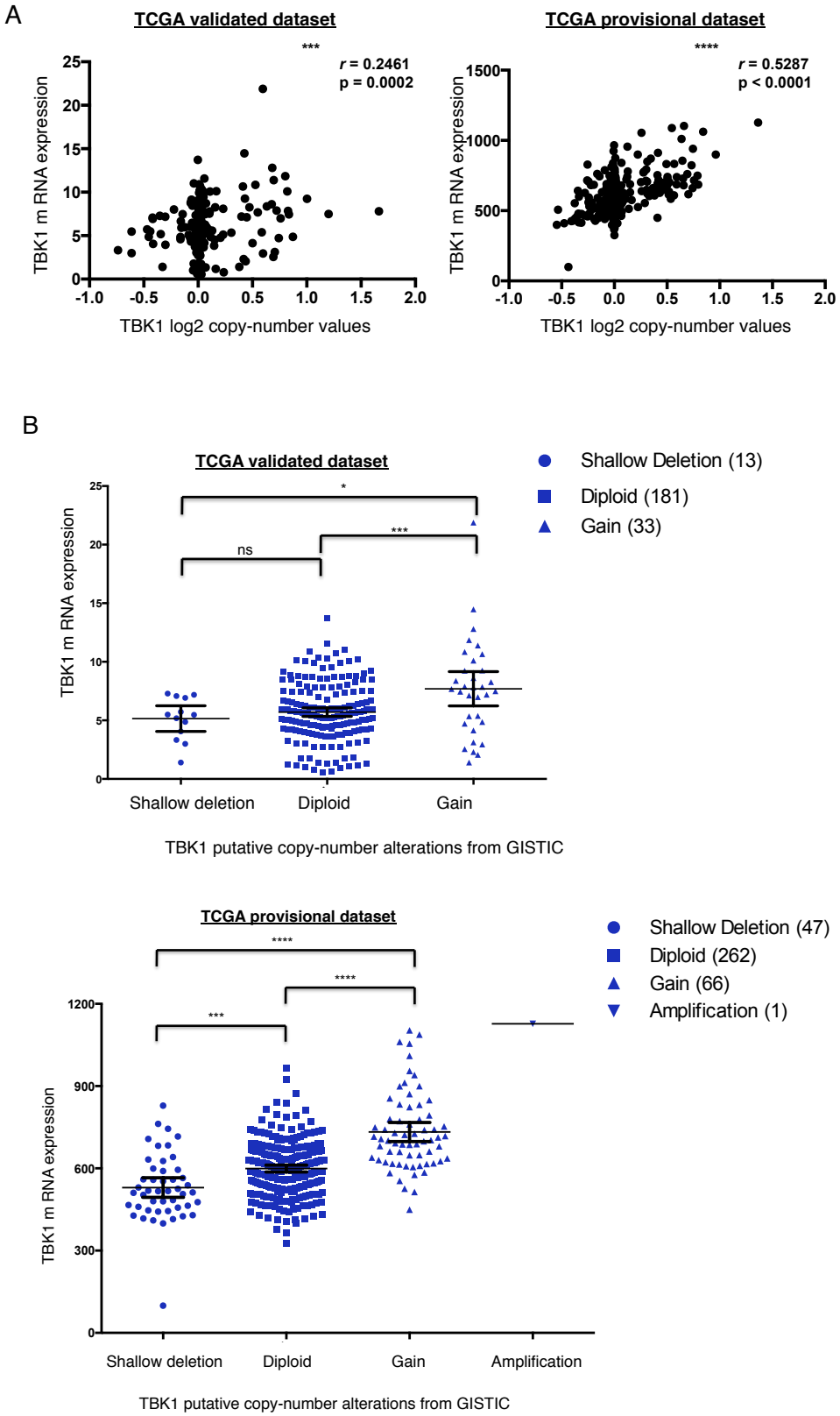

Figure 23. Copy numbers of *TBK1* significantly correlated with *TBK1* mRNA expression in colorectal adenocarcinoma samples deposited in TCGA.

Copy number and mRNA expression data were collected using the RNASeqV2 data from validated (n=227) and provisional (n=375) genomic and transcriptomic profiles of colorectal adenocarcinoma tumor samples in TCGA at www.cbioportal.org[74]. (A) The correlation between copy numbers of *TBK1* and *TBK1* mRNA expression in colorectal adenocarcinoma samples deposited in TCGA. (B) *TBK1* mRNA expression in samples with putative shallow deletions, diploid, gains or amplification with n for each group as indicated on graph. One-way ANOVA with Tukey's multiple comparisons test was used to analyze mean differences in mRNA expression levels between groups of putative copy-number alternations with the exception of the putative amplification group (n=1). Data presented as mean ± 95% confidence intervals with alpha of 0.05. p-values of <0.05, <0.01, <0.001, <0.0001 correspond with (*), (**), (***), and (***) annotations respectively.

Figure 24. *TBK1* copy number or mRNA expression in colorectal adenocarcinoma samples deposited in TCGA did not correlate with overall survival of patients.

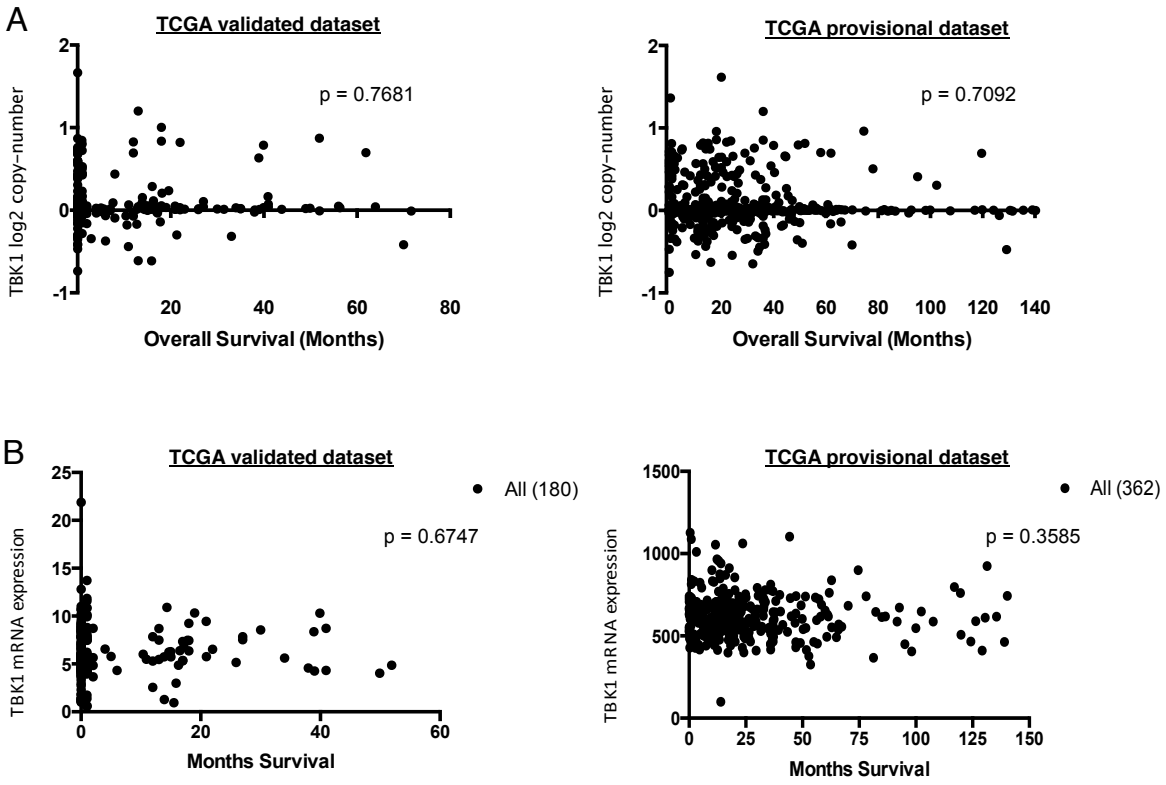

Figure 24. *TBK1* copy number or mRNA expression in colorectal adenocarcinoma samples deposited in TCGA did not correlate with overall survival of patients.

Overall patient survival data, *TBK1* copy number, and *TBK1* mRNA expression data were collected using the RNASeqV2 data from validated (n=227) and provisional (n=375) genetic profiles of colorectal adenocarcinoma tumor samples in TCGA at www.cbioportal.org[74]. (A) The correlation between copy numbers of *TBK1* in colorectal adenocarcinoma samples in TCGA and overall survival (months) of patients. (B) The correlation between copy numbers of *TBK1* mRNA expression in colorectal adenocarcinoma samples and overall survival (months) of patients. The Pearson correlation test was used to examine correlation using data from the TCGA validated and provisional datasets. p-values of <0.05, <0.01, <0.001, <0.0001 correspond with (*), (**), (***), and (***) annotations respectively.

Figure 25. *TBK1* mRNA expression in colorectal adenocarcinoma samples from disease stage IIIC correlate with survival of patients; correlation exists between levels of *TBK1* mRNA expression in samples from early and late stage of disease.

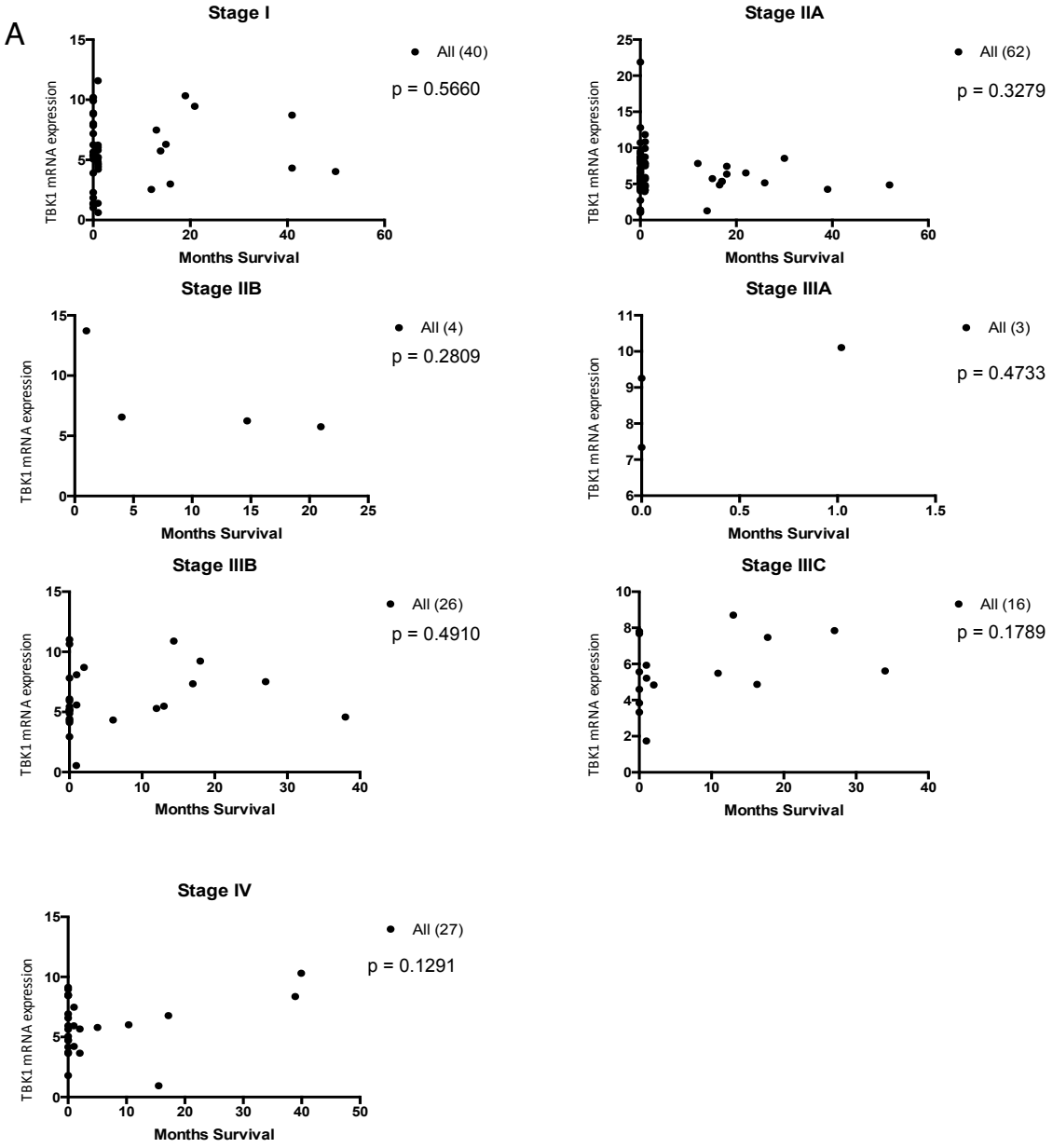

B

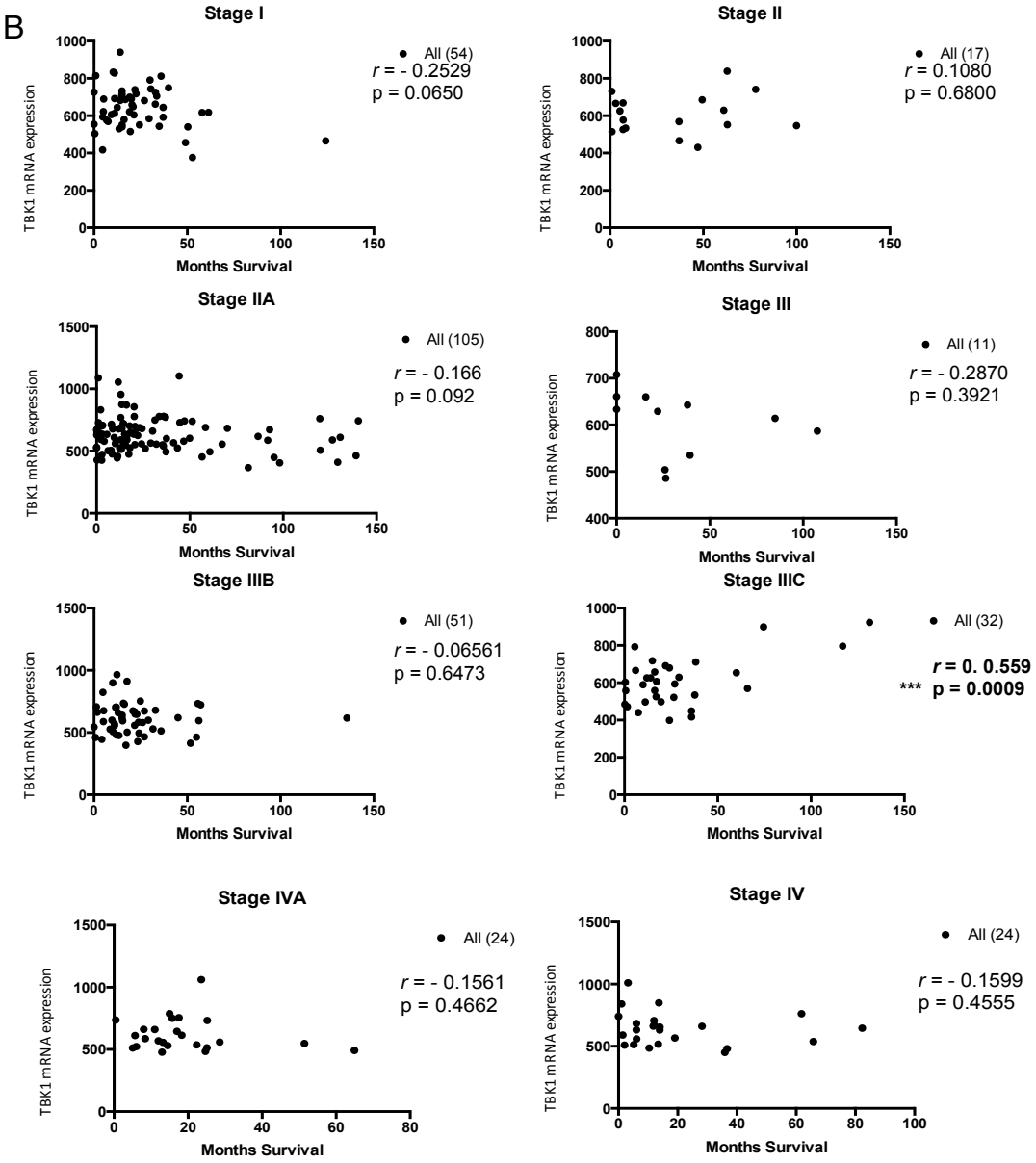
Stage I
All (54)
r = - 0.2529
p = 0.0650
Stage II
All (17)
r = 0.1080
p = 0.6800
Stage IIA
All (105)
r = - 0.166
p = 0.092
Stage III
All (11)
r = - 0.2870
p = 0.3921
Stage IIIB
All (51)
r = - 0.06561
p = 0.6473
Stage IIIC
All (32)
r = 0. 0.559
*** p = 0.0009
Stage IVA
All (24)
r = - 0.1561
p = 0.4662
Stage IV
All (24)
r = - 0.1599
p = 0.4555
TBK1 mRNA expression
Months Survival

C

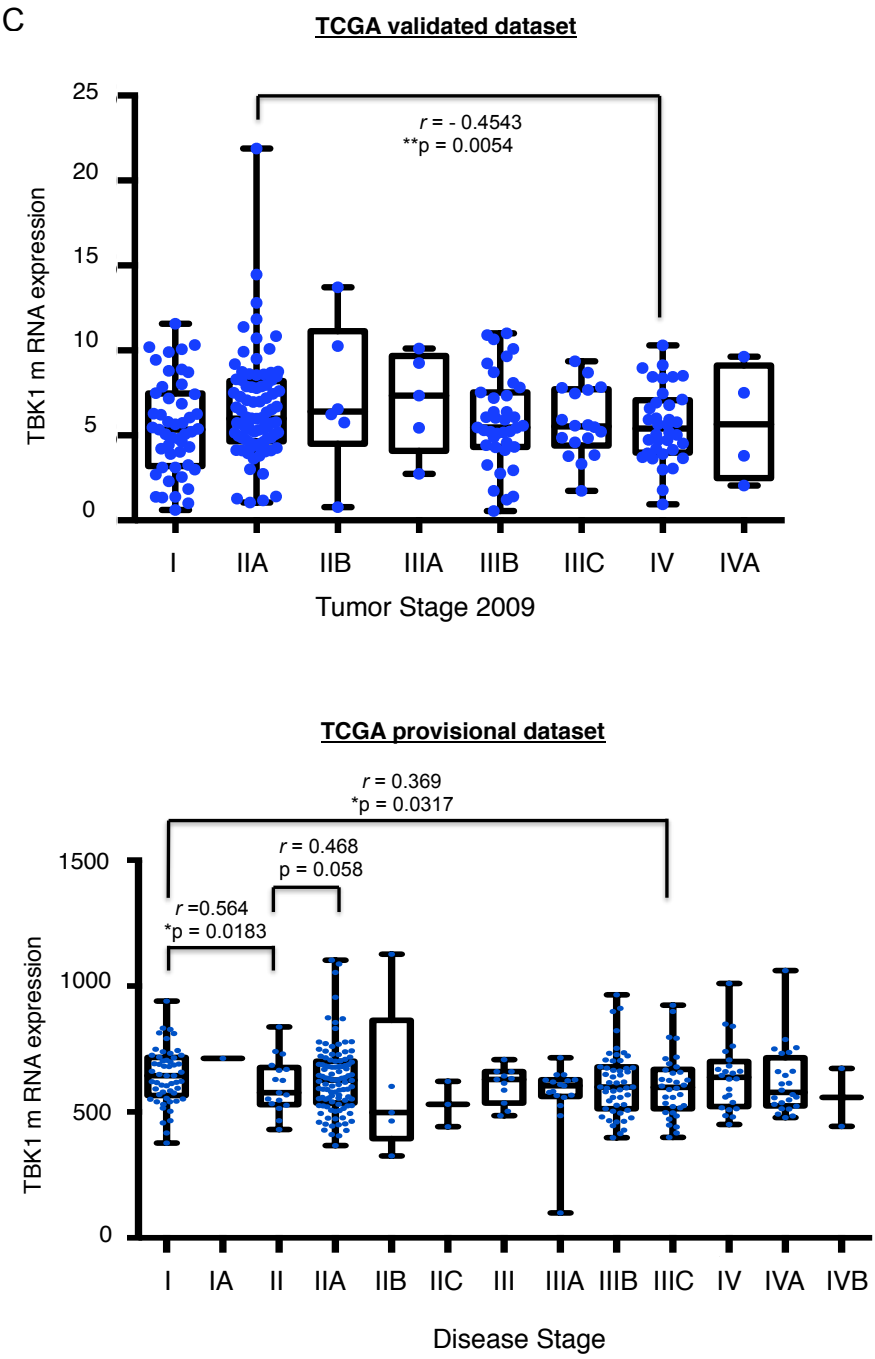
TCGA validated dataset
r = - 0.4543
**p = 0.0054
TBK1 m RNA expression
25
20
15
10
5
0
I
IIA
IIB
IIIA
IIIB
IIIC
IV
IVA
Tumor Stage 2009
TCGA provisional dataset
r = 0.369
*p = 0.0317
r = 0.468
p = 0.058
r =0.564
*p = 0.0183
TBK1 m RNA expression
1500
1000
500
0
I
IA
II
IIA
IIB
IIC
III
IIIA
IIIB
IIIC
IV
IVA
IVB
Disease Stage

Figure 25. *TBK1* mRNA expression levels in colorectal adenocarcinoma samples from disease stage IIIC correlate with survival of patients; correlation exists between levels of *TBK1* mRNA expression in samples from early and late stage of disease.

Overall patient survival data and *TBK1* mRNA expression data were collected using the RNASeqV2 data from validated and/or provisional) genetic profiles of colorectal adenocarcinoma tumor samples in TCGA at www.cbioportal.org[74]. (A) The correlation between mRNA expression of *TBK1* in colorectal adenocarcinoma samples in TCGA during each disease stage from validated dataset (n=241) and overall survival (months) of those patients. The Pearson correlation test was used to examine correlation with n for each stage as indicated on graph. (B) The correlation between mRNA expression of *TBK1* in colorectal adenocarcinoma samples in TCGA during each disease stage from provisional dataset (n=347) and overall survival (months) of those patients. The Pearson correlation test was used to examine correlation with n for each stage as indicated on graph. (C) Box and whisker plot of *TBK1* mRNA expression in samples from disease stage I through stage IV from validated dataset (top) (n=241) and provisional dataset (n=347) (bottom). The Pearson correlation test was used to examine correlation between stages of disease. p-values of <0.05, <0.01, <0.001, <0.0001 correspond with (*), (**), (***), and (***) annotations respectively.

Figure 26. *APC*, *TP53*, *KRAS*, and *PIK3CA* are among the top five most frequently mutated genes in colorectal adenocarcinomas. *APC*, *TP53*, *KRAS*, and *PIK3CA* mRNA expression correlates with copy number of its respective gene.

A

TCGA validated dataset

Mutated Gene Rank	Gene	Number of mutations	Number of samples	Frequency
1	APC	247	168	60.90%
2	TP53	122	120	43.50%
3	KRAS	94	94	34.10%
4	SYNE1	100	47	17.00%
5	PIK3CA	53	45	16.30%

B

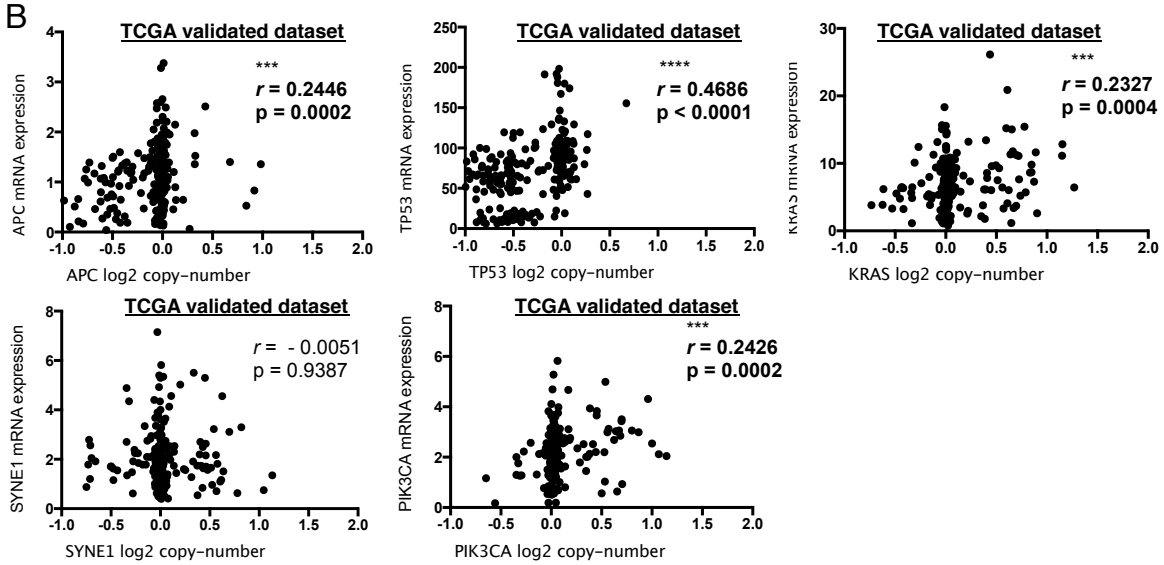

Figure 26. *APC*, *TP53*, *KRAS*, and *PIK3CA* are among the top five most frequently mutated genes in colorectal adenocarcinomas. ***APC*, *TP53*, *KRAS*, and *PIK3CA* mRNA expression correlates with copy number of its respective gene.** (A) Frequency of mutation in *APC*, *TP53*, *KRAS*, SYNE1 and *PIK3CA* in the colorectal adenocarcinoma validated dataset of TCGA. (B) Correlation between copy numbers of *APC*, *TP53*, *KRAS*, *SYNE1* and *PIK3CA* and its respective mRNA expression in the colorectal adenocarcinoma validated dataset (n=227) of TCGA . mRNA expression data were collected using the RNASeqV2 data, frequency of mutation, and copy number are data from validated and/or provisional genetic profiles of colorectal adenocarcinoma tumor samples in TCGA. www.cbioportal.org[74]. The Pearson correlation test was used to examine correlation between stages of disease. p-values of <0.05, <0.01, <0.001, <0.0001 correspond with (*), (**), (***), and (***) annotations respectively.

Figure 27. No correlation between overall survival of patients and *APC*, *TP53*, *KRAS*, *SYNE1* and *PIK3CA* copy number or mRNA expression in colorectal adenocarcinoma samples from validated TCGA dataset.

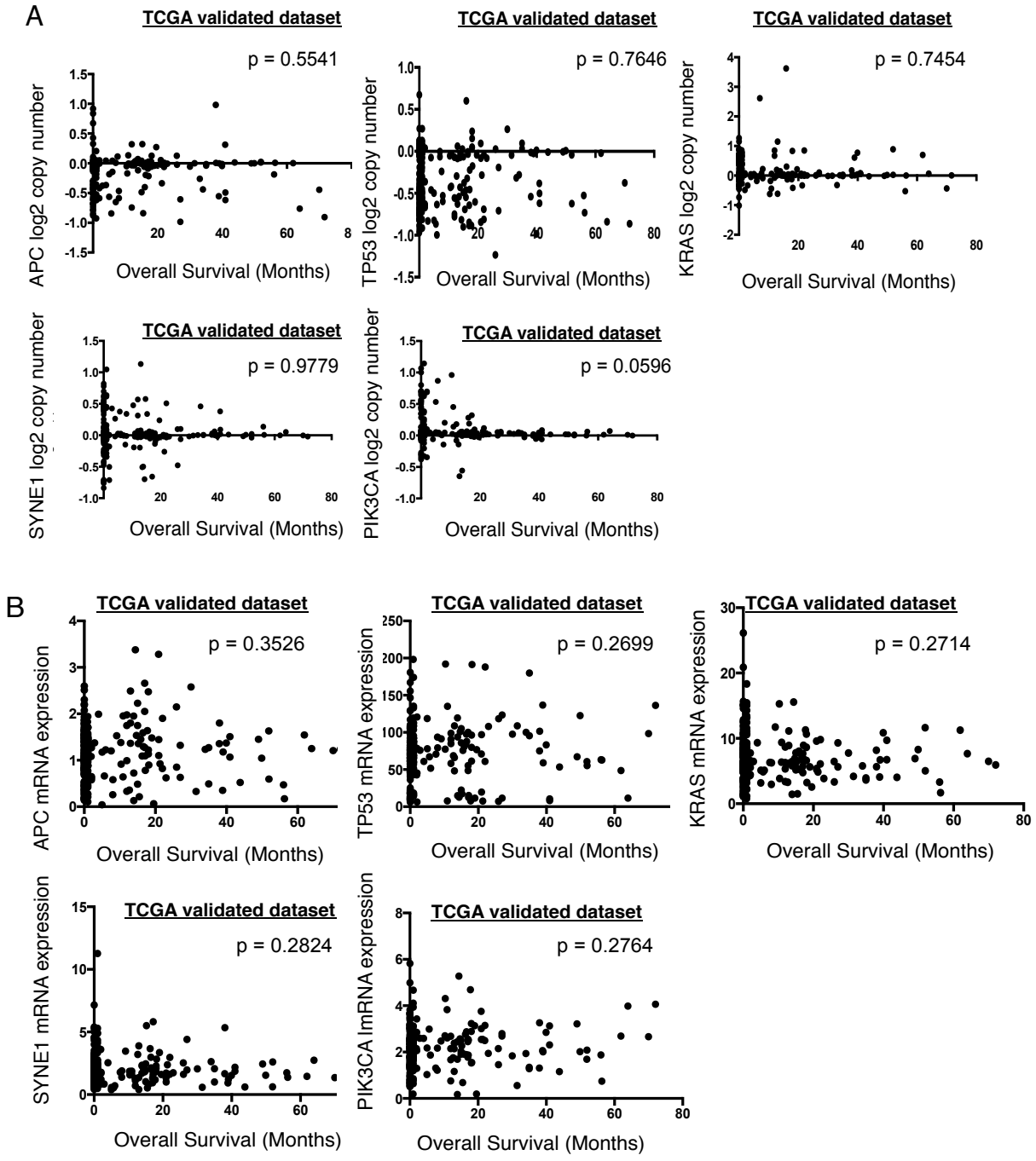

Figure 27. No correlation between overall survival of patients and *APC*, *TP53*, *KRAS*, *SYNE1* and *PIK3CA* copy number or mRNA expression in colorectal adenocarcinoma samples from validated TCGA dataset.

(A) Correlation between *APC*, *TP53*, *KRAS*, *SYNE1* and *PIK3CA* copy number in colorectal adenocarcinoma samples from validated TCGA dataset (n=255) and overall survival (months) of patients. (B) Correlation between mRNA expression of *APC*, *TP53*, *KRAS*, *SYNE1* and *PIK3CA* in colorectal adenocarcinoma samples from validated TCGA dataset (n=242) and overall survival of patients (months). mRNA expression data were collected using the RNASeqV2 data, copy number and overall survival are data from validated genetic profiles of colorectal adenocarcinoma tumor samples in TCGA. www.cbioportal.org[74]. The Pearson correlation test was used to examine correlation between stages of disease. p-values of <0.05, <0.01, <0.001, <0.0001 correspond with (*), (**), (***), and (***) annotations respectively.

Figure 28. Percentages of different types of TBK1 mutations found in the large intestine of patient colorectal adenocarcinoma samples (COSMIC and TCGA database).

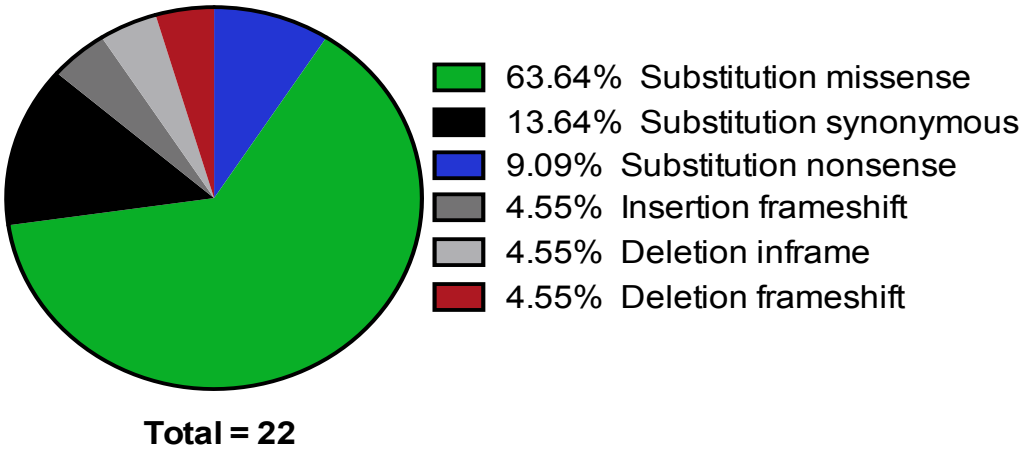

Figure 28. Percentages of different types of TBK1 point mutations found in the large intestine of patient colorectal adenocarcinoma samples (COSMIC and TCGA database).

Pie chart indicating the percentages of different types of point mutations identified in CRC patient tumor samples (excludes cultured cell line data) sequenced from adenocarcinoma tissues of the large intestine deposited in Catalogue of Somatic Mutations in Cancer (COSMIC) and The Cancer Genome Atlas (TCGA) including missense, nonsense, and synonomous mutations as well as insertion and deletion frame-shifts deletion in-frame-shift. Total of 22 mutations were found in these databases.

Table 2. Description and location of the point mutations found in the large intestine of patient tumor samples (COSMIC and TCGA database) with predicted functional impact determined by mutationassessor.org.

Point mutation	Tissue site	Type	Functional impact level	Functional impact score	Database	Region of mutation
TBK1 F56C	Colon	Missense	Medium	2.785	TCGA - validated	Protein kinase domain (p. 9 - 307)
TBK1 S347Y	Colon	Missense	Low	1.245	TCGA - validated	Ubiquitin-like domain (p. 309 - 384)
TBK1 S632L	Colon	Missense	Neutral	0.55	TCGA - validated	Potential coiled domain (p. 626 - 713); Helical scaffold dimerization domain (p. 408 - 654)
TBK1 T389I	Colon	Missense	Neutral	0.46	TCGA - validated	Near ubiquitin-like domain (p. 309 - 384)
TBK1 R357*	Colon	Nonsense	N/A	N/A	TCGA - validated	Ubiquitin-like domain (p. 309 - 384)
TBK1 A188V	Colon	Missense	Medium	2.41	COSMIC	Protein kinase domain (p. 9 - 307)
TBK1 A535T	Colon	Missense	Neutral	-0.805	COSMIC	Helical scaffold dimerization domain (p. 408 - 654)
TBK1 D720Y	Colon	Missense	Low	0.805	COSMIC	C-terminal domain (p. 658 - 745)
TBK1 E355K	Colon	Missense	Low	1.1	COSMIC	Ubiquitin-like domain (p. 309 - 384)
TBK1 L366L	Rectum	Synonymous	N/A	N/A	COSMIC	Ubiquitin-like domain (p. 309 - 384)
TBK1 L366V	Large intestine	Missense	Low	0.805	COSMIC	Ubiquitin-like domain (p. 309 - 384)
TBK1 M263V	Colon	Missense	Neutral	-0.025	COSMIC	Protein kinase domain (p. 9 - 307)
TBK1 Q289R	Colon	Missense	Low	1.22	COSMIC	Protein kinase domain (p. 9 - 307)
TBK1 R574G	Colon	Missense	Low	0.975	COSMIC	Helical scaffold dimerization domain (p. 408 - 654)
TBK1 R724C	Colon	Missense	Neutral	0	COSMIC	C-terminal domain (p. 658 - 745)
TBK1 T599T	Caecum	Synonymous	N/A	N/A	COSMIC	Helical scaffold dimerization domain (p. 408 - 654)
TBK1 T651T	Colon	Synonymous	N/A	N/A	COSMIC	Potential coiled domain (p. 626 - 713); Helical scaffold dimerization domain (p. 408 - 654)
TBK1 V275D	Colon	Missense	Neutral	-2.66	COSMIC	Protein kinase domain (p. 9 - 307)
TBK1 R440*	Colon	Nonsense	N/A	N/A	COSMIC	Helical scaffold dimerization domain (p. 408 - 654)
TBK1 E643delE	Colon	Deletion inframe	N/A	N/A	COSMIC	Helical scaffold dimerization domain (p. 408 - 654)
TBK1 L658fs*23	Colon	Deletion frameshift	N/A	N/A	COSMIC	C-terminal domain (p. 658 - 745)
TBK1 I397fs*5	Caecum	Insertion frameshift	N/A	N/A	COSMIC	Near ubiquitin-like domain (p. 309 - 384); Near helical scaffold dimerization domain (p. 408 - 654)

Table 2. Description and location of the point mutations found in the large intestine of patient tumor samples (COSMIC and TCGA database) with predicted functional impact determined by mutationassessor.org.

To predict the functional impact of the missense *TBK1* mutations listed in Table 2, each mutation was assessed using the software application at mutationasessor.org. Functional impact scores were calculated using the algorithm provided by mutationassessor.org, which is based on scores using multiple sequence alignments with an assumption that protein function is likely affected by specific substitutions of conserved residues. A “neutral” or “low” score for functional impact predicts that a specific mutation would have no influence on the function of the protein of interest whereas a “medium” or “high” score predicts that the mutation likely may alter the function of the protein[102].

Figure 29. *APC*, *KRAS*, and *PIK3CA* mRNA expression correlates with *TBK1* mRNA expression in colorectal adenocarcinomas sampled from TCGA.

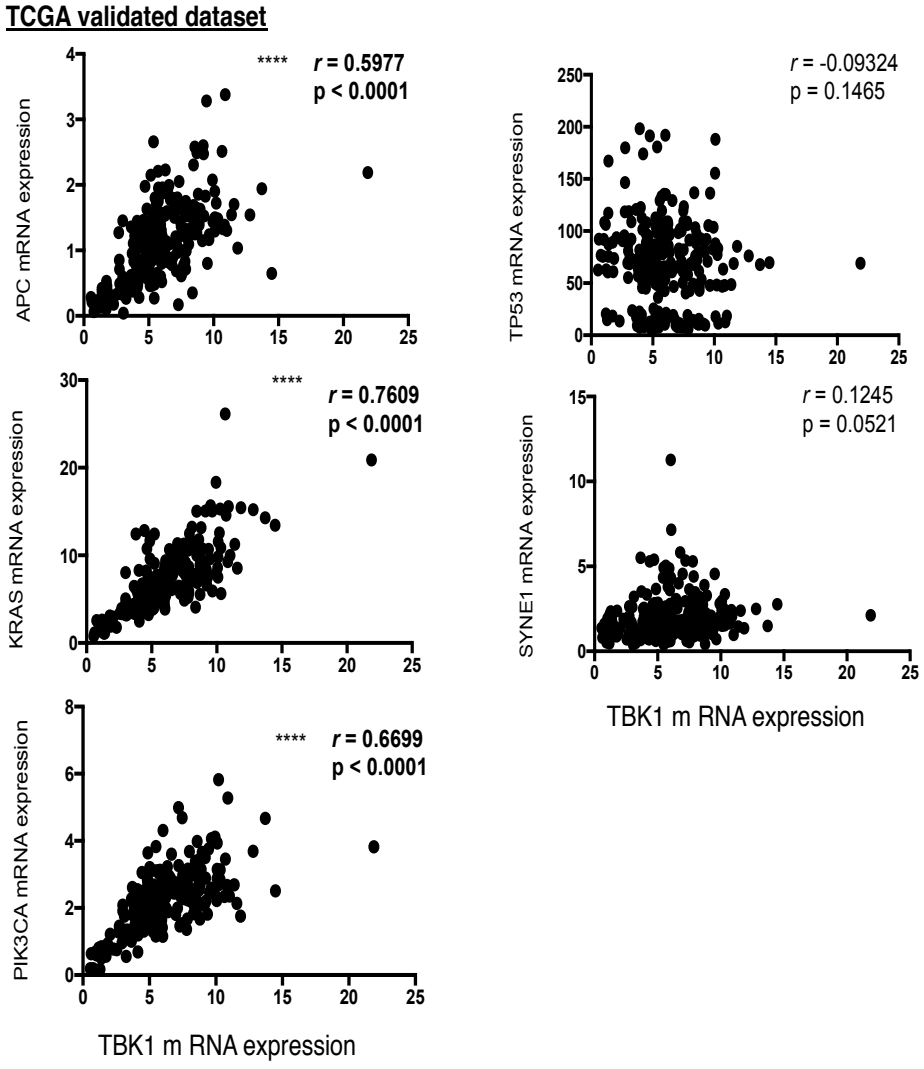

Figure 29. *APC*, *KRAS*, and *PIK3CA* mRNA expression correlates with *TBK1* mRNA expression in colorectal adenocarcinomas sampled from TCGA. Correlation between *TBK1* mRNA expression and mRNA expression of *APC*, *TP53*, *KRAS*, *SYNE1* and *PIK3CA* in the validated dataset (n=244) of TCGA. mRNA expression data were collected using the RNASeqV2 data are from validated genetic profiles of colorectal adenocarcinoma tumor samples in TCGA at www.cbioportal.org[74]. The Pearson correlation test was used to examine correlation between stages of disease. p-values of <0.05, <0.01, <0.001, <0.0001 correspond with (*), (**), (***), and (***) annotations respectively.

Figure 30. *IL10* mRNA expression correlates with *TBK1* mRNA expression in colorectal adenocarcinomas sampled from TCGA.

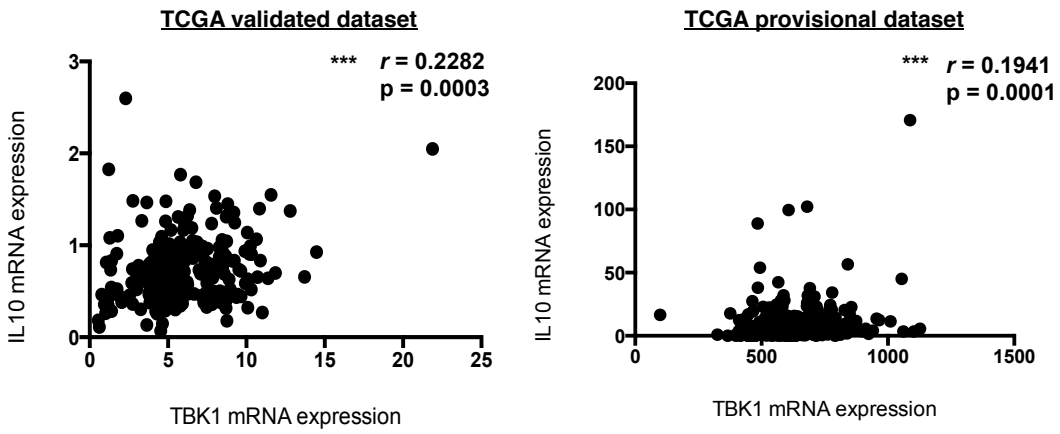

Figure 30. *IL10* mRNA expression correlates with *TBK1* mRNA expression in colorectal adenocarcinomas sampled from TCGA. Correlation between *TBK1* mRNA expression and *IL10* mRNA expression in the validated and provisional dataset of TCGA. mRNA expression data were collected using the RNASeqV2 data are from validated (n=244) and provisional (n=382) genetic profiles of colorectal adenocarcinoma tumor samples in TCGA at www.cbioportal.org[74]. The Pearson correlation test was used to examine correlation between stages of disease. p-values of <0.05, <0.01, <0.001, <0.0001 correspond with (*), (**), (***), and (***) annotations respectively.

CHAPTER 4: INVESTIGATING THE ROLE OF TBK1 IN HUMAN COLORECTAL CANCER CELLS

Chapter 4: Investigating the role of TBK1 in human colorectal cancer cells

Introduction

As discussed in previous chapters, TBK1 is involved in several signaling pathways such as pathogen recognition and immune response, inflammatory response and oncogenesis[40]. In particular, several reports have implicated TBK1 as a survival factor in cancer cells, especially KRAS-dependent lung cancer cell lines[45,60,62,66]. TBK1 knockdown by RNA interference in these human cancer cell lines promotes their apoptosis and suppresses their growth as xenograft tumors in immunocompromised mice[45,60,66]. The TBK1 knockdown has also been shown to sensitize tamoxifen-resistant breast cancer cells to tamoxifen treatment[72]. Despite these findings, the role of TBK1 in cancer regulation remained unclear and controversial prior to the commencement of this dissertation project. A recent study suggested that TBK1 knockdown by the majority of the TBK1 shRNAs has no specific effect on the survival of either KRAS-dependent or KRAS-independent human cancer cells, suggesting a potential off-target effect of the shRNAs used in previous studies[73]. Furthermore, pharmacological inhibition of TBK1 fails to significantly reduce the rate of cancer cell growth, despite the efficient blockade of the canonical TBK1 function in IRF3 phosphorylation[73]. These findings cause some confusion in the field that obviously warrants additional studies.

As described in Chapter 3 of this dissertation, our study using *Tbk1*$^{IEC\text{-}KO}$ mice in conjunction with the *Apc*$^{min/+}$ animal model of colon cancer has revealed an inhibitory role for TBK1 in regulating adenoma development. However, the role of

TBK1 in regulating the late-stages of CRC remains to be examined. We addressed this question by knocking down TBK1 in CRC cells and performing tumor formation studies using a xenograft model. In addition, we also employed a small molecule inhibitor of TBK1, MRT67307. While we have presented in this dissertation the limitations of these models, we found that TBK1 is dispensable for the survival of KRAS-competent human colon cancer xenograph tumors. We speculate that this may be attributable to the absence of T lymphocytes in this model.

Results

To knock down TBK1 in human CRC cells, we transduced human CRC HT-29 cells with either a control shRNA targeting luciferase or two different TBK1 shRNAs, TBK1 shRNA D5 and D9. The HT-29 cell line is a frequently used CRC cell line that carries *APC* mutations[104,105] but is KRAS wildtype. These cells resemble our animal studies using the $Apc^{min/+}$ mice in Chapter 3 in that they have deregulated Wnt signaling due to impaired APC function. Since TBK1 shRNA D5 had a much higher knockdown efficiency than TBK1 shRNA D9 (Figure 22A), we used the D5-transduced HT-29 cells for the xenograft model of studies. To avoid rejection of the human cells by mouse immune system, we used the lymphocyte-deficient nude (nu/nu) mice as recipients for human colon cancer cell xenograft transplantation[106]. We injected the control or TBK1 shRNA D5 knockdown HT-29 cells into nu/nu mice subcutaneously at two sites per mouse, measured the tumor size twice each week, and calculated tumor volume based on the formula volume = (length x width^2) x 0.52. We observed that TBK1 knockdown in HT-29 cells had no effect on size of tumors

developing in the immunodeficient xenograft mouse model (Figure 22B, C and D). Thus, TBK1 is dispensable for the growth and survival of CRC HT-29 cells under xenograft conditions.

Since TBK1 has been implicated in the survival regulation of KRAS-dependent cancer cells[60,62,66,73], we next performed TBK1 knockdown in a CRC cell line, LoVo, a known to carrier of *KRAS* mutations. We used the more efficient TBK1 shRNA D5 to knockdown TBK1 in LoVo cells and analyzed cell growth and cell death in culture. After TBK1 knockdown *in vitro* (Figure 23A), LoVo cells had decreased cell numbers and cell viability over time compared to control cells transduced with the luciferase shRNA-encoding vector (Figure 23B, C and D). This result is consistent with the claim in the literature that TBK1 mediates the survival of KRAS-dependent cancer cells[60,62,66,73].

To elucidate the molecular mechanism by which TBK1 mediates LoVo cell growth and survival, we examined the effect of TBK1 knockdown on the activation of two major kinases, AKT and mTORC1, associated with cell growth and survival. We measured the activation of AKT based on its phosphorylation at serine-473 and the activation of mTORC1 based on phosphorylation of a downstream protein, S6. We used the HT-29 cell line as a control, since the growth and survival of these cells are insensitive to TBK1 knockdown. Interestingly, the TBK1 knockdown by shRNA D5 resulted in inhibition of AKT activation in both the HT-29 and LoVo cells, although the effect on S6 phosphorylation was somewhat variable (Figure 24). This finding was intriguing, since TBK1 knockdown had no obvious effect on the growth of HT-29

in the xenograft model. It is possible that the reduction in AKT phosphorylation may be compensated by some other signaling pathways, particularly those downstream of the KRAS. It is also important to note that this result is based on only one TBK1 shRNA, since the shRNA D9 was inefficient in TBK1 knockdown.

The pharmacological compound MRT67307 is a TBK1 inhibitor that has been shown to inhibit the induction of IRF3 phosphorylation and IFN-β production in macrophages[107]. Since the process of shRNA knockdown is long, the system may have the potential problem of selecting abnormal cell populations with a growth advantage. So, we performed independent studies by employing the TBK1 inhibitor MRT67307. Surprisingly, MRT67307 treatment did not appreciably affect the phosphorylation of AKT as revealed using the TBK1 knockdown system with HT-29 and LoVo cells (Figure 25). Moreover, this treatment led to the drastic induction of S6 phosphorylation, indicative of mTORC1 activation. The reasons for these contradictory results are unclear, but may be due to transient nature of pharmacological inhibition as compared to the stability of the knockdown system.

Discussion

The results of this study suggest that TBK1 is dispensable for the growth and survival of CRC HT-29 cells under xenograft conditions. Taken together with our animal studies using *Apc*$^{min/+}$ mice described in Chapter 3, these findings suggest that TBK1 may not be involved in the intestinal tumor growth and/or survival of the CRC cells under KRAS-competent conditions. Furthermore, our animal studies under lymphocyte-free conditions in Chapter 3 revealed that the tumor-regulating

function of TBK1 is dependent upon the presence of functional lymphocytes. Therefore, it is possible that the function of TBK1 in CRC cell xenograph tumor growth may be masked by the absence of functional T lymphocytes.

The results of this study suggest a role for TBK1 in regulating the survival of a KRAS-dependent CRC cell line, LoVo, although not a KRAS-independent cell line, HT-29. This finding KRAS-dependent function of TBK1 is consistent with the previous work performed using lung cancer cell lines though the underlying signaling mechanism of this function is still unclear. Our attempt to elucidate this molecular mechanism revealed some inconsistent results. While TBK1 knockdown using shRNA suggests a role for TBK1 in mediating activation of AKT, inhibition of TBK1 with a pharmacologic inhibitor surprisingly did not lead to AKT inhibition. Instead, the TBK1 inhibitor strongly promoted the phosphorylation of S6, a downstream target of the metabolic kinase mTORC1. The reasons for conflicting results are unclear. As discussed above, one difference between the pharmacological inhibition and the shRNA knockdown strategies is that the former is a more transient event, whereas the latter represents a more steady state following a long period of cell selections. Another possibility is that MRT67307 may non-specifically inhibit additional kinases, thus causing the activation of the mTORC1 pathway. Alternatively, these results may reflect the loss of the adaptor function of TBK1 in knockdown systems compared to the blockade of the kinase function of TBK1 using TBK1 pharmacological inhibitor. This is possible given that other domains such as the ULD, SDD, and CTD of TBK1 mediate the recruitment of TBK1 to specific binding

partners and the substrate specificity and phosphorylation by TBK1[41-43,45,84]. Clearly, these studies further highlight the high levels of variations in *in vitro* studies using cancer cell lines, emphasizing the necessity of additional studies using different approaches including genetic animal models as presented in Chapter 3 and the recently developed CRISPR-knockout system.

.

Figure 31. TBK1 knock-down in human colon cancer cell line HT-29 has no effect on tumor size in a mouse xenograft model.

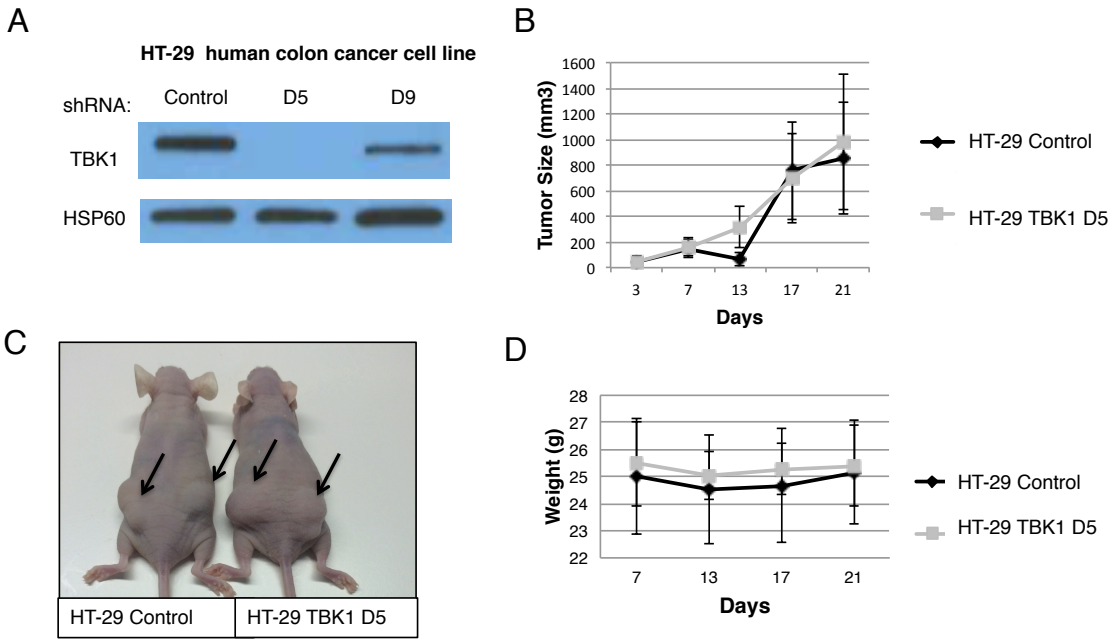

Figure 31. TBK1 is dispensable for xenograph tumor growth using KRAS-competent human HT-29. A) Western blot analysis of TBK1 in HT-29 cells transduced with a vector encoding a TBK1 shRNA (D5 or D9) or a control luciferase shRNA (control shRNA). B) Growth curve of xenograph tumors grown in nu/nu mice (n=5 each group; two tumors per mouse) injected subcutaneously with HT-29 cells transduced with control luciferase shRNA- or TBK1 D5 shRNA-encoding vectors. Data are presented as mean ± SD and are a representative of two independent experiments. C) Representative image of tumor sizes at day 21 post-injection of nu/nu mice with HT-29 cells transduced with control shRNA- or TBK1 D5 shRNA-encoding vectors. D) Change in weight (g) of the nu/nu mice post-injection with HT-29 cells transduced with control shRNA- or TBK1 D5 shRNA-encoding vectors. Data are presented as mean ± SD.

Figure 32. TBK1 knockdown in LoVo cells reduces cell viability *in vitro*.

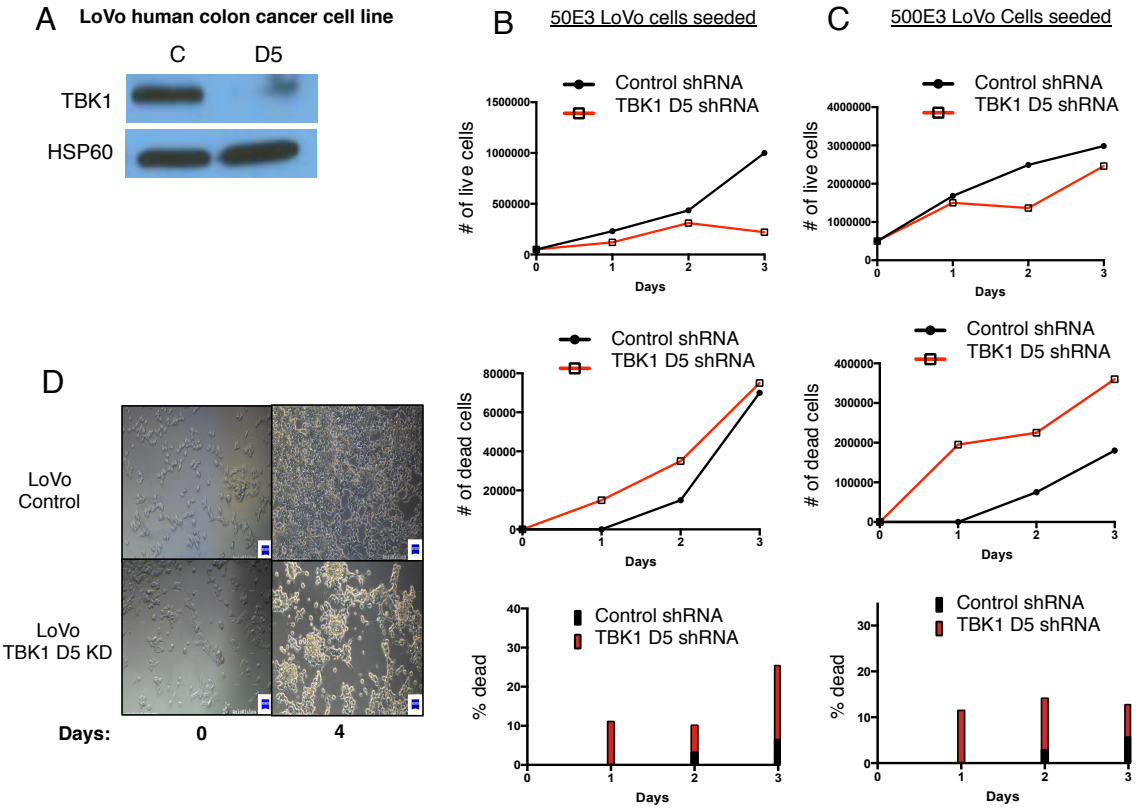

Figure 32. TBK1 knockdown in LoVo cells reduces cell viability *in vitro*. A) Western blot analysis of TBK1 in LoVo cells transduced with a vector encoding a TBK1 shRNA (D5) or a control luciferase shRNA (control shRNA). LoVo cells transduced with control luciferase shRNA- or TBK1 D5 shRNA-encoding vectors were seeded at B) 50×10^3 cells/well or C) 500×10^3 cells/well. Live (top B and C) and dead (middle B and C) cells were counted at indicated days post-seeding using trypan blue exclusion. Cell survival was determined as the percentage of dead cells (bottom B and C) in total cells counted. D) Representative images of LoVo cells transduced with a vector encoding a TBK1 shRNA (D5) or a control luciferase shRNA (control shRNA) in culture at days 1 and 4 post-seeding. Data represents one experiment.

Figure 33. TBK1 knockdown in CRC cells inhibits AKT and mTORC1 activation.

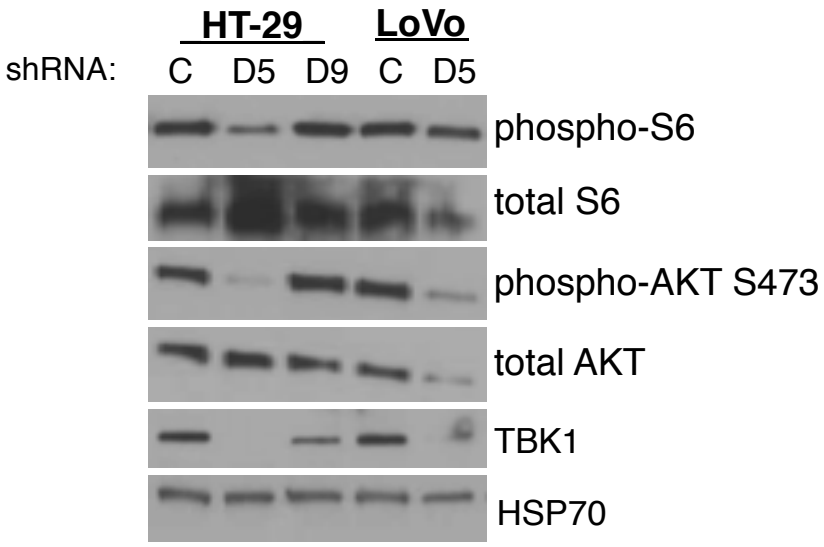

Figure 33. TBK1 knockdown in CRC cells inhibits AKT and mTORC1 activation. Western blot analysis of the indicated proteins in whole-cell lysates from HT-29 and LoVo cells stably transduced with control luciferase shRNA- or TBK1 shRNA-encoding vectors as indicated. Data represents three independent experiments.

Figure 34. Pharmacological inhibition of TBK1 activates AKT and mTOR pathways in CRC cells.

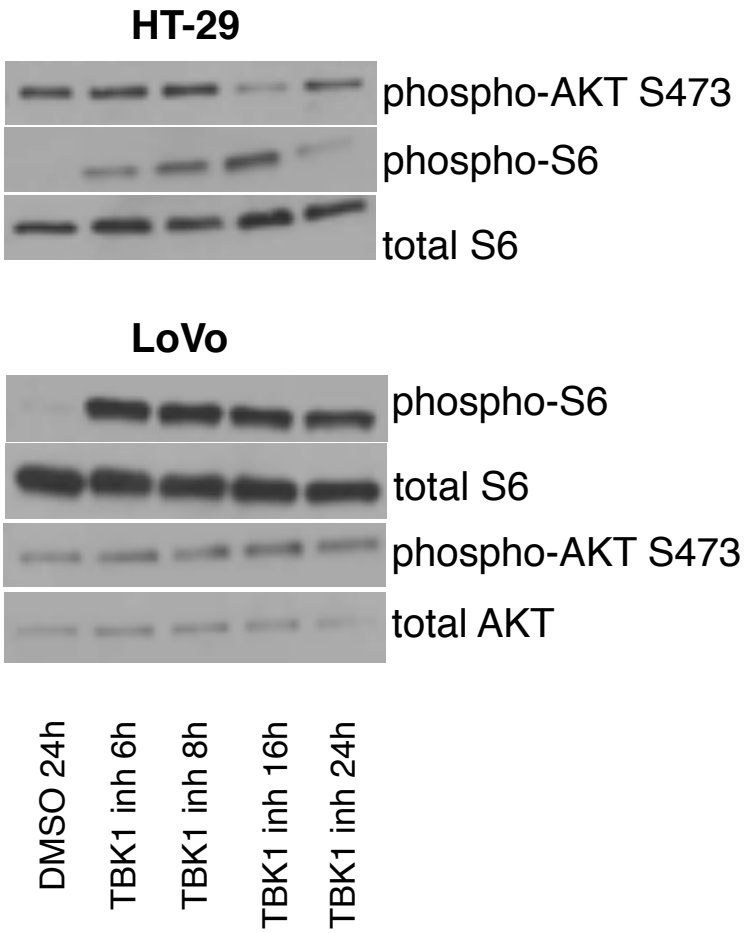

Figure 34. Figure 25. Pharmacological inhibition of TBK1 activates AKT and mTOR pathways in CRC cells. Western blot analysis of the indicated proteins in whole-cell lysates from HT-29 and LoVo cells with MRT67307 (TBK1 inh) or dimethyl sulfoxide (DMSO) at indicated times (hours). Data represents two independent experiments.

CHAPTER 5: OVERVIEW, DISCUSSION AND FUTURE DIRECTIONS

Chapter 5: Overview, Discussion and Future Directions

The primary objective of this work was to determine the role of TBK1 in the tumorigenic process *in vivo*. We present the first *in vivo* model to demonstrate TBK1's function during intestinal adenoma development and suggest a mechanism of TBK1 action. Moreover, this project presents the use of a novel approach in determining TBK1's role in early cancer development *in vivo* in addition to the xenograft model currently described in the literature for other cancer types. The following sections will summarize and discuss the major findings of this dissertation.

1. TBK1 is a novel inhibitor of intestinal adenoma growth

In Chapter 3, we generated and characterized an innovative mouse model in which TBK1 is conditionally deleted in IECs, leading to the discovery that TBK1 has a tumor-suppressive function in the intestine. In particular, IEC-specific *Tbk1* ablation promotes adenoma development in mice carrying a heterozygous mutation in the tumor suppressor *Apc* gene, an alteration commonly found in the earlier stages of CRC development[16].[18] The effect of TBK1 deficiency on adenoma formation is diminished in the absence of lymphocytes demonstrated herein by IEC-specific *Tbk1* deletion in $Apc^{min/+}$ mice having no effect on the formation of intestinal polyps under lymphocyte-free conditions. Those results suggest that IEC-specific TBK1 regulates an aspect of adaptive immune homeostasis.

Moreover, intestinal T lymphocytes, specifically Tregs, are required for immune homeostatic maintenance of the gut, suppressing inflammatory responses to commensal organisms in an IL-10-dependent manner. [33, 32] While IEC-specific

TBK1 does not seem to regulate IL-10 expression in intestinal Tregs in *Apc*$^{min/+}$ mice, it is required for IL-10 expression by IELs, another major producer of intestinal IL-10[33, 32], during the early stages of the tumorigenic process. Indeed, intestinal IELs suppression of intestinal inflammation is IL-10-mediated.[39] Thus, we identified a new role for TBK1 as an important facilitator of crosstalk between IECs and intestinal IELs that controls the expression of *Il10* under an *Apc*$^{min/+}$ background. It is important to confirm impaired IL-10 protein levels in intestinal IELs upon IEC-specific *Tbk1* deletion in *Apc*$^{min/+}$ mice to corroborate our findings. In later experiments, we will perform IL-10-specific intracellular staining and use flow cytometry to determine IL-10 protein expression in IELs at the single-cell level and we expect impaired IL-10 production by IELs after IEC-specific *Tbk1* ablation.

Given that impaired IL-10 production in the intestine is linked to enhanced inflammatory disease and intestinal tumorigenesis[37,108-111], it is likely that the diminished *Il10* expression by the IELs contributes to the elevated adenoma formation in the *Apc*$^{min/+}$*Tbk1*$^{\text{IEC-KO}}$ mice. To confirm this, we are generating *Apc*$^{min/+}$*Tbk1*$^{\text{IEC-KO}}$ mice on an IL-10-deficient background. We expect the difference between *Apc*$^{min/+}$ and *Apc*$^{min/+}$*Tbk1*$^{\text{IEC-KO}}$ mice to be abolished after *Il10* deletion.

The next question to be addressed is how TBK1 functions within IECs to affect *Il10* expression by IELs. We hypothesize that TBK1 may regulate the expression of either surface protein(s) or secretory factor(s) by IECs that in turn induces IL-10 production by IELs. Considering that the role of TBK1 is well established in regulating type I interferon induction and that IL-10 is an interferon-

responsive gene[95,112-116], it is possible that TBK1 regulates the expression of type I interferons by IECs thereby regulating IL-10 expression by IELs. While the expression levels of IFN-α and -β were comparable in the intestines of *Apc*$^{min/+}$ and *Apc*$^{min/+}$ *Tbk1*$^{IEC-KO}$ mice, it is possible that potential differences in their expression could be masked by lack of commensal stimulation of IECs during intestinal preparation prior to analysis. To overcome this technical obstacle, we will stimulate IECs with PRR agonists after intestinal preparation prior to analysis of type I interferon expression. We expect defective type I interferon expression upon PRR stimulation in IECs deficient in TBK1.

If TBK1 is dispensable for IFN expression by IECs, an alternative hypothesis may be that TBK1 regulates the expression of transmembrane protein semaphorin (Sema) 7A, thus regulating IL-10 expression by IELs. Semaphorins are classically described as regulators of neuronal cell signaling but have recently been found to function in various organs and cell types, including immune cells[114]. Specifically, Sema7A is expressed in brain, lung, intestines, thymus, lymphocytes, and macrophages[117] to name a few. It is also expressed on thymocytes preferentially during selection and during activation in the periphery[46,57,116]. Sema7a deficiency in T cells leads to a reduction in inflammatory responses, whereas its overexpression can stimulate macrophages and monocytes via interaction with $\alpha_1\beta_1$ integrin to secrete proinflammatory cytokines [118,119]. A recent study examined Sema7a in the intestine and found that its expression on IECs induces IL-10 production by intestinal macrophages to negatively regulate chemically-induced colitis[120]. We will examine

the expression level of Sema7a in IECs of *Apc*$^{min/+}$ and *Apc*$^{min/+}$*Tbk1*$^{IEC\text{-}KO}$ mice. In addition, we will employ a more systematic approach to compare gene expression profiles between the IECs of *Apc*$^{min/+}$ and *Apc*$^{min/+}$*Tbk1*$^{IEC\text{-}KO}$ mice by RNA sequencing. Together, these future studies will likely provide more insight into the mechanism underlying the IEC-specific function of TBK1 in regulating adenoma formation.

2. TBK1 is dispensable for growth and survival of KRAS-independent human CRC cells

In Chapter 4, we employed a *TBK1* knockdown system using KRAS-dependent and KRAS-independent human CRC cell lines, leading to the conclusion that, under T lymphocyte-free conditions, TBK1 is dispensable for the growth and survival of xenograph tumors derived from KRAS-independent human CRC cell lines. However, consistent with earlier findings, TBK1 regulates the survival of a KRAS-dependent CRC cell lines *in vitro*. Given the immunocompromised status of the CRC cell recipient mice, it would be interesting to determine whether the tumor-regulating function of TBK1 in KRAS-independent human CRC cells is masked by the absence of T lymphocytes similar to what we observed in our study using *Tbk1*$^{IEC\text{-}KO}$ mice in *Apc*$^{min/+}$ background. Furthermore, our attempt to elucidate the molecular mechanism underlying this function of TBK1 was met with inconsistent results further highlighting the need for multiple approaches to gain more insight.

As mentioned in Chapter 2, the use of animal models has revealed important cellular and molecular players involved in CRC development and progression. One

challenge in determining the *in vivo* function of TBK1 has been the embryonic lethality of conventional *Tbk1* KO mice[56]. In this project, we overcame this obstacle by generating *Tbk1* IEC-conditional KO mice, which provided genetic evidence that TBK1 suppresses intestinal adenoma development by regulating the intestinal adaptive immune system. It would be interesting to determine if the cell survival function of TBK1 would persist in the presence of T lymphocytes since these studies used immunocompromised hosts lacking T lymphocytes. Ironically, we show in Chapter 4 that TBK1 deficiency in KRAS-independent human CRC cells had no effect on xenograph tumor growth in immunocompromised hosts, a finding that parallels our results in Chapter 3 where the IEC specific-TBK1 deficiency has little effect on intestinal polyp formation in $Apc^{min/+}$ mice lacking lymphocytes. Further studies are needed to determine if TBK1 regulates a part of the adaptive immune homeostasis that is masked by the absence of T cells in xenograph tumor models. Furthermore, we have shown here that TBK1 inhibits intestinal adenoma development at early stages under an $Apc^{min/+}$ background. Because the survival function of TBK1 has been mainly attributed to the human cancer cells dependent upon KRAS, the question remains if TBK1 exerts similar or distinct functions in different oncogenic pathways under lymphocyte-competent conditions. The findings of this project begin to address this question, which could have significant clinical implications and impact the direction of the field. There is a strong and very significant positive correlation between *TBK1* expression and the expression of *APC* in the patient samples of colorectal adenocarcinomas, a finding that is consistent

with the results using our *Apc*$^{min/+}$ mice with IEC-specific *Tbk1* ablation presented herein. A similar trend – a strong and very significant positive correlation – was also observed between expression of *TBK1* and *KRAS* in patient samples. One could hypothesize that TBK1 negatively regulates tumor progression in *KRAS* mutant colon cancer given the strong relationship between expression of the two genes. In support of this hypothesis, levels of *TBK1* expression correlate positively between early and late stages of disease. Thus one could speculate that TBK1 functions similar in the late stages of colorectal cancer which have acquired *KRAS* and *PIK3CA* genetic mutations as it does during early stages of disease where LOH of APC commonly occurs. Additional analyses testing this idea using *KRAS* and *PIK3CA in vivo* models as presented in this dissertation using *Apc*$^{min/+}$ mice would provide a better understanding of the molecular mechanisms mediating advancement of the disease.

Chapter 6 Materials and Methods

Mice. Age-matched *Tbk1* intestinal epithelial cell-conditional KO (*Tbk1*$^{IEC-KO}$) and wildtype mice were generated by crossing *Tbk1* floxed mice [48](Taconic) with *villin*-Cre mice (Jackson Laboratory). IEC-conditional *Tbk1* mice were further crossed with *Apc*$^{min/+}$ mice (Jackson Laboratory) to generate *Apc*$^{min/+}$ or *Apc*$^{min/+}$*Tbk1*$^{IEC-KO}$ mice. In some experiments, the *Apc*$^{min/+}$*Tbk1*$^{IEC-KO}$ mice were further crossed with *Rag1*-/- (*Rag1* KO) (Jackson Laboratory) mice to generate *Apc*$^{min/+}$ *Rag1* KO or *Apc*$^{min/+}$*Tbk1*$^{IEC-KO}$ *Rag1* KO mice. The *Tbk1* floxed mice had a 129Sv/Ev background, villlin Cre transgenic mice had a mixed background, the *Apc*$^{min/+}$ and *Rag1* KO mice were of C57BL/6 background. The mice were maintained at The University of Texas M.D. Anderson Cancer Center facility under specific pathogen-free conditions. Animal experiments were performed in accordance with protocols approved by the Institutional Animal Care and Use Committee.

Antibodies and reagents. Antibodies for recognizing TBK1, phospho-AKT ser473 (D9E), AKT1 (B-1), phospho-S6 Ser235/236 (D57.2.2E), and S6 (54D2) were from Cell Signaling. β actin (C-4), HSP 60 and HSP 70 were from Sigma Aldrich. The MRT673037 TBK1 inhibitor was from Chemexpress.

Cell lines. The human colon cancer cell lines HT-29 and LoVo and the human embryonic kidney (HEK) 293 cells were cultured in DMEM (Dulbecco's modified Eagle's medium) supplemented with 10% FBS and 1% streptomycin/penicillin.

Gene silencing. To produce the lentiviral particles, the pLKO.1 vectors encoding control luciferase or encoding specific *TBK1* shRNA (either *TBK1* shRNA D5 or D9) were transfected into HEK293 cells (using the calcium method) along with the packaging vectors psPAX2 and pMD2 provided by X. Qin. Human colon cancer cell lines were then infected with packaged viruses carrying either luciferase, *TBK1* shRNA D5 or *TBK1* shRNA D9. After 48 hours, infected cells were treated with puromycin (1 ug/mL) for seven days to select for vector positive cells.

IEC isolation. Intestines were harvested, cut longitudinally and wash with PBS to remove fecal contents. Intestines were incubated in HBSS (Hank's Buffered Salt Solution) containing 10 mM EDTA at 37°C for five minutes in water bath. Supernatants were discarded and intestines incubated with PBS containing 1 mM EDTA and 1 mM DTT for 15 minutes in 37°C water bath. Suspension was shook vigorously and supernatants were collected and washed twice with ice-cold PBS.

IEL and LP cell isolation. Mice were sacrificed and intestine resected. Feces were removed by flushing with cold HBSS. The intestines were longitudinally opened, cut into ~0.5cm pieces and incubated in Solution I (5% FBS, 2 mM EDTA, 1mM DTT, 10 mM HEPES in HBSS) at 37°C for twenty minutes. Pieces were vortexed briefly and pass intestine through a (100 micron) filter. Supernatant were collected as IELs and IECs. New Solution I was added to the intestinal pieces and subsequent steps

repeated to collect more IELs. Intestinal pieces were then rinsed with HBSS with 10mM HEPES and supernatant combined with IEL and IEC collected. Percoll density gradient or CD45 bead separation was used to enrich for IELs. Intestinal pieces were incubated in Solution II (5% FBS, 1 mg/mL Collagenase D, 0.1 mg/mL Dnase I in RPMI 1640) at 37°C for 30 minutes. Suspension was vortexed briefly and filtered to collect the lamina propria cells. New solution II was added to the intestinal pieces and subsequent steps repeated. Flow-through was combined and suspension was centrifuged at 300*g* for ten minutes. Supernatant was discarded and LP cells were stained with antibody or used in indicated experiments.

Bromodeoxyuridine (BrdU) assay. BrdU incorporation assay was performed according to manufacturer's (Life Technologies) instructions. Six to eight week old mice were injected with BrdU (Sigma-Aldrich) intraperitoneally at 50 ug per gram of mouse body weight. Five hours after injection, mice were sacrificed and intestines were resected and fixed in 10% Buffered Formalin Phosphate (Fisher Scientific) overnight. Intestines were cleaned of feces, swiss-rolled, and paraffin-embedded. Five micron BrdU-labeled tissue sections were deparafinized using xylene, hydrated in series of graded ethanol as preparation for BrdU immunohistochemical staining. Per the manufacturer's kit, tissue sections were peroxidase quenched, trypsinized, denatured, blocked and incubated with biotinylated anti-BrdU antibodies. After washing with PBS, tissue was incubated with streptavidin-peroxidase, rinsed, developed, and counterstained. After tissue dehydration, tissue was mounted using

Permount (Fisher Scientific). Tissues were analyzed using brightfield filters of Olympus BX41 microscope with Olympus DP70 camera. BrdU positive cells were counted using count tool of Adobe Photoshop CS4 software and counting the number of positively labeled cells and hematoxylin stained nuclei of either crypt, villus, or microadenoma within the image from which percentage positive was determined per crypt, per villus, or per microadenoma.

TUNEL assay. For TUNEL staining, the DeadEnd Fluorometric TUNEL System (Promega) was employed. Per the manufacturer's instructions, formalin fixed five micron paraffin-embedded tissue sections were deparafinized and dehydrated using xylene and graded ethanol washes. Sections were immersed in 0.85% NaCl followed by PBS washing and 10% buffered formalin fixation. After PBS washing, sections were digested using Proteinase K solution at 20 ug/mL for 20 minutes at room temperature. Sections were PBS washed and refixed in 10% buffered formalin and rewashed in PBS. Sections were biotin blocked using Avidin/Biotin Blocking Kit from Vector Laboratories, Inc. After washing in PBS, sections were equilibrated using manufacturer-provided equilibration buffer in the TUNEL System kit. Fragmented DNA within cells were fluorescein-labeled for one hour at 37°C by using rTdT reaction mix provided by the TUNEL System kit. The reaction was terminated and washed in PBS. Prolong gold anti-fade reagent plus DAPI (Life Technologies) was used for tissue mount. Tissues were analyzed using fluorescent filters on Olympus BX41 microscope with an Olympus DP70 camera. TUNEL positive cells

were blindly counted using count tool of Adobe Photoshop CS4 software and counting the number of positively labeled cells and DAPI stained nuclei of the villus within the image from which percentage positive was determined per villus. For the microadenomas, TUNEL positive cells were counted using count tool of Adobe Photoshop CS4 software while DAPI stained nuclei were counted using Cell Profiler version 3 cell image analysis software (http://www.cellprofiler.org). The analysis pipeline included identifying region of microadenoma and cropping within individual image, saving cropped images for subsequent identification and automated enumeration of DAPI stained nuclei as determined by automated image thresholding.

Xenograft injection. Transduced HT29 cells with *TBK1* shRNA (*TBK1* KD) (2×10^6 cells) or control luciferase shRNA (2×10^6 cells) that were injected into immunodeficient nu/nu mice (n=5 each group; two injected tumors per mouse) subcutaneously. Tumor size was measured twice per week and tumor volume was calculated using the defined formula (tumor volume = (length x width^2) x 0.52). Weight of the mice was measured twice per week post injection.

Ki67 immunohistochemical staining. Mice were sacrificed and intestines were resected and fixed in 10% Buffered Formalin Phosphate (Fisher Scientific) overnight. Intestines were cleaned of feces, swiss-rolled, and paraffin-embedded. Tissue sections were deparafinized using xylene, hydrated in series of graded ethanol as

preparation for immunohistochemical staining. Antigen was retrieved by boiling tissue section in Citrate Buffer pH 6 (Sigma-Aldrich) for 20 minutes. Tissue was allowed to cool to room temperature, was blocked using 3% BSA in PBS, and incubated overnight with Ki67 (D3B5) antibody (Cell Signaling). After one hour incubation with secondary antibody, tissue was developed using DAB substrate kit (Abcam). Tissues were blindly using bright field filters of Olympus BX41 microscope with Olympus DP70 camera and counted blindly using Adobe Photoshop CS6 count tool.

Western blot. Whole-cell extracts of the cells were harvested using cell extraction buffer containing 50 mM Tris, pH 7.4, 150 mM NaCl, 1 mM EDTA, 1% NP-40, 0.5% deoxycholate, 1 mM phenylmethylsulfonyl fluoride, 50 mM p-nitrophenyl phosphate and 0.3 μM Aprotinin. Samples were extracted for ten minutes on ice and centrifuged at 13,000 RPM for one minute at 4°C. Lysates were analyzed for protein quantity using Bradford assay. Proteins were separated using SDS-PAGE and proteins were transferred to nitrocellulose membrane. Membranes were blocked using 5% non-fat dry milk at room temperature for one hour. Membranes were incubated with primary antibody indicated overnight at 4°C. Detection was performed using enhanced chemiluminescence reagents and exposed to light film.

Flow cytometry. Single-cell suspensions of IELs and lamina propria immune cells were subjected to flow cytometry using LSR II (BD Bioscience) flow cytometer.

FlowJo software was used to analyze the data. The fluorescence-labeled antibodies that were used included TCR γδ FITC-conjugated (BD bioscience), (eBioscience); CD11c Pacific Blue-conjugated (BD Bioscience); CD45 PE-conjugated (BD Bioscience); CD11b APC-Cy7-conjugated (BD Bioscience); and TCRβ APC-conjugated (eBioscience).

Real-time quantitative RT-PCR (qPCR). For RNA extraction of tissues, intestines were resected cleaned of feces using ice cold PBS. Tissues were flash frozen in liquid nitrogen and ground using a pestle and mortar. Total RNA was isolated using TRIzol reagent (Invitrogen) and subjected to cDNA synthesis using RNase H-reverse transcriptase (Invitrogen) and oligo (dT) primers. For cells, TRIzol reagent was added directly. Real-time quantitative PCR was performed in triplicates, using iCycler Sequence Detection System (Bio-Rad) and iQTM SYBR Green Supermix (Bio-Rad). The expression of individual genes was calculated by a standard curve method and normalized to the expression of beta-actin. The gene-specific primer sets used (all for mouse genes) were as follows in the table below.

Gene	**Primer**	**Primer sequence**
m*Il10*	forward	CCAGAGCCACATGCTCCTAGA
	reverse	GGTCCTTTGTTTGAAAGAAAGTCTTC
m*Tnfα*	forward	CATCTTCTCAAAATTCGAGTGACAA
	reverse	CCAGCTGCTCCTCCACTTG
m*Il6*	forward	CACAGAGGATACCACTCCCAACA

	reverse	TCCACGATTTCCCAGAGAACA
m*Il17a*	forward	AGCGATGGTGGATGGCTCATGGTTAG
	reverse	AGCTTTCCCTCCGCATTGACACAG
m*Cxcl9*	forward	TAGGCAGGTTTGATCTCCGT
	reverse	CGATCCACTACAAATCCCTCA
m*Cxcl10*	forward	CCTATGGCCCTCATTCTCAC
	reverse	CTCATCCTGCTGGGTCTGAG
m*Cxcl11*	forward	CGCCCCTGTTTGAACATAAG
	reverse	CTGCTGAGATGAACAGGAAGG
m*Ccl2*	forward	GGGATCATCTTGCTGGTGAA
	reverse	AGGTCCCTGTCATGCTTCTG
m*Ifnb*	forward	AGCTCCAAGAAAGGACGAACAT
	reverse	GCCCTGTAGGTGAGGTTGATCT
m*Ifna*	forward	AGTCCATCAGCAGCTCAATGAC
	reverse	AAGTATTTCCTCACAGCCAGCAG
m*Ifng*	forward	CAGCAACAGCAAGGCGAAA
	reverse	CTGGACCTGTGGGTTGTTGAC
m*Il17f*	forward	CCCATGGGATTACAACATCACTC
	reverse	CACTGGGCCTCAGCGATC
m*Lgr5*	forward	TCCAACCTCAGCGTCTTC
	reverse	TGGGAATGTGTGTCAAAG
m*Axin2*	forward	TCCATACAGGAGGATGCTGAAG

	reverse	TTCGTCACTCGCCTTCTTGA
m*Muc2*	forward	ATGCCCACCTCCTCAAAGAC
	reverse	GTAGTTTCCGTTGGAACAGTGAA
m*BclX*$_L$	forward	TCTGAATGACCACCTAGAGC
	reverse	GGTCAGTGTCTG GTCACTTC
m*Il22*	forward	TCCGAGGAGTCAGTGCTAAA
	reverse	AGAACGTCTTCCAGGGTGAA
m*Il1β*	forward	AAGCCTCGTGCTGTCGGACC
	reverse	TGAGGCCCAAGGCCACAGGT

Mouse *Reg3b* qPCR primers set (Primer Pair ID M_Reg3b_1- gene ID 18489) was purchased from Sigma-Aldrich.

AOM and DSS experiments. For the chemical-induced colitis model, mice were treated with dextran sodium sulfate (DDS)[121] (MP Biomedical LLC) as indicated for either five or seven days with two-day water recovery period[70]. Mice were weighed once per day during this treatment period and sacrificed at day two after water recovery. The small intestine and colons were resected, formalin-fixed, sectioned, H & E stained, and histologically scored based on the criteria in Table 1. For the carcinogen-induced, chronic inflammation-induced colon cancer model, mice were treated with a single dose of azoxymethane (AOM) (Sigma-Aldrich) and three cycles of 2.5% DSS for five days and water for 14 days[92]. Mice were weighed once per

week throughout treatment. After sacrificing the mice, the colons were resected, measured in length, and formalin-fixed overnight. Intestines were cleaned of feces and polyps were counted using Olympus SZX10 stereomicroscope.

Adenoma and microadenoma analysis. For intestinal adenoma analyses, mice were sacrificed and intestines were resected and formalin-fixed overnight. Intestinal feces were cleaned out and tissues were cut longitudinally. Using Olympus SZX10 stereomicroscope, Olympus DP70 camera, and Olympus CellSens Standard software, adenomas were counted and measured for length after staining with 0.2 % methylene blue and decolorizing with ethanol. For microadenoma analyses, mice were sacrificed and intestines were resected and formalin-fixed overnight. Intestinal feces were cleaned out and tissues were cut longitudinally and swiss-rolled. Intestines were cleaned of feces, cut longitudinally, swiss-rolled, and paraffin-embedded. H&E stained section at 100 micron intervals through 500 microns of the intestinal tissue was scored for microadenomas defined as histological dysplastic lesions characterized by focal areas of abnormally large gland(s)[17].

Statistical analysis. GraphPrism 6 (GraphPad, La Jolla, CA, USA) was used where indicated for two-tailed unpaired t-tests. p-values <0.05 and <0.01 correspond with (*) and (**) respectively. For TCGA dataset analyses, RNA expression were analyzed using the RNASeqV2 data from validated and/or provisional genomic and transcriptomic profiles of colorectal adenocarcinoma tumor samples and were accessed on December 12, 2015 at www.cbioportal.org[74]. Copy-number and overall

survival data were accessed similarly. GraphPrism 6 was used for statistical analyses and graphing. The Pearson correlation test was used to examine correlation between mRNA expressions and $\log_2$ copy-number of a gene in the TCGA datasets where correlations indicated. The survival data were visualized as correlation between mRNA expression or $\log_2$ copy-number of a gene and overall survival and analyzed using the Pearson correlation test. One-way ANOVA with Tukey's multiple comparisons test was used to analyze mean differences in mRNA expression levels between groups of putative copy-number alternations with the exception of the putative amplification group (n=1) and visualized as mean ± 95% confidence intervals with alpha of 0.05. The threshold for statistical significance in all test was $p<0.05$ with two-sided analysis. p-values of <0.05, <0.01, <0.001, <0.0001 correspond with (*), (**), (***), and (***) annotations respectively.

Bibliography

1. Jemal A, Bray F, Center MM, Ferlay J, Ward E, Forman D. Global cancer statistics. CA Cancer J Clin 2011;61:69-90.

2. Jemal A, Center MM, DeSantis C, Ward EM. Global patterns of cancer incidence and mortality rates and trends. Cancer Epidemiol Biomarkers Prev 2010;19:1893-907.

3. Howlader N NA, Krapcho M, Garshell J, Miller D, Altekruse SF, Kosary CL, Yu M, Ruhl J, Tatalovich Z, Mariotto A, Lewis DR, Chen HS, Feuer EJ, Cronin KA (eds). SEER Cancer Statistics Review, 1975-2011 Sect_01_table.01. National Cancer Institute Bethesda, MD 2014.

4. Siegel R, Naishadham D, Jemal A. Cancer statistics, 2013. CA Cancer J Clin 2013;63:11-30.

5. Siegel R, Ma J, Zou Z, Jemal A. Cancer statistics, 2014. CA Cancer J Clin 2014;64:9-29.

6. Siegel R, Desantis C, Jemal A. Colorectal cancer statistics, 2014. CA Cancer J Clin 2014;64:104-17.

7. Bailey CE, Hu CY, You YN, Bednarski BK, Rodriguez-Bigas MA, Skibber JM, Cantor SB, Chang GJ. Increasing Disparities in the Age-Related Incidences of Colon and Rectal Cancers in the United States, 1975-2010. JAMA surgery 2014:1-6.

8. Shackelford C, Elwell M. Small and Large Intestine, and Mesentery. In: Maronpot RR, ed. Pathology of the Mouse Reference and Atlas. 1st ed. Saint Louis, MO: Cache River Press; 1999:81-112.

9. Gastrointestinal Tract. In: Burkitt HG, Young B, Heath J, eds. Wheater's Functional Histology: A Text and Color Atlas. 3rd ed. Leith Walk, Edinburgh: Churchill Livingstone; 1993:247-70.

10. Finke D. Induction of intestinal lymphoid tissue formation by intrinsic and extrinsic signals. Semin Immunopathol 2009;31:151-69.

11. Murphy K, Travers P, Walport M, Janeway C. Janeway's immunobiology. 8th ed. New York: Garland Science; 2012.

12. Peterson LW, Artis D. Intestinal epithelial cells: regulators of barrier function and immune homeostasis. Nat Rev Immunol 2014;14:141-53.

13. McDole JR, Wheeler LW, McDonald KG, Wang B, Konjufca V, Knoop KA, Newberry RD, Miller MJ. Goblet cells deliver luminal antigen to CD103+ dendritic cells in the small intestine. Nature 2012;483:345-9.

14. Goto Y, Kiyono H. Epithelial barrier: an interface for the cross-communication between gut flora and immune system. Immunol Rev 2012;245:147-63.

15. Cheroutre H, Lambolez F, Mucida D. The light and dark sides of intestinal intraepithelial lymphocytes. Nat Rev Immunol 2011;11:445-56.

16. Terzić J, Grivennikov S, Karin E, Karin M. Inflammation and colon cancer. Gastroenterology 2010;138:2101-14.

17. Boivin GP, Washington K, Yang K, Ward JM, Pretlow TP, Russell R, Besselsen DG, Godfrey VL, Doetschman T, Dove WF, Pitot HC, Halberg RB, Itzkowitz SH, Groden J, Coffey RJ. Pathology of mouse models of intestinal cancer: consensus report and recommendations. Gastroenterology 2003;124:762-77.

18. Kinkler KW, Vogelstein B. Lessons from Hereditary Colorectal Cancer. Cell 1996;87:157-70.

19. Moser AR, Luongo C, Gould KA, McNeley MK, Shoemaker AR, Dove WF. ApcMin: a mouse model for intestinal and mammary tumorigenesis. Eur J Cancer 1995;A(7-8):1061-4.

20. McCart AE, Vickaryous NK, Silver A. Apc mice: models, modifiers and mutants. Pathol Res Pract 2008;204:479-90.

21. Taketo MM, Edelmann W. Mouse models of colon cancer. Gastroenterology 2009;136:780-98.

22. Yamada Y, Mori H. Multistep carcinogenesis of the colon in Apc(Min/+) mouse. Cancer Sci 2007;98:6-10.

23. Coletta PL, Muller AM, Jones EA, Muhl B, Holwell S, Clarke D, Meade JL, Cook GP, Hawcroft G, Ponchel F, Lam WK, MacLennan KA, Hull MA, Bonifer C, Markham AF. Lymphodepletion in the ApcMin/+ mouse model of intestinal tumorigenesis. Blood 2004;103:1050-8.

24. Erdman SE, Sohn JJ, Rao VP, Nambiar PR, Ge Z, Fox JG, Schauer DB. CD4+CD25+ regulatory lymphocytes induce regression of intestinal tumors in ApcMin/+ mice. Cancer Res 2005;65:3998-4004.

25. McClellan JL, Davis JM, Steiner JL, Day SD, Steck SE, Carmichael MD, Murphy EA. Intestinal inflammatory cytokine response in relation to tumorigenesis in the Apc(Min/+) mouse. Cytokine 2012;57:113-9.

26. Steinbach G, Lynch PM, Phillips RK, Wallace MH, Hawk E, Gordon GB, Wakabayashi N, Saunders B, Shen Y, Fujimura T, Su LK, Levin B, Godio L, Patterson S, Rodriguez-Bigas MA, Jester SL, King KL, Schumacher M, Abbruzzese J, DuBois RN, Hittelman WN, Zimmerman S, Sherman JW, Kelloff G. The effect of celecoxib, a cyclooxygenase-2 inhibitor, in familial adenomatous polyposis. N Engl J Med 2000;342:1946-52.

27. Kanneganti M, Mino-Kenudson M, Mizoguchi E. Animal models of colitis-associated carcinogenesis. Journal of biomedicine & biotechnology 2011;2011:342637.

28. Landskron G, De la Fuente M, Thuwajit P, Thuwajit C, Hermoso MA. Chronic inflammation and cytokines in the tumor microenvironment. Journal of immunology research 2014;2014:149185.

29. Heidland A, Klassen A, Rutkowski P, Bahner U. The contribution of Rudolf Virchow to the concept of inflammation: what is still of importance? Journal of nephrology 2006;19 Suppl 10:S102-9.

30. Hanahan D, Weinberg RA. Hallmarks of cancer: the next generation. Cell 2011;144:646-74.

31. Ernst M, Ramsay RG. Colorectal cancer mouse models: integrating inflammation and the stroma. J Gastroenterol Hepatol 2012;27:39-50.

32. Garrett WS, Gordon JI, Glimcher LH. Homeostasis and inflammation in the intestine. Cell 2010;140:859-70.

33. Hooper LV, Macpherson AJ. Immune adaptations that maintain homeostasis with the intestinal microbiota. Nat Rev Immunol 2010;10:159-69.

34. Kuhn R, Lohler J, Rennick D, Rajewsky K, Muller W. Interleukin-10-deficient mice develop chronic enterocolitis. Cell 1993;75:263-74.

35. Spencer SD, Di Marco F, Hooley J, Pitts-Meek S, Bauer M, Ryan AM, Sordat B, Gibbs VC, Aguet M. The orphan receptor CRF2-4 is an essential subunit of the interleukin 10 receptor. J Exp Med 1998;187:571-8.

36. Berg DJ, Davidson N, Kuhn R, Muller W, Menon S, Holland G, Thompson-Snipes L, Leach MW, Rennick D. Enterocolitis and colon cancer in interleukin-10-deficient mice are associated with aberrant cytokine production and CD4(+) TH1-like responses. J Clin Invest 1996;98:1010-20.

37. Ouyang W, Rutz S, Crellin NK, Valdez PA, Hymowitz SG. Regulation and functions of the IL-10 family of cytokines in inflammation and disease. Annu Rev Immunol 2011;29:71-109.

38. Kamanaka M, Kim ST, Wan YY, Sutterwala FS, Lara-Tejero M, Galan JE, Harhaj E, Flavell RA. Expression of interleukin-10 in intestinal lymphocytes detected by an interleukin-10 reporter knockin tiger mouse. Immunity 2006;25:941-52.

39. Poussier P. A Unique Subset of Self-specific Intraintestinal T Cells Maintains Gut Integrity. J Exp Med 2002;195:1491-7.

40. Helgason E, Phung QT, Dueber EC. Recent insights into the complexity of Tank-binding kinase 1 signaling networks: the emerging role of cellular localization in the activation and substrate specificity of TBK1. FEBS Lett 2013;587:1230-7.

41. Larabi A, Devos JM, Ng SL, Nanao MH, Round A, Maniatis T, Panne D. Crystal structure and mechanism of activation of TANK-binding kinase 1. Cell reports 2013;3:734-46.

42. Shu C, Sankaran B, Chaton CT, Herr AB, Mishra A, Peng J, Li P. Structural insights into the functions of TBK1 in innate antimicrobial immunity. Structure 2013;21:1137-48.

43. Tu D, Zhu Z, Zhou AY, Yun CH, Lee KE, Toms AV, Li Y, Dunn GP, Chan E, Thai T, Yang S, Ficarro SB, Marto JA, Jeon H, Hahn WC, Barbie DA, Eck MJ. Structure and ubiquitination-dependent activation of TANK-binding kinase 1. Cell reports 2013;3:747-58.

44. Ma X, Helgason E, Phung QT, Quan CL, Iyer RS, Lee MW, Bowman KK, Starovasnik MA, Dueber EC. Molecular basis of Tank-binding kinase 1 activation by transautophosphorylation. Proc Natl Acad Sci U S A 2012;109:9378-83.

45. Shen RR, Hahn WC. Emerging roles for the non-canonical IKKs in cancer. Oncogene 2011;30:631-41.

46. Mine T, Harada K, Matsumoto T, Yamana H, Shirouzu K, Itoh K, Yamada A. CDw108 expression during T-cell development. Tissue Antigens 2000;55:429-36.

47. Zhao W. Negative regulation of TBK1-mediated antiviral immunity. FEBS Lett 2013;587:542-8.

48. Jin J, Xiao Y, Chang JH, Yu J, Hu H, Starr R, Brittain GC, Chang M, Cheng X, Sun SC. The kinase TBK1 controls IgA class switching by negatively regulating noncanonical NF-kappaB signaling. Nat Immunol 2012;13:1101-9.

49. Liu S, Cai X, Wu J, Cong Q, Chen X, Li T, Du F, Ren J, Wu YT, Grishin NV, Chen ZJ. Phosphorylation of innate immune adaptor proteins MAVS, STING, and TRIF induces IRF3 activation. Science 2015;347:aaa2630.

50. Zhao Y, Liang L, Fan Y, Sun S, An L, Shi Z, Cheng J, Jia W, Sun W, Mori-Akiyama Y, Zhang H, Fu S, Yang J. PPM1B negatively regulates antiviral response via dephosphorylating TBK1. Cell Signal 2012;24:2197-204.

51. Gabhann JN, Higgs R, Brennan K, Thomas W, Damen JE, Ben Larbi N, Krystal G, Jefferies CA. Absence of SHIP-1 results in constitutive phosphorylation of tank-binding kinase 1 and enhanced TLR3-dependent IFN-beta production. J Immunol 2010;184:2314-20.

52. An H, Zhao W, Hou J, Zhang Y, Xie Y, Zheng Y, Xu H, Qian C, Zhou J, Yu Y, Liu S, Feng G, Cao X. SHP-2 phosphatase negatively regulates the TRIF adaptor protein-dependent type I interferon and proinflammatory cytokine production. Immunity 2006;25:919-28.

53. Friedman CS, O'Donnell MA, Legarda-Addison D, Ng A, Cardenas WB, Yount JS, Moran TM, Basler CF, Komuro A, Horvath CM, Xavier R, Ting AT. The tumour suppressor CYLD is a negative regulator of RIG-I-mediated antiviral response. EMBO reports 2008;9:930-6.

54. Zhang M, Wu X, Lee AJ, Jin W, Chang M, Wright A, Imaizumi T, Sun SC. Regulation of IkappaB kinase-related kinases and antiviral responses by tumor suppressor CYLD. J Biol Chem 2008;283:18621-6.

55. Charoenthongtrakul S, Gao L, Parvatiyar K, Lee D, Harhaj EW. RING finger protein 11 targets TBK1/IKKi kinases to inhibit antiviral signaling. PLoS One 2013;8:e53717.

56. Bonnard M, Mirtsos C, Suzuki S, Graham K, Juang J, Ng M, Itie A, Wakeham A, Shahinian A, Henzel WJ. Deficiency of T2K leads to apoptotic liver degeneration and impaired NF-κB-dependent gene transcription. EMBO J 2000;19:4976-85.

57. Takamatsu H, Okuno T, Kumanogoh A. Regulation of immune cell responses by semaphorins and their receptors. Cell Mol Immunol 2010;7:83-8.

58. Hiscott J. Convergence of the NF-kappaB and IRF pathways in the regulation of the innate antiviral response. Cytokine Growth Factor Rev 2007;18:483-90.

59. Yu J, Zhou X, Chang M, Nakaya M, Chang JH, Xiao Y, William Lindsey J, Dorta-Estremera S, Cao W, Zal A, Zal T, Sun SC. Regulation of T-cell activation and migration by the kinase TBK1 during neuroinflammation. Nature communications 2015;6:6074.

60. Barbie DA, Tamayo P, Boehm JS, Kim SY, Moody SE, Dunn IF, Schinzel AC, Sandy P, Meylan E, Scholl C, Fröhling S, Chan EM, Sos ML, Michel K, Mermel C, Silver SJ, Weir BA, Reiling JH, Sheng Q, Gupta PB, Wadlow RC, Le H, Hoersch S, Wittner BS, Ramaswamy S, Livingston DM, Sabatini DM, Meyerson M, Thomas RK, Lander ES, Mesirov JP, Root DE, Gilliland DG, Jacks T, Hahn WC. Systematic RNA interference reveals that oncogenic KRAS-driven cancers require TBK1. Nature 2009;462:108-12.

61. Baldwin AS. Regulation of cell death and autophagy by IKK and NF-kappaB: critical mechanisms in immune function and cancer. Immunol Rev 2012;246:327-45.

62. Ou YH, Torres M, Ram R, Formstecher E, Roland C, Cheng T, Brekken R, Wurz R, Tasker A, Polverino T, Tan SL, White MA. TBK1 directly engages Akt/PKB survival signaling to support oncogenic transformation. Mol Cell 2011;41:458-70.

63. Weidberg H, Elazar Z. TBK1 Mediates Crosstalk Between the Innate Immune Response and Autophagy. Science Signaling 2011;4.

64. Korherr C, Gille H, Schafer R, Koenig-Hoffmann K, Dixelius J, Egland KA, Pastan I, Brinkmann U. Identification of proangiogenic genes and pathways by high-throughput functional genomics: TBK1 and the IRF3 pathway. Proc Natl Acad Sci U S A 2006;103:4240-5.

65. Lu X, Kang Y. Hypoxia and hypoxia-inducible factors: master regulators of metastasis. Clin Cancer Res 2010;16:5928-35.

66. Chien Y, Kim S, Bumeister R, Loo YM, Kwon SW, Johnson CL, Balakireva MG, Romeo Y, Kopelovich L, Gale M, Jr., Yeaman C, Camonis JH, Zhao Y, White MA. RalB GTPase-mediated activation of the IkappaB family kinase TBK1 couples innate immune signaling to tumor cell survival. Cell 2006;127:157-70.

67. Mantovani A, Balkwill F. RalB signaling: a bridge between inflammation and cancer. Cell 2006;127:42-4.

68. Camonis JH, White MA. Ral GTPases: corrupting the exocyst in cancer cells. Trends Cell Biol 2005;15:327-32.

69. Waldner MJ, Neurath MF. Chemically induced mouse models of colitis. Curr Protoc Pharmacol 2009;Chapter 5:Unit 5 55.

70. Wirtz S, Neufert C, Weigmann B, Neurath MF. Chemically induced mouse models of intestinal inflammation. Nat Protoc 2007;2:541-6.

71. Kim JY, Welsh EA, Oguz U, Fang B, Bai Y, Kinose F, Bronk C, Remsing Rix LL, Beg AA, Rix U, Eschrich SA, Koomen JM, Haura EB. Dissection of TBK1 signaling via phosphoproteomics in lung cancer cells. Proc Natl Acad Sci U S A 2013;110:12414-9.

72. Wei C, Cao Y, Yang X, Zheng Z, Guan K, Wang Q, Tai Y, Zhang Y, Ma S, Cao Y, Ge X, Xu C, Li J, Yan H, Ling Y, Song T, Zhu L, Zhang B, Xu Q, Hu C, Bian XW, He X, Zhong H. Elevated expression of TANK-binding kinase 1 enhances tamoxifen resistance in breast cancer. Proc Natl Acad Sci U S A 2014;111:E601-10.

73. Muvaffak A, Pan Q, Yan H, Fernandez R, Lim J, Dolinski B, Nguyen TT, Strack P, Wu S, Chung R, Zhang W, Hulton C, Ripley S, Hirsch H, Nagashima K, Wong KK, Janne PA, Seidel-Dugan C, Zawel L, Kirschmeier PT, Middleton RE, Morris EJ, Wang Y. Evaluating TBK1 as a Therapeutic Target in Cancers with Activated IRF3. Mol Cancer Res 2014.

74. Ensembl release 83. Ensembl 2015. (Accessed December 12, 2015, at http://dec2015.archive.ensembl.org/.)

75. Kersey PJ, Allen JE, Armean I, Boddu S, Bolt BJ, Carvalho-Silva D, Christensen M, Davis P, Falin LJ, Grabmueller C, Humphrey J, Kerhornou A, Khobova J, Aranganathan NK, Langridge N, Lowy E, McDowall MD, Maheswari U,

Nuhn M, Ong CK, Overduin B, Paulini M, Pedro H, Perry E, Spudich G, Tapanari E, Walts B, Williams G, Tello-Ruiz M, Stein J, Wei S, Ware D, Bolser DM, Howe KL, Kulesha E, Lawson D, Maslen G, Staines DM. Ensembl Genomes 2016: more genomes, more complexity. Nucleic Acids Res 2015.

76. Huret JL, Ahmad M, Arsaban M, Bernheim A, Cigna J, Desangles F, Guignard JC, Jacquemot-Perbal MC, Labarussias M, Leberre V, Malo A, Morel-Pair C, Mossafa H, Potier JC, Texier G, Viguie F, Yau Chun Wan-Senon S, Zasadzinski A, Dessen P. Atlas of genetics and cytogenetics in oncology and haematology in 2013. Nucleic Acids Res 2013;41:D920-4.

77. Atlas of Genetics and Cytogenetics in Oncology and Haematology. Chromosome 12. Band 12q14. 2015.

78. Kazmierczak B, Meyer-Bolte K, Tran KH, Wockel W, Breightman I, Rosigkeit J, Bartnitzke S, Bullerdiek J. A high frequency of tumors with rearrangements of genes of the HMGI(Y) family in a series of 191 pulmonary chondroid hamartomas. Genes Chromosomes Cancer 1999;26:125-33.

79. Zhang L, Mitani Y, Caulin C, Rao PH, Kies MS, Saintigny P, Zhang N, Weber RS, Lippman SM, El-Naggar AK. Detailed genome-wide SNP analysis of major salivary carcinomas localizes subtype-specific chromosome sites and oncogenes of potential clinical significance. Am J Pathol 2013;182:2048-57.

80. Gao J, Aksoy BA, Dogrusoz U, Dresdner G, Gross B, Sumer SO, Sun Y, Jacobsen A, Sinha R, Larsson E, Cerami E, Sander C, Schultz N. Integrative

analysis of complex cancer genomics and clinical profiles using the cBioPortal. Science signaling 2013;6:pl1.

81. Cerami E, Gao J, Dogrusoz U, Gross BE, Sumer SO, Aksoy BA, Jacobsen A, Byrne CJ, Heuer ML, Larsson E, Antipin Y, Reva B, Goldberg AP, Sander C, Schultz N. The cBio cancer genomics portal: an open platform for exploring multidimensional cancer genomics data. Cancer Discov 2012;2:401-4.

82. Forbes SA, Beare D, Gunasekaran P, Leung K, Bindal N, Boutselakis H, Ding M, Bamford S, Cole C, Ward S, Kok CY, Jia M, De T, Teague JW, Stratton MR, McDermott U, Campbell PJ. COSMIC: exploring the world's knowledge of somatic mutations in human cancer. Nucleic Acids Res 2015;43:D805-11.

83. Catalogue of Somatic Mutations in Cancer. 2015.

84. Ikeda F, Hecker CM, Rozenknop A, Nordmeier RD, Rogov V, Hofmann K, Akira S, Dotsch V, Dikic I. Involvement of the ubiquitin-like domain of TBK1/IKK-i kinases in regulation of IFN-inducible genes. EMBO J 2007;26:3451-62.

85. Neely RJ, Brose MS, Gray CM, McCorkell KA, Leibowitz JM, Ma C, Rothstein JL, May MJ. The RET/PTC3 oncogene activates classical NF-κB by stabilizing NIK. Oncogene 2011;6:87-96.

86. Heavey PM, McKenna D, Rowland IR. Colorectal cancer and the relationship between genes and the environment. Nutr Cancer 2004;48:124-41.

87. Saif MW, Chu E. Biology of colorectal cancer. Cancer J 2010;16:196-201.

88. Klampfer L. Cytokines, Inflammation and Colon Cancer. Curr Cancer Drug Targets 2011;Epub ahead of print.

89. Lukas M. Inflammatory bowel disease as a risk factor for colorectal cancer. Dig Dis 2010;28:619-24.

90. Okayasu I, Ohkusa T, Kajiura K, Kanno J, Sakamoto S. Promotion of colorectal neoplasia in experimental murine ulcerative colitis. Gut 1996;39:87-92.

91. Serebrennikova OB, Tsatsanis C, Mao C, Gounaris E, Ren W, Siracusa LD, Eliopoulos AG, Khazaie K, Tsichlis PN. Tpl2 ablation promotes intestinal inflammation and tumorigenesis in Apcmin mice by inhibiting IL-10 secretion and regulatory T-cell generation. Proc Natl Acad Sci U S A 2012;109:E1082-91.

92. Tanaka T, Kohno H, Suzuki R, Yamada Y, Sugie S, Mori H. A novel inflammation-related mouse colon carcinogenesis model induced by azoxymethane and dextran sodium sulfate. Cancer Sci 2003;94:965-73.

93. Mombaerts P, Iacomini J, Johnson RS, Herrup K, Tonegawa S, Papaioannou VE. RAG-1-deficient mice have no mature B and T lymphocytes. Cell 1992;68:869-77.

94. Sheridan BS, Lefrancois L. Isolation of mouse lymphocytes from small intestine tissues. Curr Protoc Immunol 2012;Chapter 3:Unit3 19.

95. Levings MK, Sangregorio R, Galbiati F, Squadrone S, de Waal Malefyt R, Roncarolo MG. IFN-alpha and IL-10 induce the differentiation of human type 1 T regulatory cells. J Immunol 2001;166:5530-9.

96. Nagalakshmi ML, Rascle A, Zurawski S, Menon S, de Waal Malefyt R. Interleukin-22 activates STAT3 and induces IL-10 by colon epithelial cells. Int Immunopharmacol 2004;4:679-91.

97. Napolitano LM, Buzdon MM, Shi HJ, Bass BL. Intestinal epithelial cell regulation of macrophage and lymphocyte interleukin 10 expression. Arch Surg 1997;132:1271-6.

98. Clement JF, Meloche S, Servant MJ. The IKK-related kinases: from innate immunity to oncogenesis. Cell Res 2008;18:889-99.

99. How is colorectal cancer staged? 2015. (Accessed December 1, 2015, at http:///www.cancer.org/cancer/colonandrectumcancer/detailedguide/colorectal-cancer-staged.)

100. Calcagno SR, Li S, Colon M, Kreinest PA, Thompson EA, Fields AP, Murray NR. Oncogenic K-ras promotes early carcinogenesis in the mouse proximal colon. Int J Cancer 2008;122:2462-70.

101. Wang J, Kuropatwinski K, Hauser J, Rossi MR, Zhou Y, Conway A, Kan JL, Gibson NW, Willson JK, Cowell JK, Brattain MG. Colon carcinoma cells harboring PIK3CA mutations display resistance to growth factor deprivation induced apoptosis. Mol Cancer Ther 2007;6:1143-50.

102. Reva B, Antipin Y, Sander C. Predicting the functional impact of protein mutations: application to cancer genomics. Nucleic Acids Res 2011;39:e118.

103. Goncalves A, Burckstummer T, Dixit E, Scheicher R, Gorna MW, Karayel E, Sugar C, Stukalov A, Berg T, Kralovics R, Planyavsky M, Bennett KL, Colinge J, Superti-Furga G. Functional dissection of the TBK1 molecular network. PLoS One 2011;6:e23971.

104. Ilyas M, Tomlinson IP, Rowan A, Pignatelli M, Bodmer WF. Beta-catenin mutations in cell lines established from human colorectal cancers. Proc Natl Acad Sci U S A 1997;94:10330-4.

105. Brink M, de Goeij AF, Weijenberg MP, Roemen GM, Lentjes MH, Pachen MM, Smits KM, de Bruine AP, Goldbohm RA, van den Brandt PA. K-ras oncogene mutations in sporadic colorectal cancer in The Netherlands Cohort Study. Carcinogenesis 2003;24:703-10.

106. Belizario JE. Immunodeficient Mouse Models: An Overview. The Open Immunology Journal 2009:79-85.

107. Clark K, Peggie M, Plater L, Sorcek RJ, Young ER, Madwed JB, Hough J, McIver EG, Cohen P. Novel cross-talk within the IKK family controls innate immunity. Biochem J 2011;434:93-104.

108. Hofmann SR, Rosen-Wolff A, Tsokos GC, Hedrich CM. Biological properties and regulation of IL-10 related cytokines and their contribution to autoimmune disease and tissue injury. Clin Immunol 2012;143:116-27.

109. Engelhardt KR, Grimbacher B. IL-10 in humans: lessons from the gut, IL-10/IL-10 receptor deficiencies, and IL-10 polymorphisms. Curr Top Microbiol Immunol 2014;380:1-18.

110. Veenbergen S, Samsom JN. Maintenance of small intestinal and colonic tolerance by IL-10-producing regulatory T cell subsets. Curr Opin Immunol 2012;24:269-76.

111. Gomes-Santos AC, Moreira TG, Castro-Junior AB, Horta BC, Lemos L, Cruz DN, Guimaraes MA, Cara DC, McCafferty DM, Faria AM. New insights into the immunological changes in IL-10-deficient mice during the course of spontaneous inflammation in the gut mucosa. Clin Dev Immunol 2012;2012:560817.

112. Wilson EB, Yamada DH, Elsaesser H, Herskovitz J, Deng J, Cheng G, Aronow BJ, Karp CL, Brooks DG. Blockade of chronic type I interferon signaling to control persistent LCMV infection. Science 2013;340:202-7.

113. Teijaro JR, Ng C, Lee AM, Sullivan BM, Sheehan KC, Welch M, Schreiber RD, de la Torre JC, Oldstone MB. Persistent LCMV infection is controlled by blockade of type I interferon signaling. Science 2013;340:207-11.

114. Dikopoulos N, Bertoletti A, Kroger A, Hauser H, Schirmbeck R, Reimann J. Type I IFN negatively regulates CD8+ T cell responses through IL-10-producing CD4+ T regulatory 1 cells. J Immunol 2005;174:99-109.

115. Ersoy E, Kus CN, Sener U, Coker I, Zorlu Y. The effects of interferon-beta on interleukin-10 in multiple sclerosis patients. Eur J Neurol 2005;12:208-11.

116. Byrnes AA, McArthur JC, Karp CL. Interferon-beta therapy for multiple sclerosis induces reciprocal changes in interleukin-12 and interleukin-10 production. Ann Neurol 2002;51:165-74.

117. Holmes S, Downs AM, Fosberry A, Hayes PD, Michalovich D, Murdoch P, Moores K, Fox J, Deen K, Pettman G, Wattam T, Lewis C. Sema7A is a potent monocyte stimulator. Scand J Immunol 2002;56:270-5.

118. Suzuki K, Okuno T, Yamamoto M, Pasterkamp RJ, Takegahara N, Takamatsu H, Kitao T, Takagi J, Rennert PD, Kolodkin AL, Kumanogoh A, Kikutani H. Semaphorin 7A initiates T-cell-mediated inflammatory responses through alpha1beta1 integrin. Nature 2007;446:680-4.

119. Czopik AK, Bynoe MS, Palm N, Raine CS, Medzhitov R. Semaphorin 7A is a negative regulator of T cell responses. Immunity 2006;24:591-600.

120. Kang S, Okuno T, Takegahara N, Takamatsu H, Nojima S, Kimura T, Yoshida Y, Ito D, Ohmae S, You DJ, Toyofuku T, Jang MH, Kumanogoh A. Intestinal epithelial cell-derived semaphorin 7A negatively regulates development of colitis via alphavbeta1 integrin. J Immunol 2012;188:1108-16.

121. Okayasu I, Hatakeyama S, Yamada M, Ohkusa T, Inagaki Y, Nakaya R. A novel method in the induction of reliable experimental acute and chronic ulcerative colitis in mice. Gastroenterology 1990;98:694-702.

Vitae

Amber Lynn Mathews, the daughter of Jacqueline M. Stewart and Arnold Kennedy, completed high school in Kaplan, Louisiana. She earned a Bachelor of Science degree in Biological Sciences and a minor in French from Louisiana State University (LSU) in Baton Rouge, LA. After resigning as a specialist in commission-based sales, she earned a Master of Science degree in Biological Sciences from LSU, completing her master's thesis research under the advisement of Dr. Hollie Hale-Donze in the Department of Biological Sciences. In August 2010, she entered The University of Texas Graduate School of Biomedical Sciences at Houston where she joined the laboratory of Dr. Shao-Cong Sun in the Department of Immunology at The University of Texas MD Anderson Cancer Center in Houston, Texas to complete her dissertation studies.